University of Alberta

Defining the Molecular Phenotype of the Rat Retina During the Commitment Phase of Light-Induced Retinal Degeneration: A Model of Human Retinal Degenerative Disease

By

Jadwiga Maja Stepczynski

A thesis submitted to the Faculty of Graduate Studies and Research in partial fulfillment of the requirements for the degree of Master of Science

in

Molecular Biology and Genetics

Department of Biological Sciences

Edmonton, Alberta

Spring 2001

National Library of Canada
Acquisitions and Bibliographic Services
395 Wellington Street
Ottawa ON K1A 0N4
Canada

Bibliothèque nationale du Canada
Acquisitions et services bibliographiques
395, rue Wellington
Ottawa ON K1A 0N4
Canada

Your file Votre référence

Our file Notre référence

The author has granted a non-exclusive licence allowing the National Library of Canada to reproduce, loan, distribute or sell copies of this thesis in microform, paper or electronic formats.

L'auteur a accordé une licence non exclusive permettant à la Bibliothèque nationale du Canada de reproduire, prêter, distribuer ou vendre des copies de cette thèse sous la forme de microfiche/film, de reproduction sur papier ou sur format électronique.

The author retains ownership of the copyright in this thesis. Neither the thesis nor substantial extracts from it may be printed or otherwise reproduced without the author's permission.

L'auteur conserve la propriété du droit d'auteur qui protège cette thèse. Ni la thèse ni des extraits substantiels de celle-ci ne doivent être imprimés ou autrement reproduits sans son autorisation.

0-612-60502-7

Canada

University of Alberta

Library Release Form

Name of Author: Jadwiga Maja Stepczynski

Title of Thesis: Defining the Molecular Phenotype of the Rat Retinal During the Commitment Phase of Light-Induced Retinal Degeneration: A Model of Human Retinal Degenerative Disease

Degree: Master of Science

Year this Degree Granted: 2001

Permission is hereby granted to the University of Alberta Library to reproduce single copies of this thesis and to lend or sell such copies for private, scholarly or scientific research purposes only.

The author reserves all other publication and other rights in association with the copyright in the thesis, and except as herein before provided, neither the thesis nor any substantial portion thereof may be printed or otherwise reproduced in any material form whatever without the author's prior written permission.

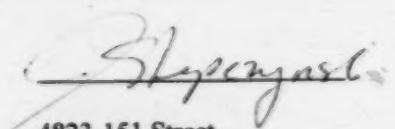

4823-151 Street,
Edmonton, Alberta
T6H 5N9

Date: April 17, 2001

University of Alberta

Faculty of Graduate Studies and Research

The undersigned certify that they have read, and recommend to the Faculty of Graduate Studies and Research for acceptance, a thesis entitled Defining the Molecular Phenotype of the Rat Retina During the Commitment Phase of Light-Induced Retinal Degeneration: A Model of Human Retinal Degenerative Disease submitted by Jadwiga Maja Stepczynski in partial fulfillment of the requirements for the degree of Master's of Science in Molecular Biology and Genetics.

Dr. Paul Wong

Dr. John Bell

Dr. Peter Constabel

Dr. Roseline Godbout

ABSTRACT

Retinal degenerative diseases are among the major causes of vision loss. The mechanisms underlying these diseases have still to be elucidated. To this end, the rat light-induced retinal degeneration (LIRD) model for human retinal degenerative disease has been developed. This model allows monitoring of the progression of retinal degeneration. By comparing the molecular phenotype of a healthy retina with that of a retina at an early stage of degeneration, the Commitment Phase of LIRD, it is possible to correlate the state of degeneration with changes in the molecular environment. During the Commitment Phase of LIRD intracellular and extracellular events are predicted to dictate whether individual cells will commit to apoptosis. The comparison of Commitment Phase retinae with healthy, control retinae through differential cross-screening lead to the identification of 54 differentially expressed transcripts. These may represent factors which are a consequence or a cause of the retinal degeneration.

ACKNOWLEDGEMENTS

This work would not have been possible without the help, support, and guidance of many. Foremost I would like to thank Dr. Paul Wong for his infectious enthusiasm, high expectations, and faith in my ability to fulfill them. Thank you to Michelle Chambers for teaching me all the techniques I needed to know in order to get my project started, for answering my plethora of questions, on all topics, and for introducing me to the true art of improvisation. Many thanks to Rhonda Kelln, Pamela Lagali, Ben McDonald, Ruby Grewal, and Micah Chrenek for the technical advice, TV chats, Florida adventures, and for generally making my time in the lab both educational and entertaining. Thanks to Brian Weiss and Daniel Barreda for much hilarity during library making, library screening and other such stress-free endeavors. Thanks to Angela Manning for keeping such great lab notes and for her willingness to share them. And finally a huge thank you to my family, Maria Percy, Marek Stepczynski, Ania Stepczynski, and Witek Stepczynski, for always pushing me to meet new challenges and supporting me completely irrespective of whether I am in the right.

"Were I to await perfection, my "thesis" would never be finished" (Tai T'ung).

Table of Contents

List of Tables----------

List of Figures ----------

Chapter 1 Introduction ----------1

A. The Mammalian Eye ----------2

B-1 Phototransduction ----------2

B-2 Retinal Degenerative Disease ----------7

B. Apoptosis and Retinal Degeneration ---------- 11

C. Genetic Models of Retinal Degenerative Disease ---------- 13

D. Induced Models of Retinal Degeneration ---------- 15

E-1 Dissecting the Rat LIRD Model ---------- 16

E-2 Apoptosis in Light Induced Retinal Degeneration ---------- 19

E-3 A Possible Trigger for LIRD: A Model for Retinitis Pigmentosa 20

E-4 LIRD and Oxidative Stress: A Model for Macular Degeneration 21

E. Gene Expression: Clues To The Mechanism of Retinal Degeneration ---------- 22

Chapter 2 Materials and Methods ---------- 24

A. Samples ---------- 25

B. Isolation of RNA ---------- 25

B-1 Isolation of Total RNA ---------- 25

B-2 Isolation of mRNA ---------- 26

C. Construction of the Commitment Phase cDNA Library ---------- 26

C-1 First Strand cDNA Synthesis ---------- 28

C-2 Second Strand cDNA Synthesis ---------- 28

C-3 Blunting the cDNA Termini ---------- 28

C-4 Ligating *Eco*R1 Adapters ---------- 28

C-5 Size Fractionation of the cDNA ---------- 28

C-6 Ligating cDNA into the Uni-ZAP XR vector ---------- 29

C-7 Packaging the Phage ---------- 29

C-8 Preparation of the Host Bacteria and Titering of the Library ---- 29

D. Screening of the Commitment Phase cDNA Library ---------- 29

D-1 Primary Commitment Phase cDNA Library Screen ---------- 29
D-1.1 Plaque Lifts ---------- 32
D-1.2 Preparation of the cDNA Probes Used in Primary Screen ---------- 32
D-1.21 cDNA Synthesis ---------- 32
D-1.22 Radioactive Labeling of cDNA Probes ------- 50
D-1.3 Hybridization and Analysis ---------- 33
D-1.31 Hybridization ---------- 33
D-1.32 Analysis ---------- 33
D-2 Secondary Commitment Phase cDNA Library Screen ---------- 34
D-3 Tertiary Commitment Phase cDNA Library Screen ---------- 35
D-3.1 Polymerase Chain Reaction ---------- 35
D-3.2 Electrophoresis ---------- 35
D-3.3 Southern Transfer ---------- 35
E. Analysis of Genes ---------- 36
E-1 RNA level ---------- 36
E-1.1 Northern Analysis ---------- 36
E-1.11 Preparation of Samples ---------- 36
E-1.12 Preparation of Formaldehyde gel and Electrophoresis ---------- 36
E-1.13 Transfer of RNA ---------- 36
E-1.14 Probe Labeling and Hybridization ---------- 36
E-1.2 Slot Blot Analysis ---------- 37
E-1.3 Nuclease Protection Assay ---------- 37
E-1.31 Designing NPA Probes ---------- 37
E-1.32 Radioactive Labeling of the Oligonucleotide Probes ---------- 37
E-1.33 Hybridization of Oligonucleotide Probe to Target mRNA ---------- 39
E-1.34 Digestion of Single Stranded Nucleic Acids - 39
E-1.35 Electrophoresis and Analysis ---------- 39

E-1.4 RT-PCR ---- 39
E-2 Analysis at the Level of the DNA ---- 41
E-2.1 Sequencing ---- 41
E-2.11 Sample Preparation ---- 41
E-2.12 Sequencing Reactions ---- 42
Chapter 3 Screening of the Commitment Phase cDNA Library ---- 43
A. Introduction ---- 44
B. Results ---- 46
B-1 Integrity of RNA Samples ---- 46
B-2 Screening of the Commitment Phase cDNA Library ---- 46
B-2.1 Primary Screen ---- 46
B-2.2 Secondary Screen ---- 46
B-2.2 Tertiary Screen ---- 49
C. Initial Characterization of Clones ---- 49
C-1 Northern Analysis ---- 49
E. Discussion and Conclusion ---- 51
Chapter 4 Sequence Comparison of Putative Differential Clones ---- 54
A. Introduction ---- 55
B. Results and Analysis ---- 55
B-1 Sequencing ---- 55
B-2 Unique Rat Sequences ---- 55
B-3 Clones with Sequence Similarities ---- 58
B-4 Matches to Known Rat Genes ---- 63
B-4.1 Clones of Genes Whose Products are Required in the Mitochondria ---- 63
B-4.2 Eye & Central Nervous System Clones ---- 63
B-4.3 Enzymes ---- 65
B-4.4 Translational Machinery ---- 67
B-4.5 Signaling Pathway Associated Clones & Transcription Factors ---- 67
C. Discussion ---- 69

Chapter 5 Expression Pattern of Transcription Factors: Evaluated Using Northern Analysis, Nuclease Protection Assay, and RT-PCR ---- 70
A. Introduction ---- 71
B. Results ---- 72
B-1 Nuclease Protection Assay ---- 72
B-2 Reverse-Transcriptase-PCR (RT-PCR) Analysis ---- 74
B-3 Northern Analysis ---- 77
C. Discussion ---- 80
Chapter 6 Ribosomal Protein Expression Over the Course of LIRD ---- 86
A. Introduction ---- 87
B. Results ---- 89
B-1 Slot Blot Analysis ---- 89
B-2 Northern Blot Analysis ---- 89
B-3 Expression Patterns During Prostate Degeneration ---- 95
C. Discussion ---- 95
C-1 Slot Blot vs. Northern Blot Analysis ---- 95
C-2 Ribosomal Proteins and Function During LIRD ---- 95
C-2.1 Ribosomal Protein Up-Regulation in Cancer Cell Lines ---- 97
C-2.2 Cell Cycle Regulation ---- 97
C-2.3 Ribosomal Proteins and Regulation ---- 98
C-2.4 Ribosomal Proteins and Apoptosis ---- 99
C-2.5 Ribosomal Proteins and Repair ---- 99
C-3 Ribosomal Proteins as a Common Phenomenon in Degeneration ---- 100
D. Conclusion ---- 100
Chapter 7 Conclusion ---- 102
References ---- 106
Appendix I Solutions ---- 123
Appendix II Abbreviations ---- 129

List of Tables

Table 1-1 Summary of Known Genetic Mutations Underlying Human Retinal Degenerative Disease ---------- 10

Table 1-2 Summary of Animal Models of Human Retinal Degeneration -------- 14

Table 4-1 Summary of Sequence Data ---------- 57

Table 6-1 Summary of Ribosomal Protein Clones and Experiments ---------- 88

List of Figures

Chapter 1

Figure 1-1 The Mammalian Eye ---------- 3

Figure 1-2 Phototransduction ---------- 5

Figure 1-3 The Visual Cycle ---------- 6

Figure 1-4 Human Retinae Undergoing Retinal Degeneration ---------- 8

Figure 1-5 Methods Used for the Detection of Apoptotic Cells ---------- 12

Figure 1-6 Stages of LIRD ---------- 18

Chapter 2

Figure 2-1 Schematic Depiction of cDNA Library Synthesis ---------- 27

Figure 2-2 Lambda Uni-ZAP XR ---------- 30

Figure 2-3 Schematic Depiction of the Commitment Phase cDNA Library Differential Cross Screen ---------- 31

Figure 2-4 Nuclease Protection Assay (NPA) ---------- 38

Figure 2-5 RT-PCR ---------- 40

Chapter 3

Figure 3-1 Identification of Genes with Altered Levels of Expression During the Commitment Phase of LIRD ---------- 45

Figure 3-2 Northern Analysis and the LIRD Profile ---------- 47

Figure 3-3 Differential Cross-Screening of the Commitment Phase cDNA Library ---------- 48

Figure 3-4 Northern Confirmation of Differential Clone Status ---------- 50

Figure 3-5 Duplicate and Triplicate LIRD Profile Northern Probed Blots-------- 52

Chapter 4

Figure 4-1 Summary of Sequencing Results ---------- 56

Figure 4-2 Hybridization Pattern of Unique Clones on LIRD Northern Blots --- 59

Figure 4-3 Sequence Comparison of Clone 2A, Mouse Opsin Gene, and Rat Opsin Gene ---------- 61

Figure 4-4 Hybridization Pattern on LIRD Profile Northern Blots of Clones of Transcripts with Sequence Similarity ---------- 62

Figure 4-5 Mitochondrial Clone 1157 on LIRD Northern Blots ---------- 64

Figure 4-6 Hybridization Pattern of Clone 12 on LIRD Northern Blots --------- 66

Figure 4-7 Hybridization Pattern of Signal Pathway Associated Clones on LIRD Northern Blots ---------- 68

Chapter 5

Figure 5-1 Nuclease Protection Assay on Light-Induced Retinal Degeneration Profile RNA ---------- 73

Figure 5-2 Densitometric Analysis of NPA Autoradiographs ---------- 75

Figure 5-3 Detection of NFκβ and Otx2 Transcript in Control and 4 h Light Treated Retinal RNA Using RT-PCR ---------- 76

Figure 5-4 Alterations in Otx2 and NFκβ Transcript Levels following 4 h Light Treatment: RT-PCR Analysis ---------- 78

Figure 5-5 LIRD Profile Northern Blot Probed with RT-PCR Product NFκβ -- 79

Figure 5-6 Comparison of Clone 1084 and Otx2 (RT-PCR Product) Hybridization Patterns on LIRD Profile Northern Blots ---------- 81

Figure 5-7 Comparison of GenBank Otx2 Sequence to Sequences of Clone 1084 and Otx2 RT-PCR Product ---------- 82

Chapter 6

Figure 6-1 Hybridization Pattern of Ribosomal Protein Clones on Slot Blots Containing Control and 4 h Light Treated Retinal RNA ---------- 90

Figure 6-2 Change in Ribosomal Protein Gene Expression Pattern Over LIRD 91

Figure 6-3 Graphical Representation of RP Expression Over the Course of LIRD: Category 1 ---------- 93

Figure 6-4 Graphical Representation of RP Expression Over the Course of LIRD: Category 2 & 3 ---------- 94

Figure 6-5 Expression Pattern of Ribosomal Proteins on Degenerative Prostate Northern Blots ---------- 96

CHAPTER 1
INTRODUCTION

A. THE MAMMALIAN EYE

The mammalian eye is a highly complex organ (figure 1-1A). The ability to see is dependent on the absorption of light, translation of light signal into an electrical signal, and the relaying of the electrical impulse encoded message to the brain. Absorption of light photons and conversion of light into an electrical impulse is facilitated by photoreceptor cells through a process termed phototransduction. Photoreceptor cells are found in the neural retina (figure 1-1B) and are among the last cell types reached by light. There are two types of photoreceptor cells, rod and cone (figure 1-1C). They differ from one another both morphologically and functionally. Rod photoreceptors are the dominant photoreceptor type in the mammalian retina. They are rod shaped, as their name suggests, and enable the perception of low levels of light. Thus, they allow for night and peripheral vision. Rod cells are concentrated around the periphery of the retina and their loss underlies retinal diseases such as retinitis pigmentosa, which will be discussed later. In humans and primates, the cone shaped cone photoreceptor cells are concentrated in the very center of the retina. Their presence there defines the foveo-macular region, a 1.5mm region that appears as a yellow tinted indentation on the surface of the retina under an electron microscope (Cohen, 1992). In rats however, there is no macular region because the cone photoreceptor cells are distributed throughout the retina and not concentrated in the central region. Cone photoreceptor cells are involved in acute and colour vision and, in humans, their loss results in the loss of central vision, a characteristic of macular degenerative diseases (Cohen, 1992).

A-1 Phototransduction Phototransduction initially requires the absorption of light by visual pigments found in photoreceptor cells. Visual pigments are G-protein coupled receptors that are located in the disc membranes of photoreceptor cell outer segments. Several different visual pigments exist; each is optimized for the absorption of a different wavelength range of visible light. This variability in wavelength absorption is attributed to the composition of the pigment. Visual pigments are composed of a specific form of apo-protein (opsin) covalently bound by a chromophore molecule, a vitamin A aldehyde (11-cis retinaldehyde) (Saari, 1992).

Figure 1-1: The Mammalian Eye

A) Schematic illustration of the eye.
B) Light micrograph of human retina. RPE, retinal pigment epithelium; OS, outer segments; IS, inner segments (OS and IS together make up the photoreceptor cells); OLM, outer limiting membrane; ONL, outer nuclear layer; OPL, outer plexiform layer; INL, inner nuclear layer; IPL, inner plexiform layer; GCL, ganglion cell layer; NFL, nerve fiber layer; ILM, inner limiting membrane.
C) Schematic illustration of the retina. R, rod photoreceptors; C, cone photoreceptors; H, horizontal cells; B, bipolar cells; A, amacrine; G, ganglion cells.
(modified from Nolte J., 1999, Rhoades *et al.*, 1996)

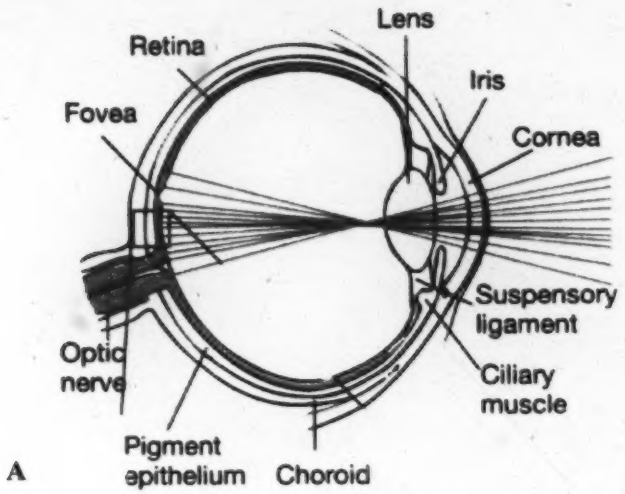
Lens
Retina
Iris
Fovea
Cornea
Suspensory ligament
Optic nerve
Ciliary muscle
Pigment epithelium
Choroid
A

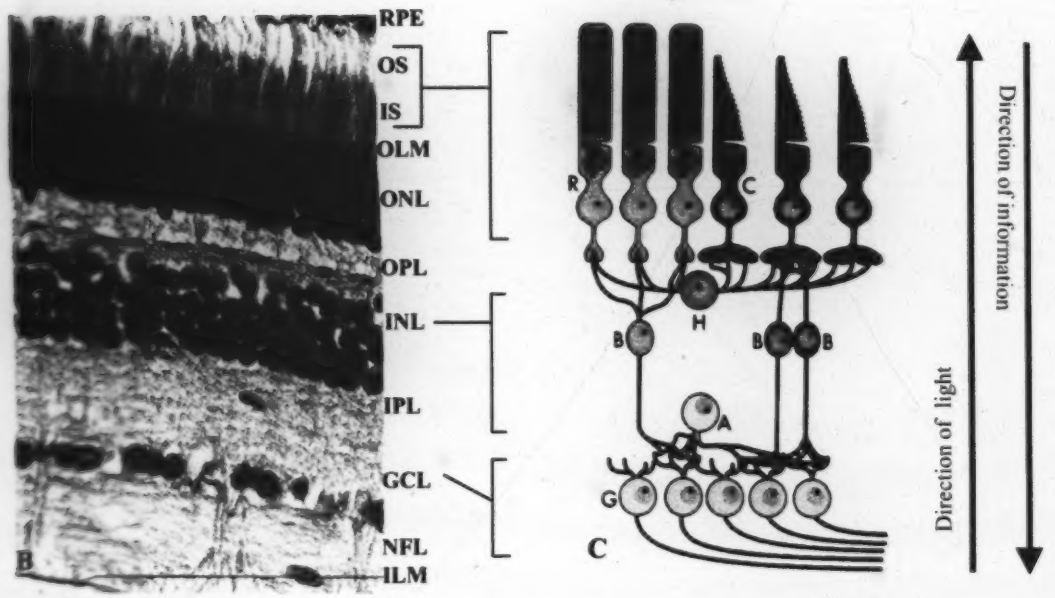
RPE
OS
IS
OLM
ONL
OPL
INL
IPL
GCL
NFL
ILM
B
R
C
H
B
B
B
A
G
C
Direction of information
Direction of light

Absorption of photons by the visual pigment activates the phototransduction pathway, which functions to link light absorption with a change in the electrical potential of the photoreceptor cell. This process, depicted in figure 1-2, is best characterized in mammalian rod photoreceptor cells, in which the major visual pigment is rhodopsin. In the absence of light, the photoreceptor, in a depolarized state, continuously releases a neurotransmitter (glutamate) from its synaptic terminal to neighboring cells. When light enters the eye, rhodopsin absorbs the light photons causing 11-cis-retinaldehyde to be converted into 11-trans retinaldehyde. This results in the dissociation of the opsin protein and chromophore, thus activating opsin. The activated opsin binds to transducin (the GTP binding protein) and induces the release of transducin's active α-subunit. Transducin proceeds to activate cyclic guanosine monophosphate phosphodiesterase (cGMP-PDE). Activated cGMP-PDE catalyzes the hydrolysis of cGMP to 5'GMP. High cGMP levels in the cell maintain cGMP-gated cation channels in an open configuration and thus maintain the cell in a depolarized state. The decrease in cGMP levels, as a consequence of cGMP-PDE activation, leads to the closure of the cGMP-gated channels and the hyperpolarization of the photoreceptor. In a hyperpolarized state the photoreceptor reduces the amount of neurotransmitter it releases. The drop in neurotransmitter release from the photoreceptor cell causes the neighboring neural cell to undergo a change in its polarization state and thus the electrical signal is transferred from cell to cell and ultimately to the brain where it is interpreted as an image (Saari, 1992).

Termination of the signal is accomplished through the inactivation of opsin. Inactivation of opsin occurs through the phosphorylation of active opsin by rhodopsin kinase and binding of the phosphorylated opsin by arrestin (s-antigen). In this state, rhodopsin is unreceptive to new light signals and incapable of activating transducin. Concomitantly the 11-trans-retinaldehyde (vitamin A derivative) that had disassociated from rhodopsin upon photon absorption is converted into all-trans retinal (figure 1-3) and is transported to the retinal
pigment epithelium (Saari, 1992) by interphotoreceptor retinoid-binding protein (IRBP). In the RPE, all-trans-retinal is converted to 11-cis retinaldehyde through a series of enzymatic reactions. The 11-cis-retinaldehyde is then transported back to the rod outer

Figure 1-2: Phototransduction

In the absence of light the photoreceptor cell is in a hyper-polarized state (A). Rhodopsin, composed of an opsin protein (apo-protein) and 11-cis retinaldehyde (chromophore), is inactive (1), as are transducin and cGMP-phospodiesterase (PDE) (2). Due to the inactive state of PDE there is a high level of cGMP in the outer segment of the photoreceptor cell. As a result the cGMP-gated cation channels are open (3) and there is a flow of positively charged ions (sodium) into the outer segment and out through channels in the cell body (4). In this hyperpolarized state the photoreceptor releases glutamate, a neurotransmitter (5).

When light photons (B) enter the retina they are absorbed by the rhodopsin chromophore (6). This results in the release of the chromophore and a configurational change in the opsin protein which renders rhodopsin active. Activated rhodopsin then activates transducin (7). The activated transducin releases its alpha-subunit, which then proceeds to activate PDE. Activated PDE catalyzes the hydrolysis of cGMP to 5'GMP (8). Thus reducing the cGMP concentration in the outer segment and causing the closure of the cGMP gated cation channels (9). This series of events changes the membrane potential of the photoreceptor cell. The now depolarized photoreceptor ceases to release neurotransmitters (adapted from Nolte, 1999).

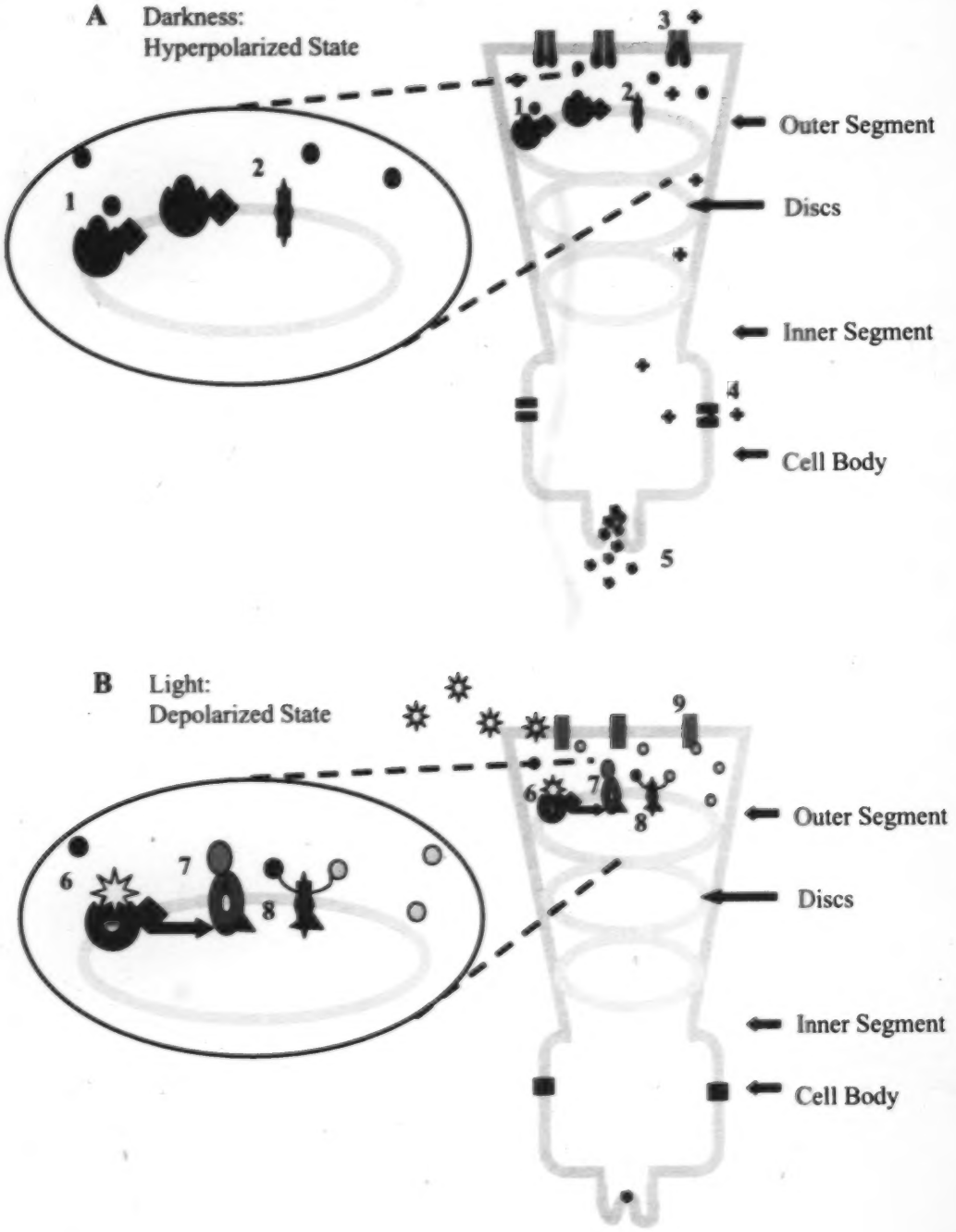
A
Darkness:
Hyperpolarized State
1
2
3
4
5
Outer Segment
Discs
Inner Segment
Cell Body
B
Light:
Depolarized State
6
7
8
9
Outer Segment
Discs
Inner Segment
Cell Body

Figure 1-3: The Visual Cycle

In its in active state (1) rhodopsin is composed of opsin and 11-cis retinaldehyde. Upon activation, through the absorption of a light photon, 11-cis retinaldehyde is converted to all trans-retinaldehyde and disassociates from the opsin protein (2). All-trans retinaldehyde is then converted to all-trans retinol by retinol dehydrogenase (3) and moved into the retinal pigment epithelium cells (RPE) by interphotoreceptor-retinol binding protein (IRBP)(4). In the RPE it is converted to all-trans retinyl ester (5), then to 11-cis retinol (6), then to 11-cis retinyl ester (7), and finally to 11-cis retinaldehyde (8). Rpe65 is necessary for the conversion of trans-retinyl ester to 11-cis retinyl ester. IRBP transports recycled 11-cis retinaldehyde back to the photoreceptor outer segment (OS)(9). The active opsin protein is deactivated through phosphorylation by rhodopsin kinase (10) and the binding of arrestin (11). In this state the opsin protein is unreceptive to new light signals and incapable of activating any more transducin molecules. Rhodopsin is reconstituted when it binds to 11-cis retinaldehyde, this causes dephosphorylation of the opsin protein, and displacement of arrestin (1).

LRAT: lecithin:retinol acyltransferase. (Redmond *et al.*, 1998; Saari, 1992)

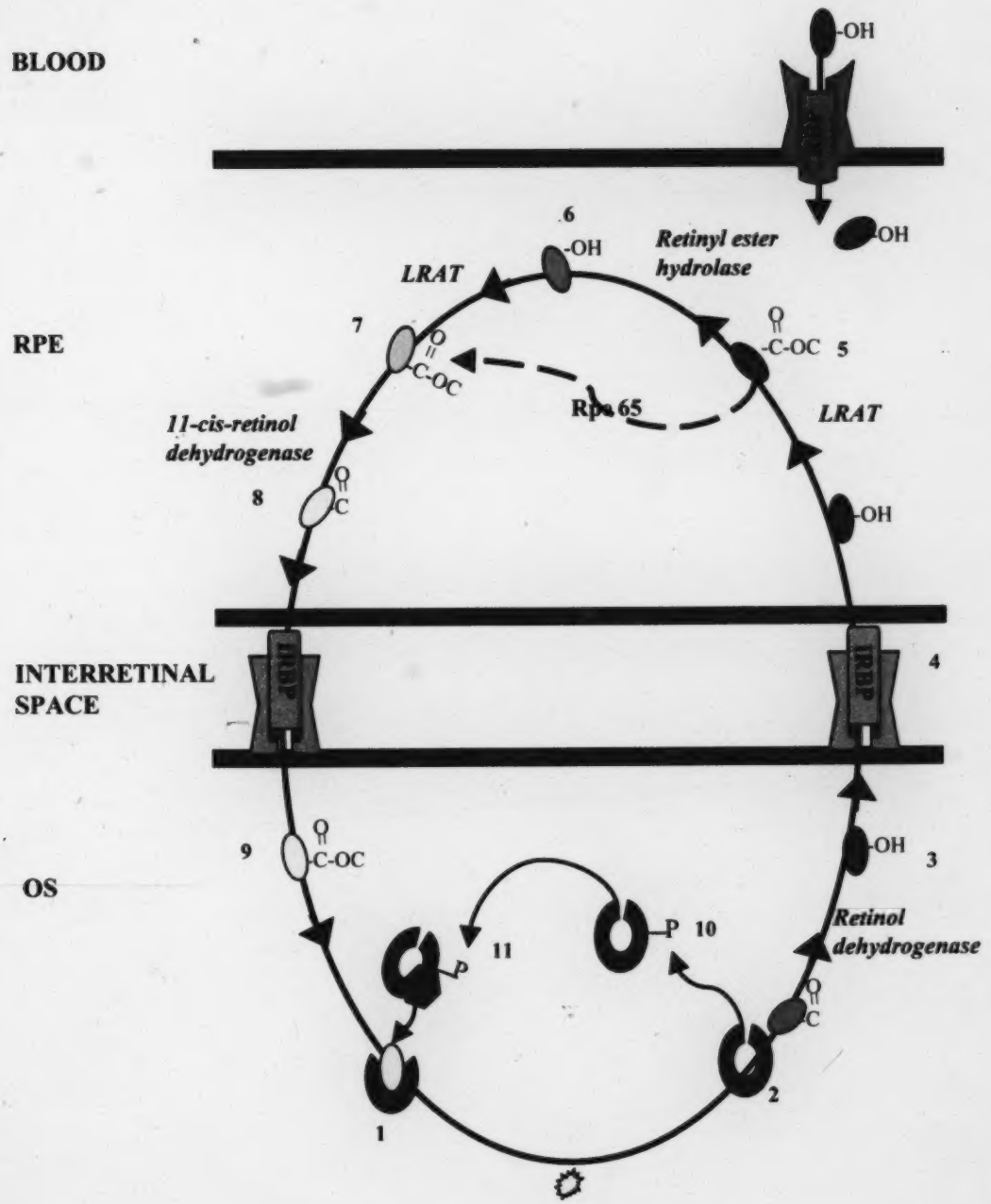
BLOOD
RPE
INTERRETINAL SPACE
OS
-OH
6
Retinyl ester hydrolase
LRAT
7
-C-OC
5
Rpe 65
11-cis-retinol dehydrogenase
8
C
LRAT
IRBP
4
9
3
P
11
10
Retinol dehydrogenase
2
1

segment (ROS) where it binds to the inactivated opsin. This binding induces the dephosporylation of the opsin and its release from arrestin. Rhodopsin is now reconstituted and again ready to absorb light. This recycling of the 11-trans retinaldehyde back to 11-cis retinaldehyde is referred to as the visual cycle.

A-2 Retinal Degenerative Diseases Given that the primary role of photoreceptor cells is to translate light impulses into electrical impulses, it is predictable that diseases affecting vision primarily involve the photoreceptor cells. The most obvious reason for the loss of vision would be the loss of photoreceptor cell function. Not surprisingly then, many of the genes identified as underlying various diseases leading to blindness are genes encoding components of the phototransduction cascade and the visual cycle or components that define the integrity of the photoreceptor cell.

There are two broad spectra of retinal degenerative diseases: diseases affecting the macular and fovea (central) region of the retina and diseases affecting the peripheral regions of the retina (figure 1-4). The former are collectively referred to as macular degenerative diseases. They include specific diseases such as Sorsby's fundus dystrophy, Stargardt macular dystrophy, Best vitelliform macular dystrophy and the heterogeneous category of age-related macular degeneration. Macular degeneration diseases are characterized by the loss
of central vision as a result of cone photoreceptor cell loss. As macular degeneration progresses rod cells also become targeted. When this occurs, patients experience loss of peripheral vision, resulting in complete vision loss. Characteristic lipofusion (oxidized lipids) deposits suggest the involvement of oxidative stress in the pathology or etiology of macular degeneration (reviewed in Zhang *et al.*, 1995). Elucidating the mechanism of macular degeneration has been hindered by the unavailability of relevant human tissue and the lack of good animal models, since only primates and birds possess a foveo-macular region.

Although animal models of peripheral retinal disease such as retinitis pigmentosa are more abundant, the mechanism underlying retinitis pigmentosa remains elusive. Retinitis pigmentosa encompasses a heterogeneous group of diseases exhibiting the opposite dystrophy pattern to macular degeneration. Retinitis pigmentosa manifests with

Figure 1-4: Human Retinae Undergoing Retinal Degeneration

A) Fundoscopic photograph of the retina of a patient with macular degeneration. The central (macular) region of the retina has degenerated while the peripheral region remains intact (Ian MacDonald).
B) Fundoscopic photograph of the retinal of a patient with retinitis pigmentosa. The reverse pattern of degeneration is observed. The macular region is intact while the peripheral region has undergone degeneration (Irene Maumenee).

A

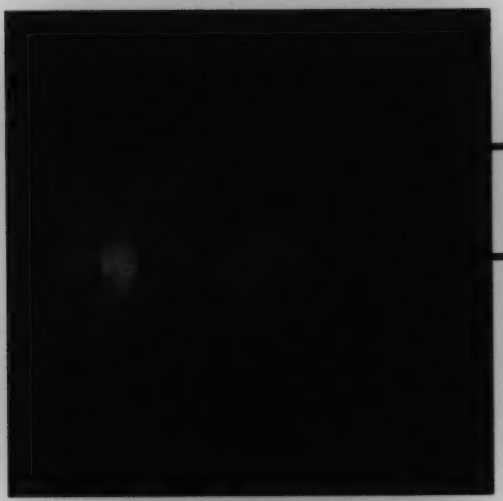

Macular Degeneration

B

Retinitis pigmentosa

a loss of night and peripheral vision as the rod cells are initially targeted for degeneration. As the disease progresses cone cell involvement is observed and results in the loss of central vision and thus complete blindness. Symptoms of retinitis pigmentosa can develop as early as infancy and correlate with the mechanism of inheritance (reviewed in Phelan *et al.*, 2000).

Despite their different pathological patterns, macular degeneration and retinitis pigmentosa can be caused by the same primary mutation (refer to table 1-1). Mutations at the ABCR and Crx loci have been implicated in both retinitis pigmentosa and macular degeneration (Rozet *et al.*, 1999; Freund *et al.*, 1998; Jacobson *et al.*, 1998; Sohocki *et al.*, 1998; Cideciyan *et al.*, 1998; Allikmets *et al.*, 1997). Such discoveries hint at the importance of the molecular environment into which these primary mutations are fixed. The effect of the retinal environment on photoreceptor cell fate is further accentuated when the expression pattern of the disease genes is considered. ABCR is expressed only in the rod photoreceptor cells but, in cases of Stargardt's dystrophy, primarily causes a dysfunction in the cone photoreceptor cells and leads to their degeneration, exemplifying the possibility that a healthy cell could be targeted for death by its mutated neighbor (Shroyer *et al.*, 1999). The above example illustrates the intricacy of the retina and the high degree of complex inter-cellular interactions that photoreceptor cells depend upon in order to function. This example also suggests that the search for disease genes cannot be confined to a search for mutations in photoreceptor cells. However, one constant remains; irregardless of in which cell the disease causing mutation originates in all cases the net effect of the primary lesion is to impair phototransduction. Mutations in rhodopsin, transducin, cGMP-PDE, and arrestin directly impede the process of phototransduction. Mutations in TIMP-3 and ABCR inhibit the visual cycle by hampering the recycling of rhodopsin. Peripherin mutations compromise the structural integrity of photoreceptor outer segments, and thus the disc membranes where phototransduction occurs (Phelan *et al.*, 2000; Dryja *et al.*, 1997). Based on these findings it is prudent to predict that any external or internal assault on the retina that induces a disruption of phototransduction could result in the death of photoreceptor cells (Wong, 1994).

Table 1-1: Summary of Known Genetic Mutations Underlying Hyman Retinal Degenerative Disease

Abbreviations: CRX: cone-rod homeobox transcription factor; TULP: Tubby like protein; ABCR:ATP binding transporter gene; RPGR: retinitis pigmentosa GTPase regulator; TIMP-3: tissue inhibitor of metalloproteinase. (reviewed in Rattner *et al.*, 1999; Phelan *et al.*, 2000)

Human Retinal Degenerative Disease	Primary Genetic Lesion (Mutated Gene)
Autosomal Dominant Retinitis Pigmentosa	Rhodopsin
	Transducin
	Peripherin
Autosomal Dominant Retinitis Pigmentosa Autosomal Dominant Cone-Rod Dystrophy	Crx
Autosomal Recessive Retinitis Pigmentosa	cGMP-Phosphodiesterase
	Rhodopsin
	Arrestin
	TULP 1
Autosomal Recessive Retinitis Pigmentosa Stargardt's Macular Degeneration	ABRC
X-Linked Retinitis Pigmentosa	RPGR
Sorby's Fundus Dystrophy	TIMP-3

B. APOPTOSIS AND RETINAL DEGENERATION

The loss of photoreceptor cells, which underlies retinal degenerative disease, occurs through apoptosis (Li *et al.*, 1995). This phenomenon is distinct from the other major process of cell loss, that of necrosis, in several fundamental ways. Necrosis usually occurs following acute injury and is a passive process resulting in the induction of an immune response and inflammation of the affected area. This leads to damage of surrounding tissue and is an undesirable and disruptive form of cell loss. Apoptosis, or programmed cell death, is a tightly controlled, genetically programmed cell death pathway. The pathway is highly regulated and can be activated by a variety of internal and external triggers. Normal development of organs and tissues, proper maturation and function of the immune system, the maintenance of checks on cell proliferation, and the elimination of harmful or non-functional cells are all dependent on the timely execution of apoptosis (Ellis *et al.*, 1991). Deregulation or improper activation of this pivotal cellular process could, therefore, have serious ramifications. Inactivation of the apoptotic pathway can lead to inappropriate proliferation of cells and result in cancer while the improper activation of the pathway could result in the elimination of healthy cells. The inappropriate activation of apoptosis is proposed to be the underlying factor in a number of degenerative diseases including Alzheimer's, Parkinson's, and Huntington's disease (reviewed in Honig *et al.*, 2000).

Apoptotic cells can be identified 1) morphologically, 2) through the detection of DNA fragmentation ladders, and 3) through the use of terminal UTP-biotin nick end labeling (TUNEL) (figure 1-5). Nuclear condensation (appearance of pyknotic nuclei), inter-cellular junction degradation, by means of extracellular matrix remodeling, and fragmentation of the cell to form apoptotic bodies comprise the series of morphologically detectable events that characterize apoptosis (Bursch *et al.*, 1990). Prior to the appearance of these morphological changes, the DNA of the apoptotic cell is cleaved into large 300,000 to 600,000 bp fragments (Bursch *et al.*, 1990). These fragments are then further cleaved to fragments that are 180 bp or multiples of 180 bp in length, representing inter-nucleosome cleavage (Bursch *et al.*, 1990). When subjected to electrophoresis on an agarose gel this fragmented DNA can be visualized as a DNA fragmentation ladder, with 180 bp steps. TUNEL is an alternative method for the detection of fragmented

Figure 1-5: Methods Used for the Detection of Apoptotic Cells

A) Morphological characteristics of nuclear condensation and cell shrinkage.
B) Example of cells exhibiting a positive terminal UTP-biotin nick end labeling (TUNEL) signal.
C) Example of a DNA fragmentation ladder with 180 bp steps .
(photographs courtesy of Dr. Sylvia Smith, Dr. Sue Gentleman, Dr. Paul Wong)

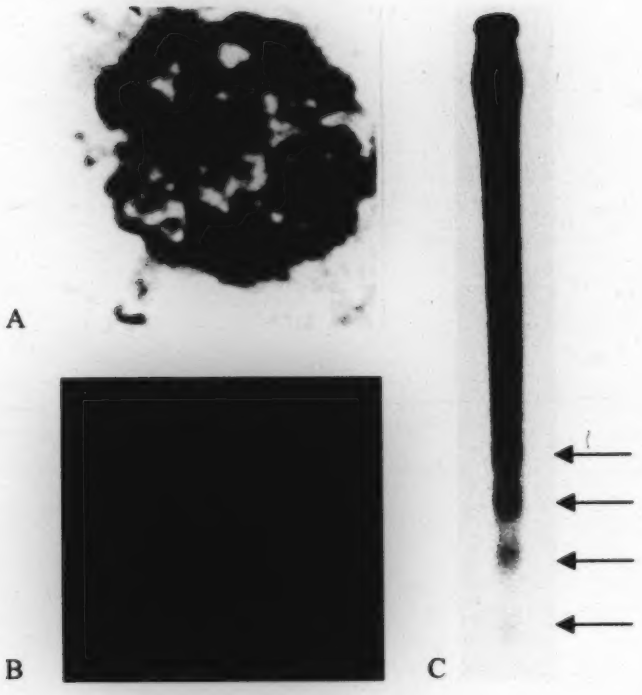
A
B
C

DNA. It allows for the detection of individual apoptotic cells by labelling all 3' DNA ends in the nucleus. Therefore, during the early stages of apoptosis when the DNA of the cell is initially being cleaved all of the resulting 3' ends will be labeled and the cell will emit a positive TUNEL signal.

Apoptosis is a highly diverse phenomenon. A large variety of triggers are able to initiate the apoptotic program, in each case the factors involved in the regulation and execution of the program can differ. Cell type, developmental stage, time of day, extracellular and intracellular environments are all factors which determine what triggers are able to induce apoptosis, which factors are involved in executing apoptosis, and how the initiation and execution of apoptosis
is regulated (Sachs *et al.*, 2000; Maslim *et al.*, 1997; Colombo *et al.*, 2000; Ruifrok *et al.* 1998; Organisciak *et al.*; 2000; Ryan *et al.*, 2000). Apoptosis may require the *de novo* synthesis of proteins, or could require the activation or deactivation of existing molecules, it may also require a change in a molecule's function (Oppenheim *et al.*, 1990; Marti *et al.*, 1998; Li *et al.*, 1995A). Details such as these remain elusive in the case of photoreceptor cell apoptosis. How the apoptotic program is regulated and executed or altered in response to the initial assault on the photoreceptor cell remains to be determined.

C. GENETIC MODELS OF RETINAL DEGENERATIVE DISEASE

Studying the progression of retinal degeneration is impossible in human patients due to the inability to obtain relevant tissue. To overcome this difficulty several animal model systems of retinal degenerative diseases, such as retinitis pigmentosa, have been established (table 1-2). The large degree of heterogeneity with respect to the genetic lesion underlying retinal degeneration in these model systems parallels the heterogeneity observed in human cases of retinal degeneration. Furthermore, despite the variety of primary genetic lesions represented in these model systems, cell loss has been demonstrated, through TUNEL staining, DNA ladder detection, and morphological analysis, to occur via apoptosis in each model examined (Portera-Cailliau *et al.* 1994, Chang *et al.* 1993; Smith *et al.*, 1995; Weiss *et al.*, 1995). This mirrors observations

Table 1-2: Summary of Animal Models of Human Retinal Degeneration

The mutated genes underlying retinal degeneration in animal models can be divided into five categories based on function. In most instances transgenic animals have been used in these models (indicated as transgenic), however, naturally occurring mutations have also been observed. Disease genes for all human retinal degenerative diseases have not yet been identified. Thus, there are instances of animal models with known genetic lesions which have not yet been mirrored in the human condition. Another interesting observation is that not all disease genes are expressed in the degenerating cells (i.e. rod or cone photoreceptor cells).
Abbreviations: ADRP: autosomal dominant retinitis pigmentosa; ARRP: autosomal recessive retinitis pigmentosa; CSNB: congenital stationary night blindness; CNG3: cyclic nucleotide-gated channel 3; ABCR: ATP binding transporter gene; NRL: neural retina leucine zipper; CRX: cone-rod homeobox transcription factor; rd: retinal degeneration; rds: retinal degeneration slow; TIMP-3: tissue inhibitor of metalloproteinase; RCS: Royal Collage of Surgeons; GC1:guanylate cyclase type 1; Mertkz: receptor tyrosine kinase gene.
(Biel *et al.*, 1999; Gal *et al.*, 2000; Morimura *et al.*, 1998; reviewed in Rattner *et al.*, 1999; Phelan *et al.*, 2000; Hafezi *et al.*, 2000)

	Mutated Gene	Animal Model	Human Disease	Expression in Affected Cells
Transducton Pathway	rhodopsin	Rat (Fisher 344)	ADRP, ARRP	yes
		Transgenic: rat, mouse, pig		
	γ -phosphodiesterase	Transgenic: mouse		yes
	ß-phosphodiesterase	rd mouse		yes
	transducin		AD, CSNB	yes
	arrestin	Transgenic: mouse	ARRP, Oguchi Disease	yes
	rhodopsin kinase	Transgenic: mouse		yes
	CNG3	Transgenic: mouse		yes
	Cyclic nucleotide gated channel		ARRP	yes
Visual Cycle	ABCR	Transgenic: mouse	ARRP, Stargardt's	no
	IRBP	Transgenic: mouse		yes
	Rpe65	Dog (Swedish briard)	ARRP Rod-cone dystrophy Leber congenital amaurosis	no
		Transgenic: mouse		
Transcription Factors	Microphthalmia gene	Vitiligo mouse		
	NRL		ADRP	yes
	CRX		ADRP, AD cone-rod dystrophy	yes
Structural & Maintenance	peripherin	rds mouse	ADRP, macular dystrophies	yes
		Transgenic: mouse		
	TIMP-3		Sorby fundus dystrophy	no
	GC1	Chicken (Rhode Island Red)		yes
	Mertkz	RCS rat Abyssinian cat Dog		no
Unknown function	Tub	Tubby mouse		yes

made in retinitis pigmentosa patients that, irrespective of the primary genetic lesion, photoreceptor cells are eliminated by means of apoptosis. The importance of molecular environment and cell:cell interactions in the pathology of retinal degenerative disease is illustrated by the fact that in several models the mutated gene is not expressed in the affected cells. The greatest limitation in using the animal models available to study human retinal degeneration is that they are predominantly in non-primate animals that lack a macula. The use of such models to study macular degenerative diseases is, therefore, seldom appropriate.

D. INDUCED MODELS OF RETINAL DEGENERATION

In 1966, Werner K. Noell *et al.* demonstrated that light could induce the degeneration of photoreceptor cells in healthy rat retinae. Since then many models of LIRD have appeared. The differences between these models are the wavelength and intensity of light and the species of rat used. These types of alterations appear to have an effect on the mechanism and rate by which photoreceptor cells apoptose.

Noell *et al.* (1966) discovered that exposing albino rats with wild type photoreceptor cells to green light for 24 h causes a reduction in the amplitude of ERG signal (a test used to evaluate the function of photoreceptor cells), which correlated with the disorganization and degeneration of the outer nuclear layer and rhodopsin bleaching. Damage caused by this exposure is cumulative and, once initiated, the damage progresses in the absence of light. Furthermore, exposure to red light, which cannot be absorbed by rat rod photoreceptor cells, unlike green light that is absorbed by rat rod photoreceptors (by rhodopsin), has no adverse effect on the retina (Noell *et al.*, 1966; Morrow *et al.* 1999). Taken together, these results suggest that the ability of green light to cause retinal degeneration is due to its absorption by rhodopsin. Further evidence of the involvement of rhodopsin in the degenerative process comes with the observation that rats reared in constant darkness are more susceptible to light damage than cyclic light-reared (12 h light, 12 h dark cycle) animals. Dark-reared rats have more rhodopsin protein and more tightly packed rhodopsin molecules in their outer segment discs than do cyclic light-reared animals (Noell *et al.*, 1966; Organisciak *et al.*, 1998). If the potential of green light to induce retinal degeneration is dependent on interactions between photons and

rhodopsin, it follows that higher levels of rhodopsin in a cell will cause it to be more vulnerable to light-induced damage. Hence, dark-reared rats should be more susceptible to light damage. The discovery that damage initiated by light exposure could continue in the absence of light suggests that absorption of photons by rhodopsin may begin a sequence of light independent reactions that eventually lead to the death of rod and cone photoreceptor cells (Organisciak *et al.*, 1995). The loss of both cone and rod photoreceptor cells, even though rhodopsin is a rod photoreceptor cell specific protein, suggests that cell:cell signaling is involved in the definitive degeneration process. This observation parallels the documented progress of human retinitis pigmentosa in which the initial loss of rod photoreceptor cells is followed by a loss of cone photoreceptor cells.

Three hypotheses on how light exposure leads to retinal degeneration were initially postulated (Noell *et al*, 1966). The first hypothesis stipulates that the action of light on natural pigment will convert the pigment into a catalyst. In this state the pigment will catalyze reactions between an activated substrate and a free oxygen species, yielding peroxide. These peroxides, and other free radical species, can cause damage to DNA, proteins, and lipids. The second hypothesis is founded upon the observation that O_2 consumption in the retina decreased in response to steady light exposure. This could be attributed to a metabolic change, possibly involving a metabolite involved in intracellular membrane function control. However, the rapid rate at which histological changes observed in response to light treatment occur argue against this proposed mechanism of action. The third hypothesis proposes that accumulation of toxic photoproducts could induce degeneration by tipping the balance between DNA damage and DNA repair toward DNA damage. Vitamin A was suggested as such a toxic photoproduct. Even a small amount of vitamin A causes mitochondrial swelling and induces the release of proteolytic enzymes from isolated lysosomes (Noell *et al.*, 1971; Dingle, 1963; Lucy *et al.*, 1963). However, the majority of vitamin A in photoreceptor cells after rhodopsin bleaching is in the esterified form, a form that is unable to cause the effects described above.

D-1 Dissecting the Rat LIRD Model The extent and rate of retinal degeneration can be precisely manipulated in the LIRD model. This is advantageous because it allows for the

dissection of the degenerative process, something that cannot be accomplished using the genetic retinal degeneration models. Dissection of the degenerative process is possible due to the ease with which variables, such as light intensity, duration of light exposure, or animal body temperature, can be altered to effect a change in the rate and degree of retinal degeneration (Noell *et al.*, 1966; Organisciak *et al.*, 1998, Organisciak *et al.*, 1994). By using green light (490 nm- 580 nm) at an intensity of 1500 lux and manipulating the duration of light exposure, a predictable and reproducible degenerative profile of LIRD in rats has been produced. This profile is composed of four discrete phases: 1) commitment, 2) execution, 3) stress response, and 4) recovery. This division is primarily founded on the expression of three marker genes: interphotoreceptor retinoid-binding protein (IRBP), heme oxygenase-1 (HO-1), and clusterin (Wong *et al.*, 1995) (figure 1-6). IRBP is a gene normally expressed in functioning photoreceptor cells (refers to figure 1-3). Therefore, it serves as a marker for the presence of functional photoreceptor cells (Nickerson *et al.* 1998). The heat shock protein HO-1 is induced as part of the oxidative stress response (Kutty *et al.* 1985; Le *et al.* 1999). Hence, its induction in the LIRD model is indicative of an oxidative stress environment in the retina. Clusterin is proposed to be involved in the aftermath of apoptosis, potentially in the clean up of apoptotic bodies and lipids. Clusterin is used as a marker of recovery, or of a post-apoptotic environment (Wong *et al.*, 1994).

A 4 h exposure to 1500 lux green (490-580 nm) light causes a decrease in the levels of IRBP mRNA detected in the rat retina. This light treatment and marker gene expression pattern define the Commitment Phase of retinal degeneration. This degree of light assault on the retina is hypothesized to result in a change in the molecular phenotype of the neural retina, specifically of the rod photoreceptor cells. This altered molecular environment is representative of the priming of rod photoreceptor cells to initiate the apoptotic program. However, the Commitment Phase does not mark the initiation of the apoptotic program. DNA fragmentation ladders are not detected following 4 h of light treatment. However, examination of 4 h light-treated retinae following a two week period of recovery under dark conditions reveals that 80% of the photoreceptor cells are lost (Darrow *et al.*, 1997). This suggests that a 4 h light treatment is sufficient to commit the photoreceptor cells to an apoptotic fate. It also demonstrates that following the initial

Figure 1-6: Stages of LIRD

The rat LIRD model of human retinal degeneration was divided into four discrete phases based on the expression pattern of three marker genes: interphotorecptor retinoid-binding protein (IRBP), heme oxygenase-1 (HO-1), and clusterin. IRBP is a marker for photoreceptor cell function, HO-1 is a marker for an oxidative stress environment, and clusterin is a marker for a post apoptotic environment. Each of the four phases of LIRD are induced by a specific length of exposure to green (490-580 nm) light (1500 lux). The commitment phase is induced by a 4 hour light exposure, the execution phase is induced by a 8 hour light exposure, a 16 hour light exposure induces an oxidative stress phase and a 12 hour light exposure following a 24 hour recovery period under dark conditions induced the recovery phase (Wong *et al.*,1995).

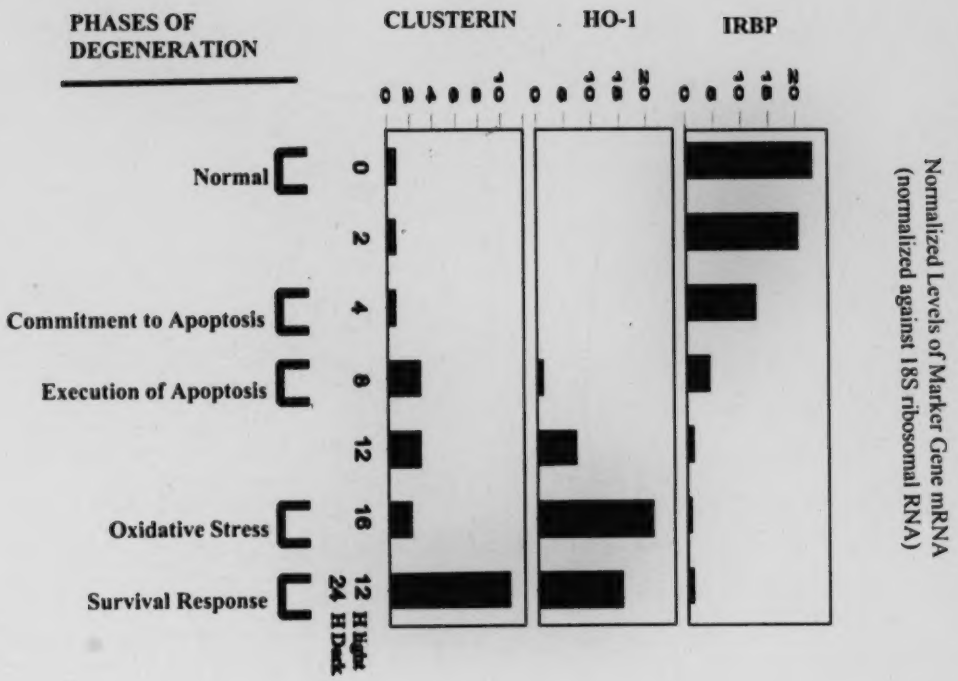
PHASES OF DEGENERATION
CLUSTERIN
HO-1
IRBP
Normal
Commitment to Apoptosis
Execution of Apoptosis
Oxidative Stress
Survival Response
0
2
4
8
12
16
12 H Light
24 H Dark
Normalized Levels of Marker Gene mRNA
(normalized against 18S ribosomal RNA)

light dependent trigger event, the mechanism underlying LIRD is light independent. The 4 h light treatment marks an unique opportunity to glimpse the transitional point between trigger (light) and response (apoptosis or survival).

An 8 h light treatment is marked by a further decrease in IRBP mRNA levels, and an increase in HO-1 and clusterin mRNA levels. The substantial decrease in IRBP suggests that normal photoreceptor cells are disappearing at this stage of the process. The slight increase in HO-1 transcription also indicates that this apoptotic environment has an element of oxidative stress. The 8 h light treatment is also the minimal light treatment required to induce the immediate appearance of a DNA fragment ladder. Thus, the 8 h treatment is hypothesized to represent the execution phase of retinal degeneration, a time of active photoreceptor cell death.

A 16 h light treatment results in the loss of detectable IRBP expression, a peak in HO-1 mRNA levels and relatively unaltered (compared to 8h treatment) clusterin mRNA levels. The high HO-1 mRNA levels suggest that the retina is responding to a peak oxidative stress environment. Hence, this phase is hypothesized to define the stress response phase of LIRD.

The last phase of LIRD, designated the recovery phase, is produced by subjecting the rat retinae to a 12 h light treatment followed by a 24 h recovery period in the dark. At this phase there is minimal expression of IRBP, decreased but still high level of HO-1 mRNA and a peak in clusterin mRNA levels. The minimal IRBP expression signifies that the majority of photoreceptor cells have been lost but that some remain and are functioning. The decrease in HO-1 mRNA levels suggest the recession of oxidative stress, while the high levels of clusterin expression suggest a response by the surviving retinal cells to the loss of the photoreceptor cell population.

D-2 Apoptosis in Light Induced Retinal Degeneration Evidence of apoptotic photoreceptor cells in the LIRD model has been obtained using morphological, and DNA ladder detection methods. As in human retinitis pigmentosa, rod photoreceptors are the primary targets of light induced degeneration (Cicerone, 1976; Kuwabara et al 1976; LaVail 1976), and the initial loss of rod photoreceptors is followed by the loss of cone photoreceptors. Also in the LIRD model, as in human retinal degeneration, the

photoreceptor cells develop normally and function normally until apoptosis is initiated. In most genetic models of retinal degeneration the primary genetic lesion interferes with normal photoreceptor cell development. This poses a problem since normal retinal development, including photoreceptor cell development, is dependent on apoptosis (Cohen, 1992). The overlap between developmentally programmed photoreceptor apoptosis and apoptosis induced by genetic lesions could create a unique degeneration process, one that may not necessarily be caused purely by the genetic lesion itself. If the overlap is not actually altering the effects of the primary lesion, the presence of regulating elements for both the appropriate and inappropriate apoptotic programs could make the task of identifying the role of molecules more difficult. Furthermore, the developmental stage of a cell can have an affect on the triggers that are able to induce apoptosis and perhaps even on the method by which apoptosis is executed (Diaz *et al.*, 1999). Thus to elucidate the mechanism of retinal degeneration, mature photoreceptor cells should be studied.

The *en mass* loss of rod photoreceptors caused by light exposure is extremely helpful in the search for the mechanism of retinal degeneration. Such a synchronized and large loss of cells indicates a synchronized and drastic change in the retina's molecular environment, both intracellular and extracellular. Effectively, this serves as an amplification of the degenerative mechanism to levels that can be detected by molecular biology techniques.

D-3 A Possible Trigger for LIRD: A Model for Retinitis Pigmentosa Rhodopsin mutations, or mutations in phototransduction, are responsible for a significant portion of retinitis pigmentosa cases (refer to table 1-1). Effects of light exposure on the retina could be mimicking the effects of such mutations (Noell *et al.*, 1966; Wong, 1994A; Grimm *et al* 2000). As stated earlier, one of the first clues that the absorption of photons by rhodopsin is the trigger for LIRD was the observation that dark-reared rats, which have large amounts of rhodopsin tightly packed in their outer segments, are more susceptible to light damage than cyclic reared rats, whose rhodopsin levels are lower (Organisciak *et al.*,1994, 1998, Penn *et al.*,1987). Further evidence for rhodopsin's role in LIRD comes from experiments with Rpe 65-deficient and Rho -/- mice (Grimm *et al.*,

2000). Both mouse mutants are devoid of rhodopsin. Rpe 65 is a protein expressed in the retinal pigment epithelium (RPE) cells and is necessary for production of 11-cis-retinyl esters and thus for the recycling of vitamin A (Redmond *et al.*, 1998; refer to figure 1-3). Rho -/- mice contain a mutation in their rhodopsin encoding gene which prevents the expression of the rhodopsin protein. Thus, Rpe 65-deficient mice lack the ability to regenerate rhodopsin once it has been bleached by light, while Rho -/- mice do not express rhodopsin's opsin protein, thus also preventing formation of rhodopsin. In both cases these mutations afford the animals protection from light induced degeneration. This suggests that the absorption of light by rhodopsin is responsible for the initiation of photoreceptor cell degeneration in the LIRD model. In our LIRD model the wavelength of light used to induce degeneration, green light (490-580 nm), is absorbed specifically by rhodopsin. Thus in our LIRD model, light exposure causes a malfunctioning of rhodopsin. This could translate into a malfunctioning of the phototransduction pathway and result in an impaired photoreceptor cell, which then becomes committed to apoptosis.

D-4 LIRD and Oxidative Stress: A model for macular degeneration Lipofuscin, the accumulation of oxygen-damaged lipids, is characteristic of macular degeneration (Organisciak *et al.*, 1999, 1996; Adler *et al.*, 1999). This type of lipid damage is indicative of an environment under oxidative stress. Light exposure induces an oxidative stress environment in the LIRD model. The induction in HO-1 expression is evidence for this phenomenon. HO-1 is known to be responsible for the degradation of heme via an alpha-meso bridge-specific cleavage. HO-1 is induced in response to oxidative stress and protects against oxidative damage, although how it affords this protection is unknown (Maines, 1992; Stocker, 1990; Kutty *et al.*, 1995; Chen *et al.*, 2000). Induction of HO-1 gene expression occurs during the stress response phase of LIRD (refer to figure 1-6). Treatment of rats with anti-oxidants such as dimethylthiourea (DMTU) and ascorbic acid prior to light exposure protects against photoreceptor cell loss (Organisciak *et al.* 1992, 1995, 1999; Spect *et al.*, 1999) and damage to polyunsaturated fatty acids (Wiegand *et al.*, 1983). Since this type of oxidative damage is observed in macular degeneration (Cai *et al.*, 2000; Nicolas *et al.*, 1996), it is possible that, as in LIRD, oxidative stress also causes or mediates the loss of photoreceptor cells in macular degeneration. Thus,

understanding how oxidative damage occurs, and how the oxidative stress environment is contributing to the loss of photoreceptor cells could aid in unraveling mechanisms underlying macular degeneration and retinitis pigmentosa.

E. GENE EXPRESSION: CLUES TO THE MECHANISM OF RETINAL DEGENERATION

The ability of one mutation to cause two opposite patterns of degeneration, peripheral to central (retinitis pigmentosa), and central to peripheral (macular degeneration), suggests that a model for the mechanism(s) of one degenerative pattern could also serve as a model for those underlying the other. The approach taken toward understanding the mechanism underlying retinal degeneration in the LIRD model of retinal degeneration was to determine the changes in gene expression over the course of degeneration. These changes are hypothesized to constitute a response to the light exposure, induction of rod photoreceptor specific apoptosis, and the execution of an apoptotic program. This thesis focuses on the response of the retina to a 4 h light exposure, an exposure that induces the Commitment Phase, the time point at which the cells are primed to undergo apoptosis. The changes in retinal gene expression that occur as a consequence of this 4 h light exposure are hypothesized to reflect the immediate response of the cell to this adverse external assault and the initial events necessary for inducing the apoptotic pathway.

Photoreceptor cells are primed for apoptosis during the Commitment Phase, while other retinal cells are positioned to survive. Thus, the relaying of two types of signals is envisioned to be taking place at this time: signals that transmit the extent and nature of the assault and signals that initiate the appropriate cellular response. Therefore, it is expected that the expression of signal pathway related genes, including genes encoding transcription factors, or any gene whose product is involved in regulation, should be altered in response to light exposure. The role of these factors would be expected to be "long term", meaning that they would be responsible for the commitment of cells to the apoptotic program but would not necessarily be involved in the execution of this program. Signal pathways associated with survival as well as immediate stress response genes would also be expected to be active during the Commitment Phase.

To identify genes whose expression is altered by 4 h of light exposure, a Commitment Phase (4 h light treatment) cDNA library was differentially cross-screened (described in Chapter 3 and 4). A large proportion of the genes identified in this manner were found to encode ribosomal proteins. This is an unexpected but interesting finding (see Chapter 6). Another group of genes whose expression was identified as changing in response to 4 h light treatment were those of transcription factor encoding genes. The details of the preliminary characterization of their role in LIRD is presented in Chapter 5. The results in this thesis provide a framework from which the direction of future experiments can be developed. They provide clues as to what pathways are altered in response to light treatment and what factors could be participating in the degeneration process.

CHAPTER 2
MATERIALS AND METHODS

A. SAMPLES

Albino Sprague-Dawley rats were used for these experiments. The rats were divided into 5 treatment groups, including the control treatment group. All rats were reared under dark conditions until they were 61 days old. At 61 days of age the rats were exposed, for various lengths of time, to 1500 lux green (490-580 nm) light. The treatment groups consisted of rats exposed to 4 h, 8 h, 16 h or 12 h of light. The rat retinae were enucleated immediately after light treatment with the exception of the 12 h light treatment group. The retinae of these rats were not enucleated until after a 24 h recovery period under dark conditions. The control treatment group's retinae were enucleated at 61 days of age without ever having been exposed to intense light. All light treatments were performed in the Organisciak lab (D.T. Organisciak, Wright State University, Dayton, Ohio). The recovered retinae were flash frozen on dry ice and stored at -70^0C. A minimum of five animals were used per treatment group. Northern profiles of rat prostates during regression were obtained from Dr. M. Tenniswood (University of Notre Dame, Southbend, Indiana).

B. ISOLATION OF RNA

B-1 Isolation of total RNA Total RNA was extracted from the retinae of the above treatment groups using the standard RNazol method (Chomczynski *et al.*, 1987). Approximately 10 retinae were used to generate the total RNA needed to synthesize cDNA for use as probe, to construct the cDNA library and to produce the necessary Northern blots. The retinal tissue was homogenized using a Polytron and 1 mL of RNazol B (Tel -Test Inc. Friendswood, Texas). After homogenization, another 1 mL of RNazol B together with 200 μL of chloroform were added to the sample. The sample was shaken vigorously and placed on wet ice for a minimum of 15 minutes in order to ensure that the RNases remained inactive and to allow the phenol contained in the RNazol B and chloroform to separate the proteins. Centrifugation of the sample resulted in the separation of the protein, DNA, and RNA into different phases. Proteins settle in the organic phase, DNA at the interphase (because RNazol B destroys DNA's hydrophilic interactions) and RNA in the aqueous phase (due to RNazol B's promotion of RNA-guanidinium and water molecule complexes). The aqueous layer, containing RNA, was

isolated and an equal volume of isoproponal was added in order to precipitate RNA overnight at -20^0C. Following a 15 minute centrifugation at 4^0C the RNA pellet was washed with 70% cold ethanol and re-suspended in a maximum of 50 µL of DEPC treated water. The RNA was then flash frozen on dry ice and stored at -70^0C.

To assay the integrity of the extracted RNA, 3 µL of each RNA sample was run on a formaldehyde 1% agarose gel. The RNA was verified as undegraded by observing the crispness of the 18S and 28S ribosomal bands on the formaldehyde gel (detailed in sections E-1.11 and E-1.12).

B-2 Isolation of mRNA Poly (A) mRNA was isolated form total RNA using the Oligotex mRNA mini kit (Qiagen, Mississauga, Ontario). Isolation of mRNA from tRNA and rRNA increases cloning efficiency of mRNA. According to the protocol (supplied in the kit), total RNA was incubated at 65°C for 3 minutes to denature any secondary structures. The RNA was then incubated at room temperature with an oligo dT_{30} primer linked to latex particles. This allowed for the oligo dT_{30} to bind to the mRNA's poly A tail. The mixture was centrifuged, causing the latex bound mRNA to pellet. Once the mRNA pellet was washed it was transferred to a spin column. The latex particles linked to the mRNA through the oligo dT_{30} bind to the column, thus, upon centrifugation, RNA that lacks a poly A tail and does not bind the oligo dT_{30}, flows through the column. To elute the mRNA from the column the salt concentration was decreased, causing the mRNA to dissociate from the oligo dT_{30} and flow through the column. The mRNA was quantified on an ethidium bromide agarose plate.

C. CONSTRUCTION OF THE COMMITMENT PHASE cDNA LIBRARY

The Stratagene ZAP cDNA synthesis and ZAP cDNA Gigapack III Gold Cloning kits were used in the construction of the rat retina Commitment Phase (4 h light treated) cDNA library (Stratagene, LaJolla CA.). The procedure is depicted in figure 2-1. All reaction buffers, enzymes, primers, and vector were provided with the ZAP cDNA Gigapack III Gold Cloning kit and all were used at volumes and concentrations described in the manufacturers' protocols.

Figure 2-1: Schematic Depiction of cDNA Library Synthesis

C-5* size fractionation not shown on diagram.

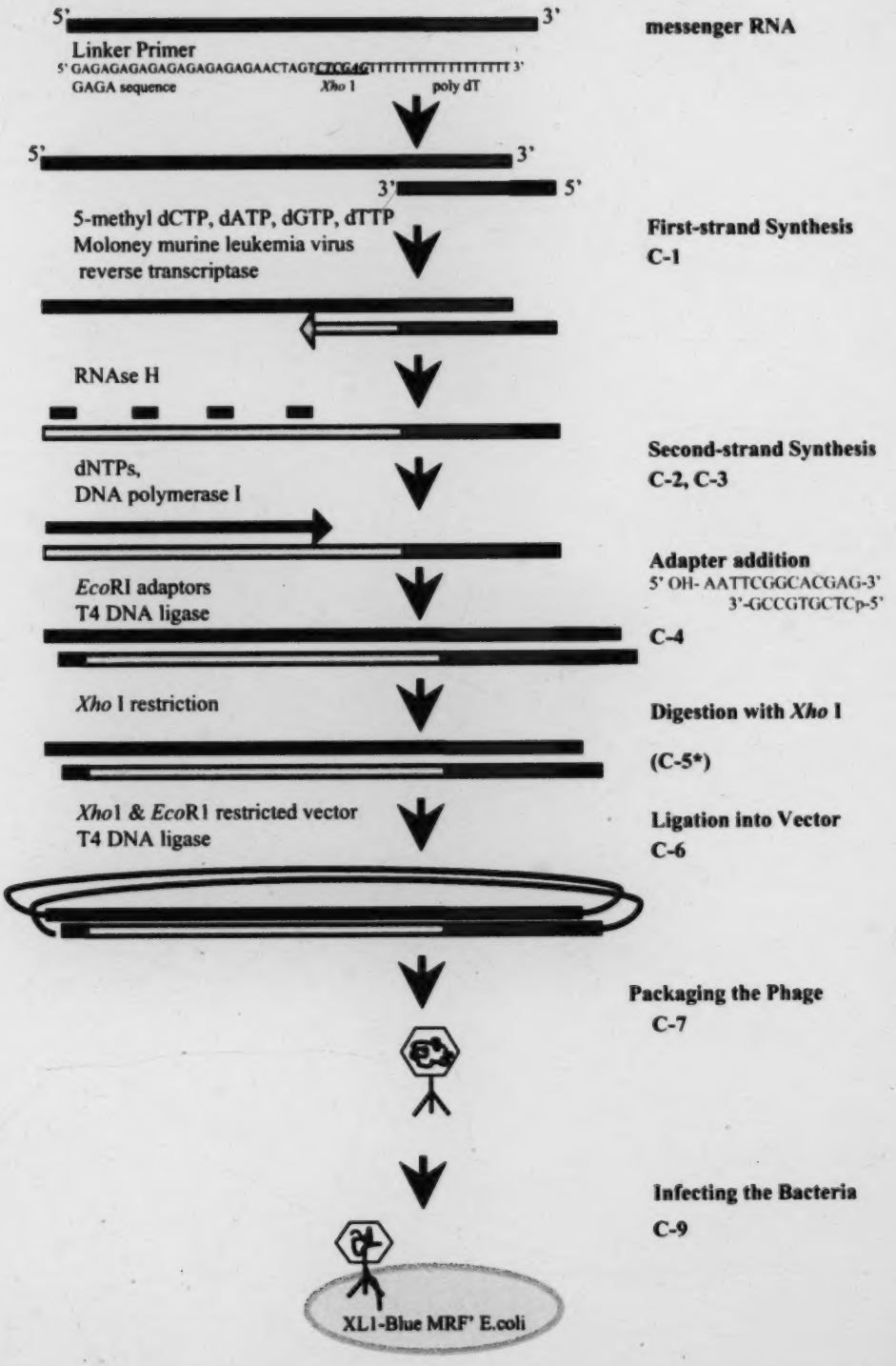
5'
3'
messenger RNA
Linker Primer
5' GAGAGAGAGAGAGAGAGAACTAGTCTCGAGTTTTTTTTTTTTTTTT 3'
GAGA sequence
Xho I
poly dT
5'
3'
3'
5'
5-methyl dCTP, dATP, dGTP, dTTP
Moloney murine leukemia virus
reverse transcriptase
First-strand Synthesis
C-1
RNAse H
dNTPs,
DNA polymerase I
Second-strand Synthesis
C-2, C-3
EcoRI adaptors
T4 DNA ligase
Adapter addition
5' OH- AATTCGGCACGAG-3'
3'-GCCGTGCTCp-5'
C-4
Xho I restriction
Digestion with Xho I
(C-5*)
Xho1 & EcoR1 restricted vector
T4 DNA ligase
Ligation into Vector
C-6
Packaging the Phage
C-7
Infecting the Bacteria
C-9
XL1-Blue MRF' E.coli

C-1 First Strand cDNA Synthesis The first strand of cDNA was synthesized from purified mRNA using Moloney-Murine leukemia virus reverse transcriptase (MMLV-RT) and a 50 base pair, linker primer containing the *Xho*1 restriction endonuclease recognition site and a poly dT region. RNAse H was added to the first strand reaction mix in order to degrade the mRNA template, thus leaving the first strand of cDNA.

C-2 Second Strand cDNA Synthesis The digested fragments of mRNA generated by RNAse H served as primers for DNA polymerase I in the synthesis of the second strand of cDNA. [α^{32}P] dATP (800 Ci/mmol) is used in the reaction as a marker so that cDNA can be detected when it is run through a sepharose column for size fractionation purposes.

C-3 Blunting the cDNA Termini Pfu DNA polymerase was used to produce blunt ended cDNAs from C-2. This was done so that the *Eco*R1 adapters could later be ligated to these blunt ends.

C-4 Ligating *Eco*R1 Adapters *Eco*R1 adapters were ligated to both the 5' and 3' blunt ends of the newly synthesized cDNA. The adapters were 9- and 13- mer oligonucleotides containing the *Eco*R1 recognition site. These adapters allow for the addition of a second restriction enzyme site and thus for directional cloning of the cDNA. The cDNA was then digested with *Xho*1 so as to leave an *Eco*R1 site at the 3' end and a *Xho*1 site at the 5' end. This facilitated the directional cloning of the cDNA fragments into the Uni-ZAP XR vector.

C-5 Size Fractionation of the cDNA Size fractionation was accomplished using a drip column filled with Sepharose CL-2B gel filtration medium. This was performed to separate full length cDNAs from smaller, partial, cDNA fragments and *Eco*R1 adapters released by *Xho*1 digestion. The drip columns were assembled with a 1 mL sterile pipette and 10 mL syringe. The cDNA was extracted from the fractions with phenol-chloroform and precipitated using cold 100% ethanol.

C-6 Ligating cDNA into the Uni-ZAP XR vector The Uni-ZAP XR vector can accommodate DNA inserts up to 10 kb. The vector is double digested with *Eco*R1 and *Xho*1 to facilitate the directional cloning of the cDNA. The site at which the cDNA is inserted is flanked by T3 and T7 promoter sequences, thus allowing for PCR amplification of the inserted cDNA fragment using T7 and T3 primers (figure 2-2) (BioServe, MD).

The size fractioned cDNA was ligated into the Uni-ZAP XR vector using T4 DNA ligase (2 day incubation at 4^0C). The cDNA fragments are ligated into the vector such that the poly (A) tail is next to the T3 primer site.

C-7 Packaging the Phage The packaging extract (Gigapack III Gold) used to package the phage contained all of the proteins coded for by the phage and usually synthesized using the host bacteria's transcriptional and translational machinery. This step is necessary for the generation of recombinant phage capable of infecting the host bacteria.

C-8 Preparation of the Host Bacteria and Titering of the Library The host bacteria strain used was the RecA$^-$ *E. coli* XL1-Blue MRF'. The bacterial cells were grown in LB broth supplemented with 0.2% (w/v) maltose and 10mM $MgSO_4$ to an OD_{600} of 1.0, usually overnight at 30^0C in a shaking incubator. The bacterial cells were spun down at 2800 rpm, and resuspended in 10 mM $MgSO_4$ (to an OD_{600} of 1.0). To determine the titer of the library 200 µL of this bacterial culture was infected with either 4:1 or 1:1 dilution of the Commitment Phase (4 h light treatment) cDNA library (the packaged phage). The bacterial cells and phage were left at room temperature for 5 minutes and then incubated at 37^0C for 15 minutes. The infected bacteria were then added to 15 mL of NZY top agar (50^0C) and poured onto NZY plates (137 mm diameter). The plates were left to incubate overnight at 37^0C. The number of plaques on each plate was counted to determine the titer of the cDNA library.

D. SCREENING OF THE COMMITMENT PHASE cDNA LIBRARY

D-1 Primary Commitment Phase cDNA Library Screen (figure 2-3A) 2 µL of the packaged phage from the Commitment Phase cDNA library were used to infect 200 µL

Figure 2-2: Lambda Uni-ZAP XR

A. Schematic of lambda Uni-ZAP XR vector used in Commitment Phase cDNA library synthesis.

B. A schematic of the multiple cloning site and T7, T3 primer sites. (Adapted from the Stratagene ZAP cDNA synthesis and ZAP cDNA Gigapack III Gold Cloning kit manuals).

A

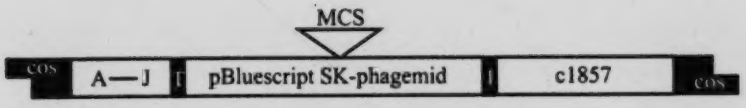
MCS
cos
A—J
pBluescript SK-phagemid
c1857
cos

B

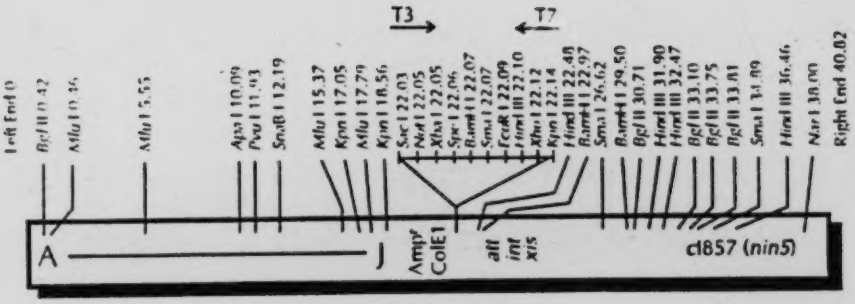
T3
T7
Left End 0
Right End 40.02
A
J
Amp'
ColE1
att
int
xis
c1857 (nin5)

Figure 2-3: Schematic Depiction of the Commitment Phase cDNA Library Differential Cross-Screen

A) Primary Differential Cross-Screen

B) Secondary Differential Cross-Screen

C) Tertiary Screen Differential Cross-Screen

A.

1° Screen

2ul of packaged phage from the 4 hour library are used to infect 200ul of E.coli bacterial cells

The infected bacterial cells were plated out on NZY plates and incubated overnight at 37°C. Approximately 1000 plaques were detected per plate.

Duplicate plaque lifts were taken from each plate. Asymmetric notches and pin holes were made in the nylon membranes to aid in determining orientation in later analysis.

Probed with ^{32}P labelled cDNA from the 4 hour light-treatment group

Probed with ^{32}P labelled cDNA from the Dark (control) treatment group

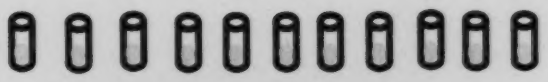

Phage stocks were made of all differentially expressed clones

B.

2° Screen

3ul of each phage stock were used to infect bacterial lawn on gridded NZY plate. Incubated overnight at 37°C.

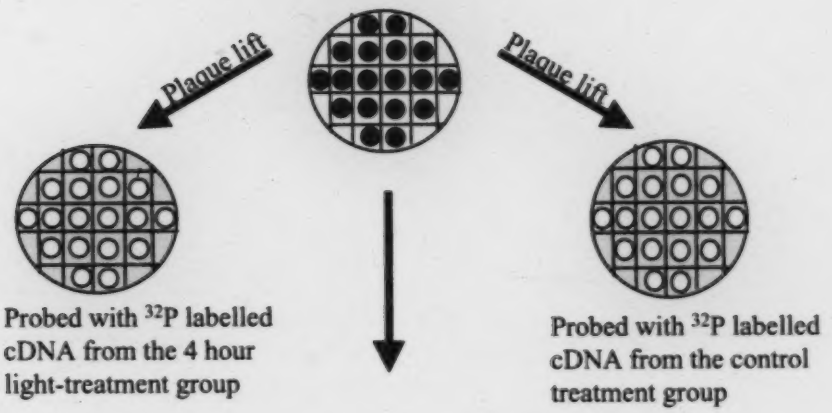
Plaque lift
Plaque lift
Probed with ^{32}P labelled cDNA from the 4 hour light-treatment group
Probed with ^{32}P labelled cDNA from the control treatment group

C.

3° Screen

PCR amplified differentially expressed clones and the PCR products were size fractionated on duplicate agarose gels.

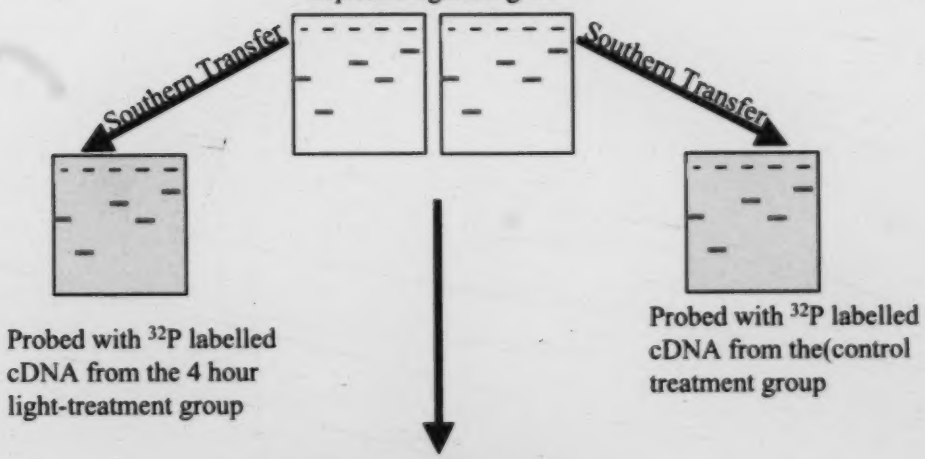
Southern Transfer
Southern Transfer
Probed with ^{32}P labelled cDNA from the 4 hour light-treatment group
Probed with ^{32}P labelled cDNA from the(control treatment group

Confirm Differential Expression Status by Northern Analysis

of *E.coli* cells suspended in 10 mM $MgSO_4$ (OD_{600} 1.0) for each NZY plate. A 5 minute room temperature incubation was used to facilitate attachment of the phage to the bacterial pili. A 15 minute incubation at 37°C followed in which bacterial cells complete one cell cycle and infection by the phage occurs. The infected bacterial cells were then mixed with 20 mL of NZY top agar and poured onto the NZY plate. The plates were left incubating at 37°C overnight. Approximately 1000 plaques were detected on each of the 10 plates used. Thus the titer of the Commitment Phase cDNA library was approximately 500 pfu/μL.

D-1.1 Plaque Lifts Once plaques were visible, plates were refrigerated at 4°C for at least 1 h prior to performing plaque lifts. Duplicate plaque lifts were performed for each plate. Nylon membranes (Gene Screen Plus, Biotechnology Systems, Boston MA) were divided into two sets. One set of plates, to be used for the first plaque lift, was notched in two asymmetrical places. The second set of plates was notched in three places. These notches or "lift tabs" were made so that the autoradiograph, membrane, and plate could be properly aligned later. Membranes were placed on the plates for 1 minute for the first lift and 2 minutes for the second lift. While on the plate, 3 asymmetrical "orientation" holes were made on the membranes with a sterile needle and traced onto the plate to further aid in the accurate alignment of master plate, membrane, and autoradiograph. Once removed from the plate, the membranes were treated with O.5 M NaOH for 4 minutes and then with 1.0 M Tris-HCl, pH 7.5 for 2 minutes. Following this treatment the membranes were dried on Blotting paper (Rose Scientific Ltd. Edmonton, Canada) and UV cross-linked using a Stratagene UV cross-linker (Stratagene, LaJolla, CA).

D-1.2 Preparation of cDNA Probes Used In Primary Screen

D-1.21 *cDNA synthesis* The total cDNA population from the control and 4 h treatment groups was synthesized, from purified mRNA (see section B-1), using a combination of the 5' and 3' RACE systems for Rapid Amplification of cDNA Ends (GIBCO BRL, Gaithersburg MD). The synthesis of the first strand of cDNA was achieved using an oligo T containing AP primer (anchor primer, CUA CUA CUA CUA GGC CAC GCG TCG ACT AGT ACG GGI IGG GII GGG IIG) and Superscript II Reverse Transcriptase. RNase H was added so as to eliminate the RNA from the RNA/DNA complexes. The first strand cDNA was isolated using Glassmilk spin columns and Gibco binding

solution. The DNA was eluted using deionized water. To synthesize the second strand of cDNA, the first strand of cDNA was tailed with dCTP and TdT. Using the tailed cDNA as a template PCR was used for amplification, thus generating double stranded cDNA. Abridged anchor primer (GIBCO BRL, Gaithersburg, MD) and UAP (universal amplification primer) primer were used in this PCR reaction that consisted of a:

94°C 1 min. denaturing phase
55°C 1 min. annealing phase
72°C 6 min. elongation phase
25 cycles
final elongation at 72°C for 7min

D-1.22 ***Radioactive labeling of cDNA probes*** cDNA probes used in the library screens were triple labeled with [α^{32} P] (3000Ci/mmol) dGTP, dATP, and dCTP. In accordance with the Gibco random primer labeling kit (GIBCO BRL, Gaithersburg MD) protocol the probe was boiled for 5 minutes to denature the DNA. Following this treatment the Random Primer mix, dTTP, radioactively labeled nucleotides, reaction buffer, and Klenow fragment were added. The reaction was left at room temperature for at least 2 h. The probe was then purified using STE select D G50 Sephadex columns (5 Prime 3 Prime Inc., Boulder Colorado). The probes were either used immediately or stored at -20°C. Prior to use, 100 µl of sheared salmon sperm DNA (10 mg/mL) (5 Prime 3 Prime Inc., Boulder, Colorado) was added to the probe and the probe was boiled for 5 minutes.

D-1.3 Hybridization and Analysis Primary differential screening was accomplished by probing the first set of membranes with cDNA derived from the 4 h light-treatment tissue and probing the second set of plaque lift membranes with cDNA derived from the retinae of the control group rats (preparation of probes described above, section D-1.2).

D-1.31 ***Hybridization*** Prior to hybridization, blots were washed in 2X SSC (sodium chloride tri-sodium citrate) for approximately 20 minutes. After this initial wash, the blots were prehybridized in Hybrisol II (Intergen, New York) for at least 3 h and up to 14 h. The prehybridizations were carried out at 65°C.

Hybridizations were carried out in hybrisol II at 65°C for at least 16 h. The blots were then subjected to two 15 minute washes with 2X SSC, followed by one wash in 2X SSC, 0.1%SDS for 30 minutes, and a final, 10 minute, wash in 0.1X SSC, 0.1%SDS. All

washes were carried out at 65^{0}C. As a last step, the blots were rinsed in 2X SSC before being placed on 2X SSC pre-wetted Blotting paper (Rose Scientific Ltd., Edmonton, Canada) and wrapped in Saran wrap. Blots were exposed to Kodak X-OMAT film (Eastman Kodak Company, Rochester, New York) for approximately 2 days at -70^{0}C before being developed.

D-1.32 ***Analysis*** Autoradiographs from the control cDNA probed membranes were compared to those from the 4 h treatment cDNA probed membranes. Signals that showed a different level of intensity on one set of autoradiographs compared to the other were matched to plaques on the NZY master plates. This was done by aligning the orientation holes and lift tabs on the membranes, autoradiograph, and NZY plates. The plaques matching the signal were picked using sterile Pasteur pipettes and placed in 500 µL of SM buffer. This was done to establish a stock of each phage containing an insert whose expression levels differed in the control cDNA population compared to the 4 h treatment cDNA population. To maintain the sterility of the phage stock, two drops of chloroform were added to the SM buffer. The phage stocks were then numbered and stored at 4^{0}C.

D-2 Secondary Commitment Phase cDNA Library Screen (figure 2-3B)

Approximately 30 mL of an overnight XL Blue *E. coli* culture (LB broth, O.2% maltose, 10 mM $MgSO_4$) was used to generate enough cells to create a bacterial lawn on twenty-two, gridded (into 1 cm by 1 cm squares) NZY plates (137 mm diameter), thus providing cells for the phage to infect. The cells were spun down for 10 minutes at 2800 rpm and resuspended in 10 mM $MgSO_4$ to an OD_{600} of approximately 1.0. 667 µL of these cells was added to 40 mL of NZY top agar and poured onto each of the NZY plates. The plates were incubated at 37°C for 30 minutes. 3 µL of each phage stock (section D-1.32) was dotted onto the appropriately numbered square on the NZY plates. The plates were incubated overnight at 37°C. After 1 h of refrigeration, duplicate plaque lifts were taken of each plate (section D-1.1). One set of membranes was probed with cDNA derived from the retinae of the control rats and the other set with cDNA derived from the retinae of the 4 h light treatment group rats. The probe labeling, hybridization and analysis were

carried out as outlined in sections D-1.22 and D-1.3. This constituted the secondary Commitment Phase cDNA library differential cross-screen.

D-3 Tertiary Commitment Phase cDNA Library Screen (figure 2-3C) The tertiary screening consisted of a PCR amplification of the differentially expressed clones followed by size fractionation of the PCR products on an agarose gel, transfer of the DNA onto nylon membranes and probing of the membrane with either radiolabeled control cDNA or radiolabeled 4 h treatment group cDNA.

D-3.1 Polymerase Chain Reactions (PCR)

PCR reactions were carried out according to manufacture's instructions (GIBCO BRL, Gaithersburg MD) using T7 and T3 primers (BioServe, MD.), nucleotides (GIBCO BRL, Gaithersburg MD), 2.5 units Taq enzyme, and 10X PCR buffer (GIBCO BRL, Gaithersburg MD). The PCR reactions consisted of:

94^0C, 3 minute denaturing

94^0C, 1 minute denaturation
50^0C, 5minute annealing
72^0C, 3.5 minute elongation
30 cycles

72^0C, 7 minute elongation

D-3.2 Electrophoresis

PCR products amplified from the phage stocks were separated on 1% agarose (FMC BioProducts, Rockland Maine) gels using TAE buffer and standard gel electrophoresis technique (Sambrook *et al.* 1989). Products were visualized over UV light following ethidium bromide staining.

D-3.3 Southern Transfer

Southern transfers were performed using standard methods (Sambrook *et al.* 1989, Southern, 1975). Nylon membrane and agarose gels were first soaked in 0.4 M NaOH in order to improve efficiency of transfer. Capillary action was used to transfer the DNA from the gel to the membrane. 0.4 M NaOH was used as the transfer buffer. The

membrane was washed in 2X SSC after the completion of the transfer, prior to being UV cross-linked.

For tertiary screening of the library two sets of gels were run for all of the samples. One set was probed with control cDNA while the other set was probed with 4 h light treatment group cDNA. The probe generation, labeling, hybridization, and analysis were carried out as described in sections D-1.2 and D-1.3.

E. ANALYSIS OF GENES

E-1 RNA Level

E-1.1 Northern Analysis

E-1.11 ***Preparation of Samples*** 1.5 µg of total RNA was mixed with 11% (v/v)10X MOPs buffer, 20% (v/v) formaldehyde, 57% (v/v) deionized formamide, and 3% (v/v) ethidium bromide (1 mg/mL) in a total volume of 30 µl (refer to Solutions in Appendex I). This served to stain the RNA and to denature any secondary structures. The samples were heated in a 55^0C water bath for 15 minutes, to further denature the RNA, and cooled on ice. Samples containing a loading dye were subjected to electrophoresis on a 1% agarose formaldehyde gel.

E-1.12 ***Preparation of Formaldehyde gel and Electrophoresis*** Total RNA from each treatment group, including the control group, was separated on a 1% agarose formaldehyde gel using standard protocols (Sambrook *et al.*, 1989). Samples were electrophoresed at 100 volts for 15 minutes and then at 30 volts for approximately 18 h.

E-1.13 ***Transfer of RNA*** After separation on a formaldehyde 1% agarose gel the RNA was transferred to a nylon membrane. The transfer was accomplished via capillary transfer using 10X SSC as the buffer. The membrane was soaked in 2X SSC prior to the transfer. UV cross-linking ensured RNA adhesion to the membrane.

E-1.14 ***Probe Labeling and Hybridization*** All Northern analyses were performed at least twice on duplicate blots to confirm results. Probes used on Northern blots were labeled with [α^{32}P] dCTP using the Gibco random primer labeling kit (GIBCO BRL, Gaithersburg MD, see section D-1.22). Prehybridization, hybridization, and washes were as described in D-1.3 except that:

1) Probes used here were derived from specific single clones.

2) When the blot and probe contained nucleic acid from different species the hybridizations and washes were performed at 52^{0}C.

3) In cases where the blot and probe contained nucleic acid from same species the hybridizations and washes were performed at 65^{0}C.

E-1.2 Slot Blot Analysis Slot blots were constructed using the Minifold II Slot-blot system (Schleicher & Schuell, Keene NH) apparatus. 2X SSC was used as a buffer to ensure that the nylon membrane, onto which the RNA was transferred, remained wet for the duration of the transfer. Approximately 0.2 µg of total RNA from each experimental group (including control) was transferred onto individual Slot blots. The RNA was prepared as described in section E-1.11. After the transfer was complete the membranes were U.V. cross-linked. Prehybridization, hybridization and washes were performed as described in section E-1.14.

E-1.3 Nuclease Protection Assay The Multi-NPA RNA/DNA/Oligo Probe Protection Assay Kit (Ambion, Austin, Texas) was used to detect specific mRNAs whose levels were too low to be detected via Northern analysis. The theory behind the technique is illustrated in figure 2-4. The protocol consists of radioactively labeling the 5' end of the oligo probes used, allowing for the oligo probes to hybridize to their target mRNA sequences, digesting all single stranded nucleic acids including the non-homologous 3' ends of the oligonucleotide probes, and separating the completed reaction products on 8 M urea, 12% polyacrylamide denaturing gels in order to quantify the amount of target mRNA present in each sample.

E-1.31 ***Designing NPA Probes*** Nucleotide sequences for the p53, Otx2, c-fos, and Crx probes were chosen based on sequences present in GenBank (http://www.ncbi.nlm.gov). Chosen sequences were checked to ensure that the only known sequences to which they have a strong sequence identity to the target sequence. A non-homologous 3' tail was added to the sequence (BioServe Biotechnologies Laurel, MD) (figure 2-4).

E-1.32 ***Radioactive Labeling of the Oligonucleotide Probes*** The KinaseMax 5' End-Labeling Kit (Ambion, Austin Texas) was used to label the oligonucleotide probes. T4 Polynucleotide Kinase was used to catalyze the forward reaction. In this reaction the gamma phosphate from [γ^{32}P]ATP is transferred to the 5'OH of the oligonucleotide probe.

Figure 2-4: Nuclease Protection Assay (NPA)

A) Table of oligonucleotide probe sequences used for the nuclease protection assay (the sequence of the 3' non-homologous tail is underlined).

B) Illustration of the NPA reaction.

A.

Oligonucleotide Probe	Protected Fragment Length (nt)	Total Fragment Length (nt)	Sequence
18S	40	48	Purchased from Ambion
p53	20	28	CCA TAG TTG CCT TGG TAA GTC ATT CTA C
Otx 2	29	37	CTA TAA CCT GAA GCC TGA GTA TAG CCT ATA TTA C
cFos	14	24	GAG GTC CAC AGC TTC ACT ATT CTC
CRX	10	18	GGT ATG GAT CTA TAT TCT
28S	35		Purchased from Ambion

B.

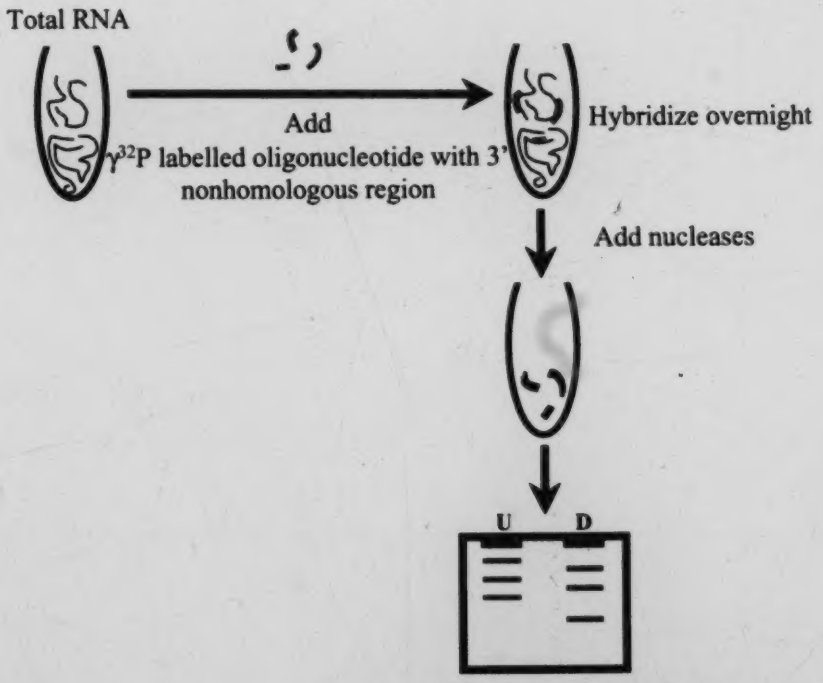

Run on 12% polyacrylamide, 8M urea gel.
Visualize by autoradiography

E-1.33 ***Hybridization of Oligonucleotide Probe to Target mRNA*** 1μg of total retina RNA from the control and each of the four treatment groups was used in these reactions. Radioactive oligo probe was added in excess to each treatment group RNA. In accordance with the protocol provided by the manufacturer, the RNA and oligo probe were concentrated by precipitating the sample with 0.5 M NH_4OAc and 2.5 volumes cold ethanol and then resuspended in 10ul of hybridization buffer. The hybridization reaction was left overnight at 37^0C.

E-1.34 ***Digestion of Single Stranded Nucleic Acids*** A mixture of nucleases suspended in a digestion buffer was added to the hybridization reaction. The digestion reaction was incubated at 37^0C for 30 minutes. This resulted in the digestion of all unbound oligo probes, non-target RNA and the non-homologous 3' end of the oligo probe, which does not bind to the target RNA. Following incubation, nuclease inactivation buffer was added. The oligo-bound target RNA was then precipitated using cold 100% ethanol, washed using cold 70% ethanol, re-suspended in loading dye, and loaded onto an 8 M urea, 12% polyacrylamide gel.

E-1.35 ***Electrophoresis and Analysis*** A 10 cm by 15 cm by 0.75 mm Protean II polyacrylamide electrophoresis system (Bio-rad Hercules, CA) gel apparatus was used for electrophoresis. Samples were heated at 90^0C for 3 minutes prior to being loaded on the 8 M urea, 12% polyacrylamide gel. Samples were electrophoresed at 160 volts for 10 minutes, then at 100 volts for approximately 6 h. Once electrophoresis was complete the gel was placed on blotting paper, wrapped in Saran wrap and exposed to Kodak X-OMAT film. The film was then developed and the intensity of the probe's signal compared and used to determine the relative amount of target RNA present in each of the five samples.

E-1.4 RT-PCR Life Technologies (Gibco-BRL, Gaithersburg MD) SuperScript One-Step RT-PCR with Platinum Taq was used to carry out RT-PCR experiments. Gene specific primers for Otx2 mRNA, NFκβ mRNA, and 18S ribosomal RNA were designed using GenBank sequences and ordered from Gibco-BRL Custom Primers (figure 2-5). The enzymes, buffers, and nucleotides used were provided with the kit and all components were used at concentrations and volumes specified in the manufacturer's protocol. cDNA was synthesized using reverse transcriptase and gene specific primers.

Figure 2-5: RT-PCR

A) Sequences of the gene specific primers used in the RT-PCR reactions

B) Schematic illustration of RT-PCR

A.

Primer	Primer Number	Sequence
Otx2 Left	R4760A02	TGCTGGCTCGACTTC CTACT
Otx2 Right	R4713A05	GGTACCCATGGGAC TGAGTG
NFκβ Left	R4713A02	CTTCTCGGAGTCCCT CAGTG
NFκβ Left	R4713A03	CCAATAGCAGCTGGA AAAGC
18S Left	R4713A06	GAACGCGTGCATTTA TCAGA
18S Right	R4713A07	CTTGGATGTGGTAGC CGTTT

B.

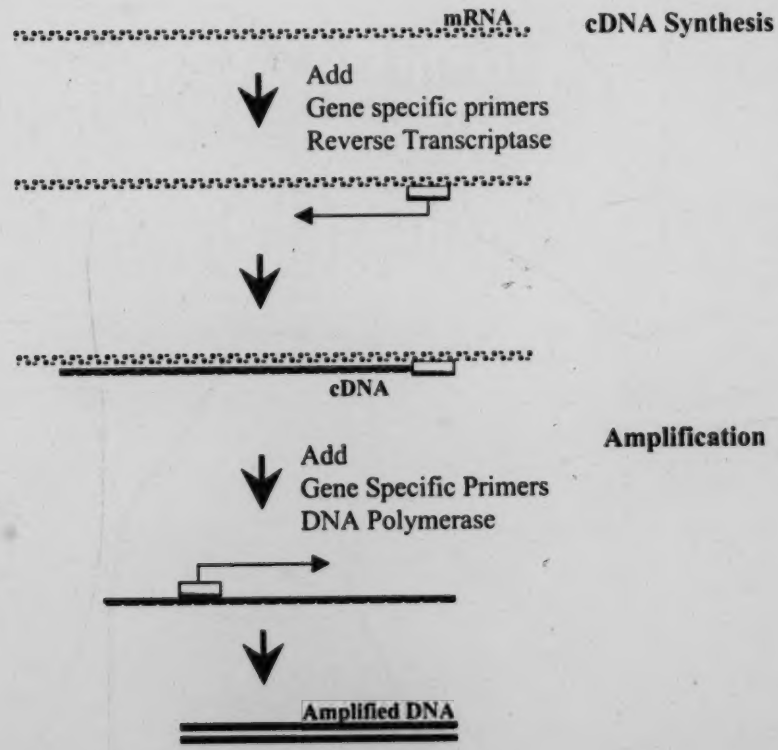

The cDNA was then amplified using the same gene specific primers and DNA polymerase. The following RT-PCR cycles were used:

cDNA Synthesis	30 min at 50^0C
	2 min. at 94^0C
PCR Amplification	15 sec at 94^0C
	30 sec at 58^0C
	2 min at 72^0C
	30 cycles
Final Extension	10 min at 72^0C

Following this RT-PCR reaction 1 μL of the RT-PCR product was subjected to an additional PCR amplification:

PCR Amplification	15 sec at 94^0C
	30 sec at 58^0C
	2 min at 72^0C
	30 cycles
Final Extension	10 min at 72^0C

The primes used in this reaction were the same as those used in the original RT-PCR reaction.

E-2 Analysis at the Level of the cDNA

E-2.1Sequencing All clones found to be differentially expressed were sequenced and the sequences subjected to a BLAST search in order to determine the clone's identity.

E-2.11 ***Sample preparation*** The PCR amplified clone inserts (section D-3.1) were prepared for sequencing using either the QIAquick Gel Extraction kit or the QIAquick PCR Purification kit (Qiagen, Mississauga, Ontario).

The PCR purification kit was used to isolate amplified clone inserts where only one highly amplified product was seen when the PCR reaction was separated on a 0.8% agarose gel and visualized over UV light after ethidum bromide staining. This protocol is effective at purifying single and double stranded DNA fragments ranging from 100 bp to 10 kb in length. The PCR reaction was run through a column containing QIAquick

silica-gel membrane. This membrane absorbs DNA in the correct salt concentration and pH. Both these conditions are achieved by adding the appropriate amount of buffer PB and wash buffer PE provided with the kit. DNA is eluted from the membrane by decreasing the salt concentration and increasing pH. This is achieved through the addition of deionized water to the column.

The QIAquick Gel Extraction kit also employs a QIAquick silica-gel column. This method of DNA isolation was used when more than one PCR product was amplified from a given phage stock solution. The PCR reactions were separated on 0.8% agarose gels and the DNA was excised from the gel and placed into a microfuge tube. Buffer QG was added to the gel slice and the sample was heated. The QG buffer solubilized the gel slice and created the optimal conditions for DNA binding to the silica-gel column. The remainder of the procedure was identical to that employed in the PCR purification described above. This method of DNA purification is effective for purifying DNA ranging from 70 bp to 10 kb in length.

E-2.12 ***Sequencing reactions*** Both full and half reactions from the ABI Prism DNA Sequencing Kit (PE Applied Biosystems, Warrington, U.K.) were used for automated sequencing. Reactions were carried out using either SK primer (priming off the 5'end of mRNA inserts in the lambda Uni-ZAP XR vector) or T7 primer (priming off the 3' end of mRNA inserts in the Uni-ZAP XR vector). The sequencing reaction consisted of 25 cycles of:

30 second, 96^0C denaturation phase

15 second, 50^0C annealing phase

4 minute, 60^0C elongation phase

The sequencing reactions were then purified using the Centri Spin Sephadex columns (Princeton separations, Lakewood, New Jersey) and lyophilized in a vacuum centrifuge. The reactions were sent to the Biological Sciences Sequencing Facility for analysis using a PE Applied Biosystems 377 automated sequencer.

CHAPTER 3

SCREENING OF THE COMMITMENT PHASE cDNA LIBRARY

A. INTRODUCTION

During an early stage of retinal degeneration it is expected that photoreceptor cells are committing to apoptosis but have not yet initiated the process. Initial results suggest that exposing Sprague-Dowley rats to green light (490-580 nm) at an intensity of 1500 lux leads to such an early degenerate state, or Commitment Phase, in the rat retinae (Wong *et al.*, 1995). This phase of retinal degeneration is of interest because the initiation of the apoptotic (in the case of photoreceptor cells) or survival (in the case of the other neural retina cells) programs occurs at this interval. Two options exist for cells during this phase of retinal degeneration: 1) to fix light-induced damage and survive the light assault, or 2) to initiate the apoptotic program because the damage incurred is too extensive. In both cases a change in the cell's molecular environment will occur; the expression of genes whose products are required to initiate either survival or death will be up-regulated while the expression of genes encoding antagonistic proteins will be down-regulated. Identifying the genes whose expression changes following a 4 h light treatment could lead to identifying factors involved, either directly or indirectly, in the initiation of retinal degeneration.

To identify genes whose expression is altered in response to the 4 h light treatment, a Commitment Phase cDNA library was differentially cross-screened using cDNA probes derived from total RNA populations of control and 4 h light treated rat retinae (figure 3-1). The hybridization pattern of Commitment Phase cDNA clones was compared. The intensity of the hybridization signal is a reflection of the amount of transcript, complementary to the cDNA clone
sequence, that is present in the total RNA population of the control or 4 h light treated retinae. Clones whose signal is stronger when probed with control retina cDNA as compared to 4 h light treated retina cDNA represent transcripts whose levels are decreased in response to the 4 h light treatment. Transcription of genes whose products are involved in establishing the apoptotic phenotype would be expected to be up-regulated in response to a 4 h light exposure and thus would have the opposite hybridization pattern.

Figure 3-1: Identification of Genes with Altered Levels of Expression During the Commitment Phase of LIRD

Schematic of the experiments used in the isolation of light repressed and light induced retinal genes.

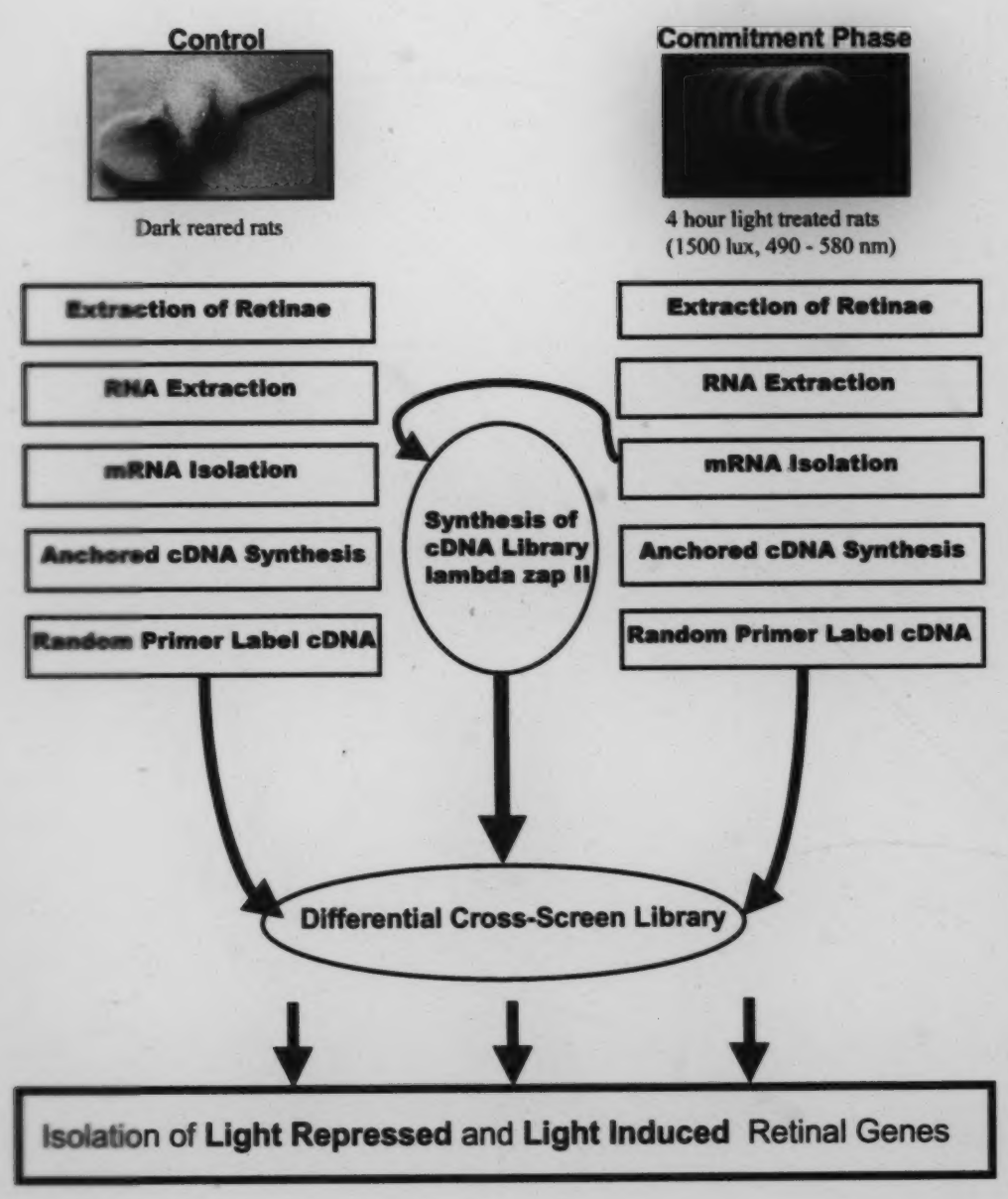
Control
Dark reared rats
Commitment Phase
4 hour light treated rats
(1500 lux, 490 - 580 nm)
Extraction of Retinae
RNA Extraction
mRNA Isolation
Anchored cDNA Synthesis
Random Primer Label cDNA
Synthesis of cDNA Library lambda zap II
Extraction of Retinae
RNA Extraction
mRNA Isolation
Anchored cDNA Synthesis
Random Primer Label cDNA
Differential Cross-Screen Library
Isolation of Light Repressed and Light Induced Retinal Genes

B. RESULTS

B-1 Integrity of RNA Samples Following extraction, total RNA was size fractioned on formaldehyde agarose gels to ensure that it was not degraded. The crispness of the 28S and 18S ribosomal RNA indicates that the RNA is of good quality (figure 3-2A). Northern analysis of the profile using a rat opsin probe, a marker of rod photoreceptor cell number, was used to confirm the expected profile of retinal degeneration (figure 3-2B). The Commitment Phase cDNA library and cDNA probes were made only after the integrity of the RNA samples were tested.

B-2 Screening of the Commitment Phase cDNA Library

B-2.1 Primary Screen The Commitment Phase cDNA library is representative of the different mRNA species present in the retina following a 4 h light treatment. 10, 000 cDNA clones from the library were differentially cross-screened using two different retinal cDNA probes: control probe and 4 h treatment group probe (figure 3-3A). Both probes were derived from total retinal RNA populations and random primer labeled with alpha [α^{32}P] dCTP, dATP, and dGTP (refer to Chapter 2, D-1.21). As a result, upon hybridization, cDNA clones of highly abundant mRNA sequences display a higher intensity signal than do cDNA clones of medium or low abundant transcripts. This allows for the detection of mRNAs whose levels have been altered following a 4 h light treatment.

In the primary screen, 10, 000 cDNA clones in Uni-ZAP XR phage vectors were plated onto NZY plates. Each plaque in the bacterial lawn contained one specific cloned cDNA in multiple copies. Duplicate plaque lifts were performed on the plates. One set was probed with control retina cDNA probe and the other with cDNA probe derived from retinae subjected to a 4 h light treatment. The expression pattern of individual clones was compared between the control and 4 h treatment groups and 2,300 clones were found to putatively contain sequences whose levels altered in response to light treatment. The differential expression pattern of these clones was tested in a secondary screen.

B-2.2 Secondary Screen A secondary screen was necessary since the NZY plates used in the primary screen contained approximately 1000 plaques each which sometimes made it difficult to determine exactly which plaque on the NZY plate corresponded to the

Figure 3-2: Northern Analysis & the LIRD Profile

A) A) An example of a typical RNA gel. The crispness of the 28S and 18S ribosomal bands indicates that the RNA is of good quality, not degraded. Sizes of the RNA ladder fragments are indicated along the left side of the gel photo.

Lane 1: RNA ladder,

Lane 2: total RNA from control retinae,

Lane 3: total RNA from 4 hour light treated retinae;

Lane 4: total RNA from 8 hour light treated retinae;

Lane 5: total RNA from 16 hour light treated retinae;

Lane 6: total RNA from 12 hour light followed by 24 hour dark treated retinae.

B) Opsin expression over the course of LIRD is expected to decrease due to the loss of photoreceptor cells. Hence, when a LIRD profile Northern blot is probed with an opsin probe the hybridization signal is expected to decrease as LIRD progresses. This type of hybridization pattern is shown on an LIRD profile Northern blot made from the RNA extracted for this thesis project. The LIRD profile Northern blot contains total retinal RNA as indicated in the figure. The opsin probe hybridizes to four different transcripts, which correspond to the different opsin transcripts that are present in the photoreceptor cells.

A

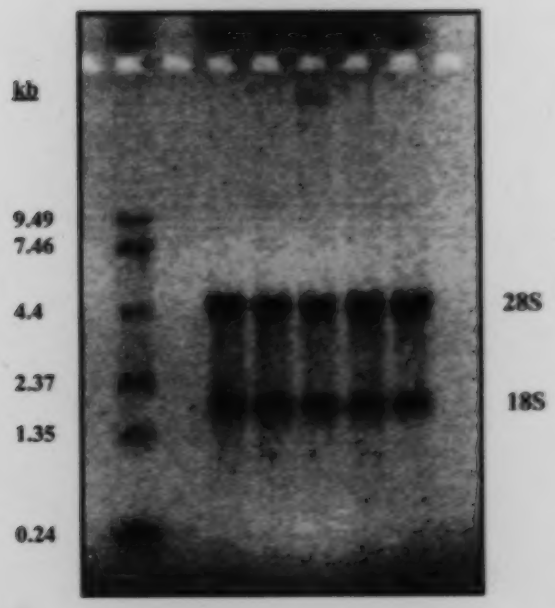
kb
9.49
7.46
4.4
2.37
1.35
0.24
28S
18S

B

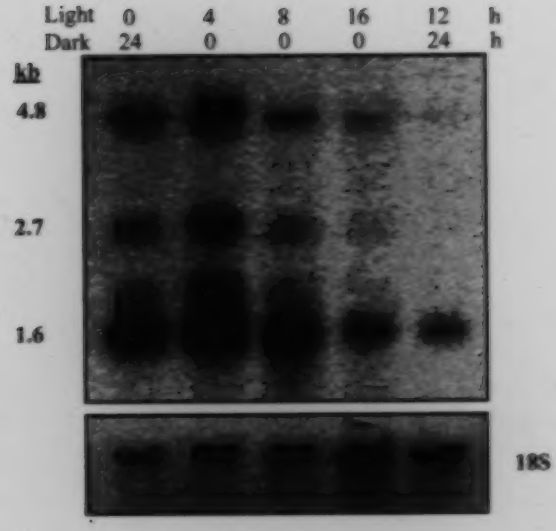
Light 0 4 8 16 12 h
Dark 24 0 0 0 24 h
kb
4.8
2.7
1.6
18S

Figure 3-3: Differential Cross-Screening of the Commitment Phase Library

Schematic depiction of Differential Cross-Screening of the Commitment Phase cDNA Library. Representative autoradiographs shown.
A) The primary screen of 10, 000 phage identified 2,300 differential clones. On the autoradiographs, the red circles indicate light repressed clones (stronger hybridization signal with control cDNA probe than with 4 h light treatment cDNA probe) and the green circles indicate light induced clones (hybridization signal stronger with cDNA from 4 h light treated retinae than with control cDNA).
B) The secondary screen of the 2,300 clones identified 200 clones as differentially expressed. On the autoradiographs the red star indicates light repressed clones and the green star light induced clones.
C) The tertiary screen identified 54 differentially expressed clones. The red arrows on the autoradiograph indicate light repressed clones while the green arrows indicate light induced clones.

A.

Plate out Commitment phase library

Duplicate plaque lifts taken of library plates
Total of 10 000 clones screened

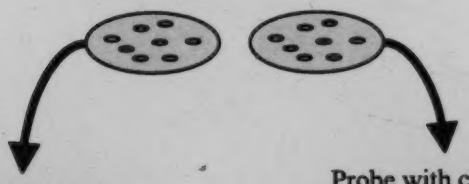

Probe with cDNA from
4 hour treatment group

Probe with cDNA
from Dark treatment
group (control)

Differentially expressed clones were picked. Clones whose expression increased following light treatment are indicated by green circles. Clones whose expression is reduced following light treatment are indicated by red circles.
A total of 2300 clones were isolated.

Phage stocks were made of all differentially expressed clones

B.

Phage Dot Analysis
Two microliters of each of the 2300 clones is
dotted out onto a bacterial lawn

Duplicate plaque lifts of the phage dot plates are taken

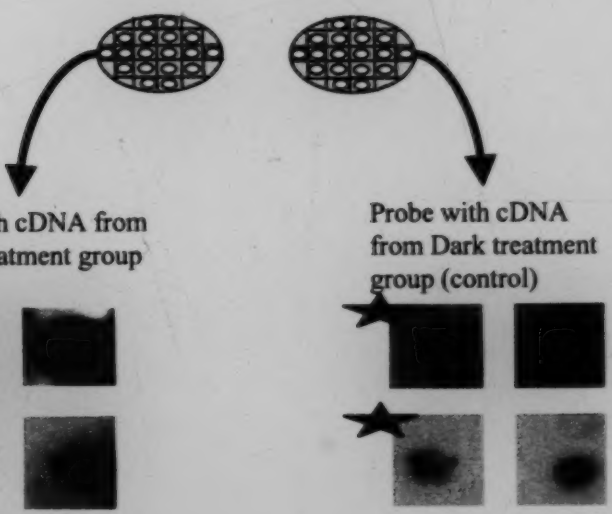

Differentially expressed clones were picked. Clones whose expression increased following light treatment are indicated by green stars. Clones whose expression is reduced following light treatment are indicated by red stars.
A total of 200 clones were isolated.

C.

PCR based Analysis

PCR amplified clones from secondary screen are run on duplicate agarose gels and Southern transfers are performed.

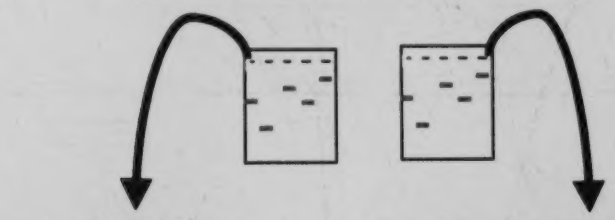

Probe with cDNA from 4 hour treatment group

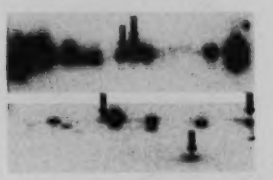

Probe with cDNA from Dark treatment (control) group

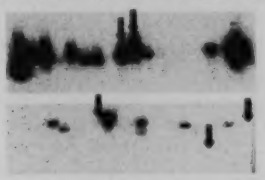

Differentially expressed clones were picked. Clones whose expression increased following light treatment are indicated by green arrows. Clones whose expression is reduced following light treatment are indicated by red arrows.
A total of 54 clones were isolated.

signal on the autoradiograph. To ensure that no clone with a differential expression pattern would be missed, several clones from an area were isolated. The secondary screen was used to more precisely determine which clones were differentially expressed.

The secondary cross-screen consisted of dotting out 2ul of phage stock, isolated from the primary screen, onto a gridded NZY plate containing a lawn of XL1-Blue MRF' *E.coli* bacterial cells (figure 3-3B). Again, duplicate plaque lifts were taken. One set of membranes was probed with control cDNA and the other set with 4 h light treatment cDNA. The differential status of 200 clones was confirmed after secondary screening of the 2,300 clones isolated from the primary screen. The remaining clones were found to be non-differential or false positives.

B-2.3 Tertiary Screen Each of the clones remaining after the secondary screen were amplified using PCR (refer to Chapter 2, D-3.1). The PCR products were electrophoresed on duplicate agarose gels and transferred onto nylon membranes (figure 3-3C). These membranes were then probed either with control cDNA probe or 4 h light treatment cDNA probe. The hybridization patterns of the PCR amplified clone inserts were compared and 54 of the 200 clones screened maintained their differential status.

C. INITIAL CHARACTERIZATION OF CLONES

C-1 Northern Analysis To confirm the isolation efficiency of clones by the differential cross-screen technique, a chosen subset of 12 clones from the 54 identified was subjected to Northern analysis. The inserts from these clones were PCR amplified and random primer labeled with [α ^{32}P] dCTP. The clone inserts were then used as probes on Northern blots containing total control (0 h of light treatment) and 4 h light treated retinal RNA. Representative Northern blots for 12 of the clones are shown in figure 3-4.

As predicted, two general trends were observed in the hybridization patterns of these clones. One set of clones showed an increased level of mRNA following 4 h of light exposure while the other set of clones showed decreased levels of mRNA following light treatment. In a number of cases, (clone 1005 and clone1114) a single probe detected several transcripts which displayed different expression profiles over the course of retinal degeneration. For example, clone 1005 hybridized to three transcripts. The largest transcript was down-regulated in response to the 4 h light treatment, while the

Figure 3-4: Northern Confirmation of Differential Clone Status

The inserts of putative differentially expressed clones isolated from the differential cross-screen of the Commitment Phase cDNA library were amplified, radiolabeled and used to probe LIRD profile Northern blots. Representative Northern blot results are shown. The Northern blots contain total RNA isolated form the retinae of control (0 h of light exposure) rats and total RNA isolated from the retinae of 4 h light treated rats. Two general trends were observed:

A) the cloned transcripts were induced in response to light exposure

or,

B) levels of cloned transcript mRNA decreased in response to light exposure.

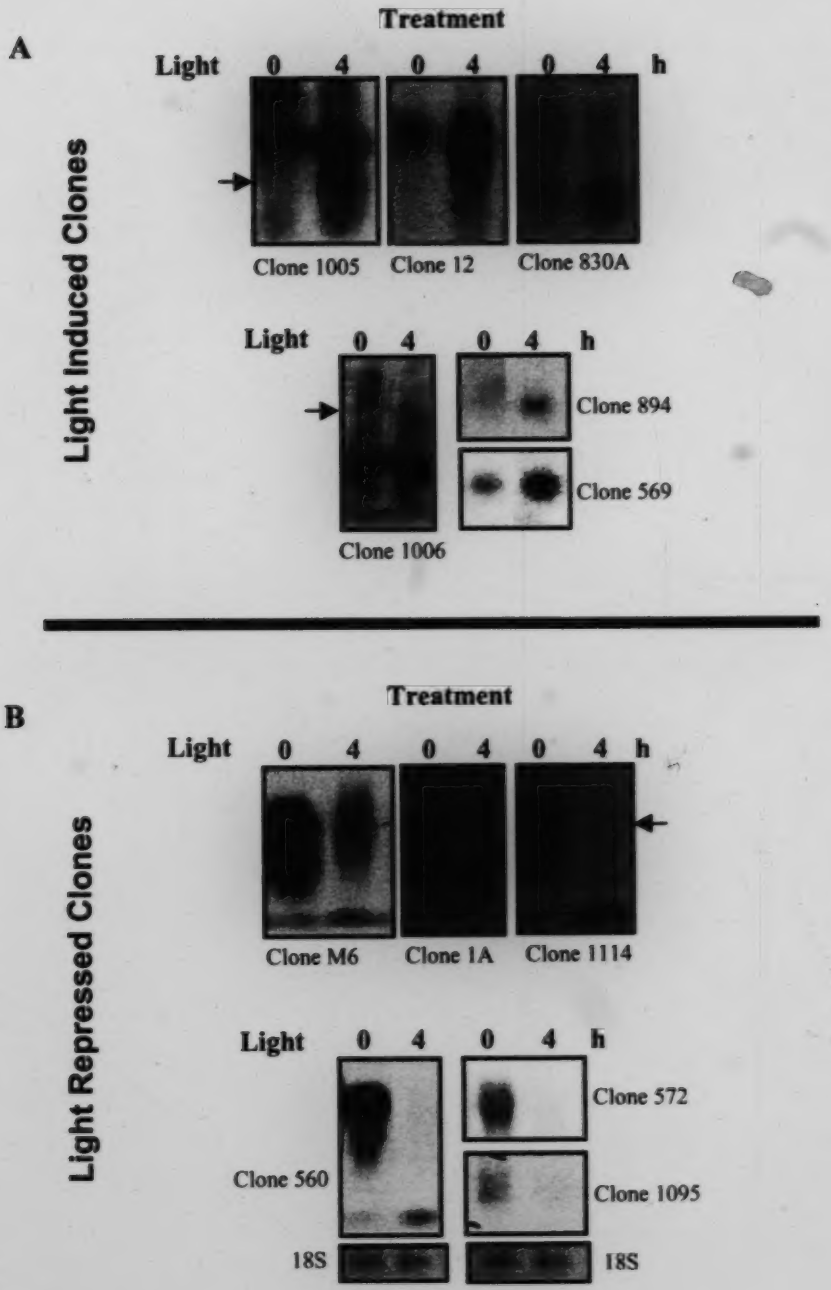
A
Treatment
Light
0 4 0 4 0 4 h
Clone 1005
Clone 12
Clone 830A
Light Induced Clones
Light
0 4 0 4 h
Clone 894
Clone 569
Clone 1006
B
Treatment
Light
0 4 0 4 0 4 h
Clone M6
Clone 1A
Clone 1114
Light Repressed Clones
Light
0 4 0 4 h
Clone 572
Clone 560
Clone 1095
18S
18S

smallest transcript was up-regulated. Clone 1114 also hybridized to two transcripts. The larger transcript is down-regulated following light exposure while the small transcript is up-regulated. Northern blot analysis was repeated at least two times on duplicate Northern blots to ensure the reproducibility of the results (figure 3-5).

D. DISCUSSION AND CONCLUSION

From the initial 10, 000 clones screened a total of 54 clones was isolated following three rounds of differential cross-screening. The high percentage of clones isolated in the primary differential cross-screen that were eliminated (98%) in subsequent screens can be attributed to 1) the large number and size of plaques present on each of the NZY plates in the primary screen, 2) the specificity and nature of the probe, 3) the nature of the clone insert sequence. When the autoradiographs and master plates were aligned following the primary cross-screen, clones surrounding the putative clone identified as differentially expressed were also picked. This was done as a precautionary measure to ensure that no differential clone would be lost as a result of misalignment. Therefore the majority of the clones picked in the primary cross-screen were expected not to contain differentially expressed transcripts. A further complexity was introduced by the total cDNA probes used. Since transcript sequences contain regions of partial DNA sequence similarity to many different transcripts (conserved regions among gene family members, alternately spliced transcripts, chance DNA sequence similarity between transcripts) the hybridization signals observed were not always a result of specific hybridization between probe, representing a single discrete gene (of the transcript cDNA present in the clone) and the clone insert. For this reason it is important that the differential expression of the clones identified through the cross-screen be confirmed using Northern analysis.

By performing Northern analysis, probe and target are switched. The clone insert becomes the probe and the total retinal RNA population becomes the target, thus, making it possible to determine if the clone insert hybridized to different transcripts. This result was routinely observed. The different sized transcripts on the Northern LIRD profile blots could correspond to alternately spliced variants of the cloned transcript, to different members of the gene family to which the cloned transcript belongs, or to unrelated

Figure 3-5: Duplicate and Triplicate LIRD Profile Northern Probed Blots

Duplicate and triplicate Northern blot analysis was performed to establish the reproducibility of results and the reproducibility in making consistent Northern blots for analysis. The inserts of clones identified as differentially expressed in the differential cross-screen of the Commitment Phase cDNA library were amplified, radiolabeled, and used to probe two or three different LIRD profile Northern blots (JS and PW are different LIRD profile Northern blots). The Northern blots contain total RNA from the retinae from dark-reared rats as indicated. The Northern blots were made from two different sets of rats, PW blots from one set and JS blots from another.

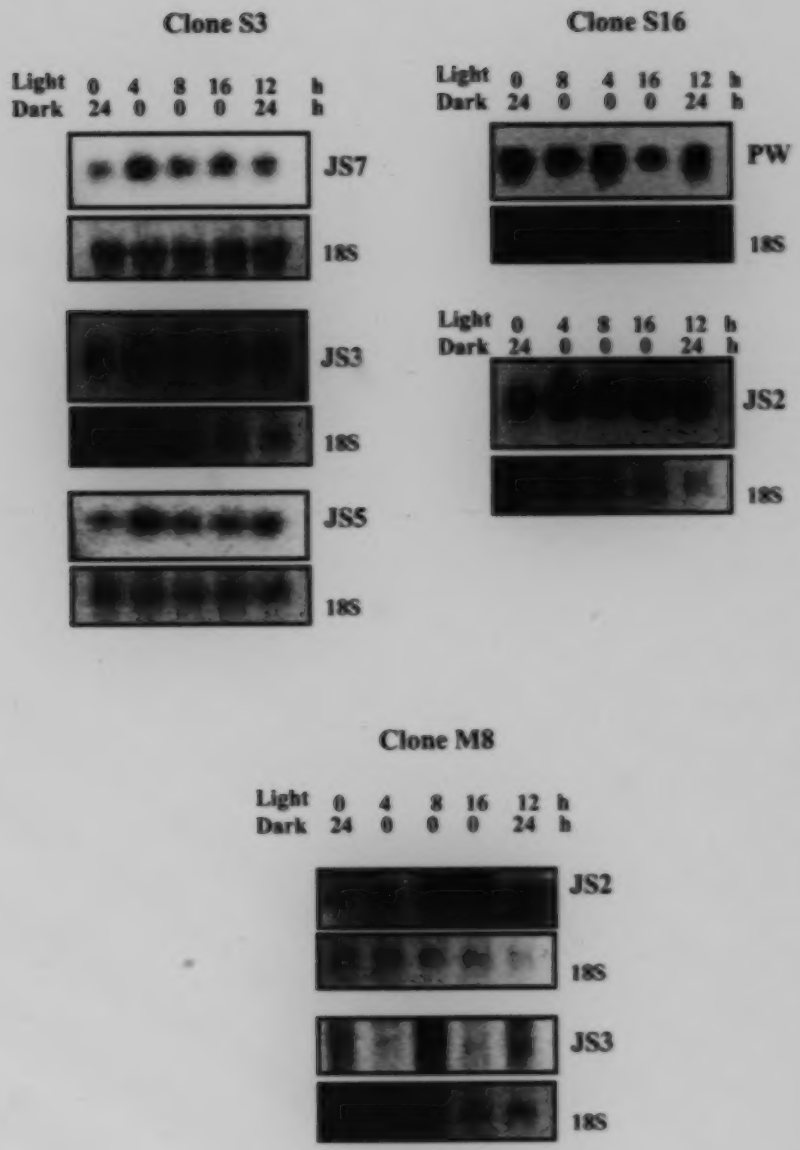
Clone S3
Light 0 4 8 16 12 h
Dark 24 0 0 0 24 h
JS7
18S
JS3
18S
JS5
18S
Clone S16
Light 0 8 4 16 12 h
Dark 24 0 0 0 24 h
PW
18S
Light 0 4 8 16 12 h
Dark 24 0 0 0 24 h
JS2
18S
Clone M8
Light 0 4 8 16 12 h
Dark 24 0 0 0 24 h
JS2
18S
JS3
18S

transcripts that by coincidence contain regions of sequence homologous to the cloned transcript.

From the 10,000 clones initially cross-screened, the expression of 0.5% was shown to be altered in response to the 4 h light treatment. Although this appears to be a small fraction, it is reasonable, since 1% of screened transcripts have been reported to be differentially expressed in other model systems of tissue involution (Guenette *et al.*, 1994; Ishida *et al.*, 1992). Therefore, the differential cross-screening of the Commitment Phase cDNA library was successful.

CHAPTER 4

SEQUENCE COMPARISON OF PUTATIVE DIFFERENTIAL CLONES

A. INTRODUCTION

As part of the characterization of clones isolated in the Commitment Phase cDNA library differential cross-screen, all clones were subjected to sequencing and sequence analysis. Sequencing was performed at the Biological Science Sequencing Facility and the sequences analyzed using the GenBank database. Nine of the clones with sequence similarity to known genes, did not show identity to any known rat gene sequences but did show similarity to *Mus musculus* or *Homo sapiens* gene sequences. The remaining clones can be divided into five categories based on their sequence-derived putative identification: mitochondria associated, eye and central nervous system, enzyme, translational machinery, signal pathway-associated and transcription factors (figure 4-1). In order to confirm the success of the differential cross-screen, a random set of 26 differential clones were used to probe Northern LIRD profile blots (representative results are shown throughout the thesis). In all cases a differential profile (although sometimes subtle) was observed.

B. RESULTS AND ANALYSIS

B-1 Sequencing Single pass sequencing was performed on all 54 differential clones (refer to E-2.1). Not all of the clones contained readable sequences. Of the 54 clones sequenced 11 did not yield readable sequence sufficient for further analysis. The sequences of the remaining 42 clones were analyzed for sequence homologies using the GenBank database (www.ncbi.nlm.nih.gov/BLAST/) (summary of search results in figure 4-1). With the aid of this database, putative identities were assigned to 33 clones. The sequences of the other five clones did not match those of any known genes contained in the database at the time of the search (table 4-1).

B-2 Unique Rat Sequences Approximately 9% of the clones contained transcripts with no DNA sequence identity to known genes, demonstrating that differential cross-screening is an effective method for the identification of novel genes. Five of the 54 clones were assigned unique status. Single pass sequencing of these five clones yielded long stretches of readable sequence, on average 414 nucleotides in length. BLAST database searches revealed either no significant sequence similarities or found similarities

Figure 4-1: Summary of Sequence Results

Clones whose insert sequences showed sequence similarity to known rat genes were categorized under Known . Clones whose inserts had no significant sequence similarity to any gene sequence in the GenBank database were classified as Unique . Clones whose insert sequences showed sequence similarity to genes other than rat genes were classified as Similar . The clones comprising the Known category were further divided into five categories based on the type of genes to which they showed sequence similarity.

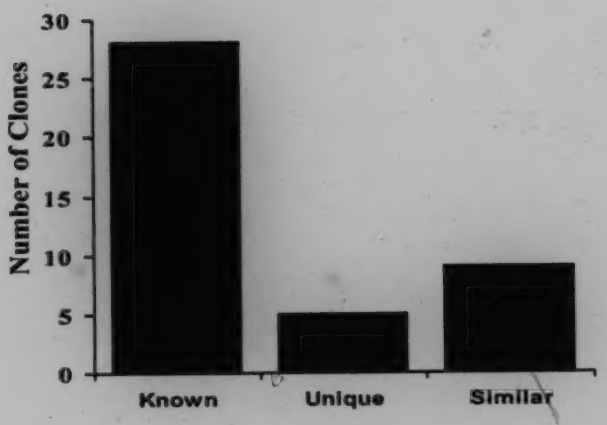

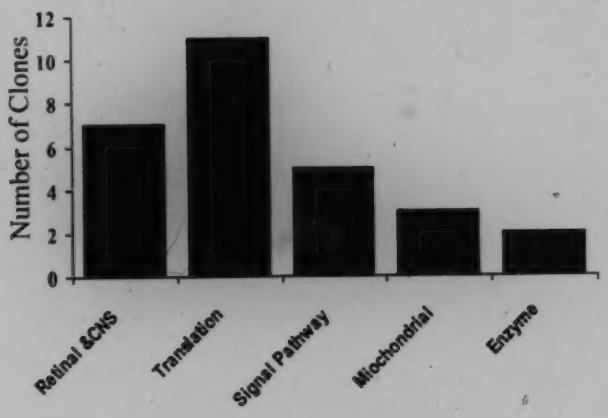

Known Gene Sequences

Clone Number	Putative Clone ID	Section
Unique		B-2
894	Unique/ *M. Musculus* chromosome 14 clone UWGC	
17	Unique/ rat EST AA957529	
2269A	No matches to known sequences	
2161A	No matches to known sequences	
1A	*Homo sapiens* DNA sequence from clone LL22NC03-5H6	
Similar Sequences		B-3
2A	*M. musculus* opsin gene	
246	*M. musculus* beta-A2-crystallin mRNA	
830A	*M. musculus* beta-B1-crystallin mRNA	
841	*M. musculus* gamma-S-crystallin mRNA	
1005	*M. musculus* guanine nucleotide binding protein	
1530	*M. musculus* external transcribed spacer B2 element	
1362A	*M. musculus* rab3A gene	
	Homo sapiens proteasome inhibitor p131	
577	*M. musculus* hemochromatosis gene	
1114	*Homo sapiens* protein tyrosine kinase 7	
Mitochondrial		B-4.1
1157	cytochrome c oxidase subunits I, II, III, and ATPase subunit 6	
716	Cytochrome c oxidase VIa	
130B	Coupling factor 6 of mitochondrial ATPsynthase complex	
25	ATP synthase subunit 8 and 6 gene	
Eye & Central Nervous System		B-4.2
12	Retina S-antigen (arrestin)	
3A	Opsin gene	
705	Brain ID transcript (BC1 RNA)	
1212A	Alpha-A-crystallin	
219	Alpha-A-crystallin	
1014	Beta-B3-crystallin	
330A	Beta-B1-crystallin	
Enzymes		B-4.3
748	Gamma-b3-glutathione-S-transferase	
1137	Triosephosphate isomerase	
Translation Associated		B-4.4
1287	Ribosomal protein S16	
M8	Ribosomal protein L7	
569	Ribosomal protein L30	
830B	Ribosomal protein L12	
736A	18S, 5.8S, and 28S genes	
736B	Ribosomal protein L7	
1755A	Elongation factor 2	
325	18S rRNA	
986	Ribosomal protein L19	
959	18S, 5.8S, and 28S genes	
Signaling Pathway Associated		B-4.5
1095	Neonatal glycine receptor	
M7	GTP-binding protein (G-alpha-O)	
767	Guanine nucleotide binding protein G-O, alpha subunit	
1102	Rat enhancer of split homologue (R-esp1)	
1084	Otx2 (homeobox domain)	
Unreadable Sequence		
1337, M6, 560, 1006, 572, 574, 1290		
1110, 1113, 1362B, 2214		

Clone Number	GenBank Accession #	Identity	Expected Size (bp)	Score	E-value	Medline number
Unique						
894						
17						
2269A						
2161A						
1A						
Similar Sequences						
2A	M55171	366/410	9483	432	e-119	91056108
246	AJ272227.1/ MMU27227	345/379	701	494	e-137	
830A	AF106853.1	430/472	873	595	e-168	
841	NM_009967.1	512/575	703	722	0	98234460
1005	NM_008140.1	360/381	1053	583	e-164	89214143
1530	X56974	197/201	2062	371	e-100	
	X72966		6348	214	2e-53	93319503
1362A	NM_006814.1	442/506	3188	490	e-136	99290307
577						
1114	NM_2821	138/154	4187	151	e-34	97037064
Mitochondrial						
1157	M27315	265/265	7632	525	e-147	85022618
716	X72757	92/93	4447	168	4e-39	
130B	X54510	475/479	573	912	0	92339904
25	AF115771.1	412/425	961	737	0	96118462
Eye & Central Nervous System						
12	X51781	290/322	1482	424	e-116	
3A	U22180	213/258	1047	228	2e-57	91236741
705	U25484	69/69	93	137	3e-31	95334379
1212A	(RN)U47922	409/418	1056	771	0	
219	(RN)U47922	439/443	1056	842	0	
1014	X05899.1	258/302	747	307	2e-81	85175137
330A	NM_012936.1	439/456	750	720	0	85175137
Enzymes						
748	J02744	463/499	1208	799	0	87222405
1137	L36250	260/286	1348	387	e-105	
Translation Associated						
1287	X17665	444/457	544	807	0	90235982
M8	M17422	403/418	778	630	e-179	87308300
569	K02931	390/392	392	753	0	86006278
830B	X53504	297/297	664	589	e-166	9102567
736A	V01270			728	0	
736B	M17422	667/695	778	1140	0	87308300
1755A	Y07504.1	434/460	2626	720	0	89252028
325	X01117	419/432	1874	755	0	
986	J02650.1	417/422	701	807	0	87109220
959	V01270	287/306	8647	488	e-135	
Signaling Pathway Associated						
1095	X57281	228/230	3865	434	e-120	91200276
M7	M17526	175/190	2068	200	e-49	88007678
767	M12671	306/358	1106	339	4e-91	
1102	L14462	134/134	1356	266	e-69	
1084	S81922	196/197	211	383	e-104	96108898
Unreadable Sequence						
1337, M6, 560, 1006, 572, 574, 1290						
1110, 1113, 1362B, 2214						

to sequences derived from other clones (human YACs or BACs) or to ESTs (expressed sequence tags). All cDNAs in this category were used as probes on Northern blots containing the LIRD profile. Three of the unique clones hybridized to more than one transcript on LIRD profile Northern blots (figure 4-2).

Clone 2161A hybridized to two transcripts and both were induced following 4 h light treatment. Expression of both transcripts remained elevated following 8 h light exposure and then decreased to levels approximating those seen in control retinae.

Clone 17 hybridized to multiple transcripts, the smallest of which was induced following 4 h light treatment. mRNA levels of this transcript decreased following 8 h light treatment and fell to undetectable levels following 16 h light exposure. A slight increase of mRNA levels was observed following the 12 h light 24 h dark treatment. The larger transcript yielded a much more intense hybridization signal.

Levels of this transcript are elevated over the course of LIRD with the exception of the 16 h light treatment.

Clone 1A hybridized to two transcripts, the mRNA levels of both decrease over the course of LIRD. Expression of the larger transcript was undetectable following 4 h light treatment while mRNA corresponding to the smaller transcript persisted until the 16 h treatment after which expression decreases to undetectable levels.

The hybridization pattern of **clone 2269** does not appear to differ significantly between the control and 4 h light treated retinae (densitometry and normalized data reveal that there is a slight decrease in mRNA following 4 h light treatment). However, transcript levels show an increase following an 8 h light treatment, a decrease following 16 h light treatment, and finally an increase during the 12 h light 24 h dark treatment. Transcr levels at the 12 h light 24 h dark treatment did not, however, reach levels observed in control retinae.

Clone 894 has an especially interesting expression pattern because its transcript is expressed solely following 4 h light treatment.

B-3 Clones With Sequence Similarities There are 9 clones which fall into this category. The sequences of the clones in this category do not match any known characterized rat gene sequences. For this reason an exact identity could

Figure 4-2: Hybridization Pattern of Unique Clones on LIRD Northern Blots

Clones 2161A, 2269, 894, 17, 1A were identified as containing unique transcripts upon differential cross-screening of the Commitment Phase cDNA library. The five clone inserts were amplified, radiolabelled, and used to probe LIRD profile Northern blots. Representative autoradiographs for each probe are shown. The blots contain total RNA extracted from control and light treated rat retinae as indicated. The 18S ribosomal RNA detected on RNA gels was used as a loading standard. Densitometry and normalization to the 18S ribosomal RNA was performed for each band detected on the Northern blots (values represent the average of at least three separate readings). The results of this analysis are presented in graph form with each transcript being represented by a different colored column on the graph (transcripts are coded by color as shown in the table below).

Clone	Putative ID	Clone insert size (kb)	Size of sequence searched (bp)	Transcript size on LIRD Northern Blots (kb)
2161A	unique	1.3	272	1.5, 0.6
17	unique	0.6	468	2.4, 1.1
1A	unique	0.8	340	5.6, 4.5
2269	unique	1.5	499	2.2
894	unique	1.7	489	1.1

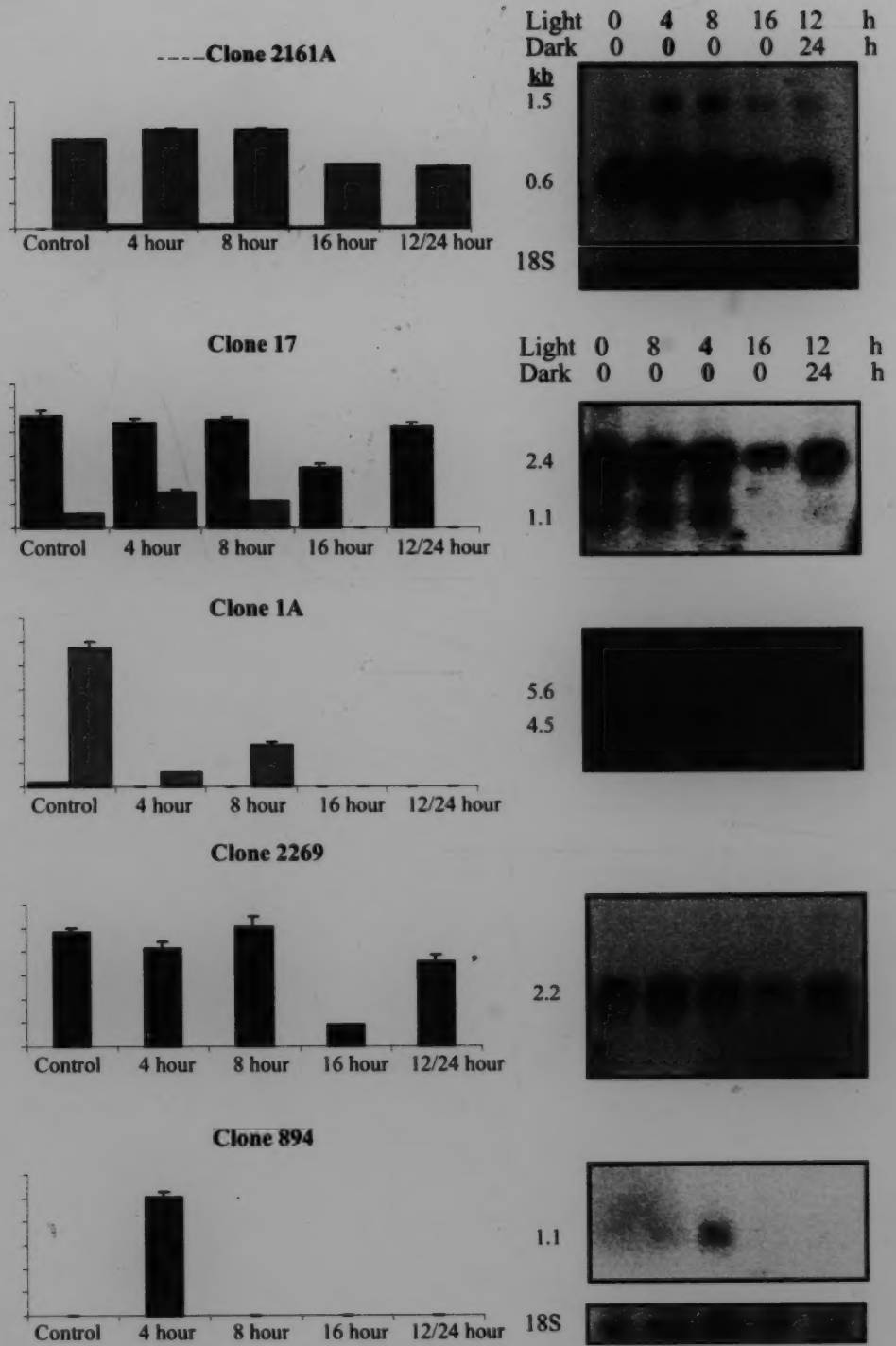
----Clone 2161A
Control
4 hour
8 hour
16 hour
12/24 hour
Light 0 4 8 16 12 h
Dark 0 0 0 0 24 h
kb
1.5
0.6
18S
Clone 17
Control
4 hour
8 hour
16 hour
12/24 hour
Light 0 8 4 16 12 h
Dark 0 0 0 0 24 h
2.4
1.1
Clone 1A
Control
4 hour
8 hour
16 hour
12/24 hour
5.6
4.5
Clone 2269
Control
4 hour
8 hour
16 hour
12/24 hour
2.2
Clone 894
Control
4 hour
8 hour
16 hour
12/24 hour
1.1
18S

not be assigned. However, these clones showed sequence similarity with genes characterized in other species. The greatest amount of sequence similarity was found between the rat clones identified and known mouse genes. Of these the majority (4 out of 9 clones) show sequence similarity to eye specific genes including mouse opsin (clone 2A), mouse beta-A2-crystallin (clone 246), mouse beta-B1-crystallin (clone 830A) and mouse gamma-S crystallin (clone 841). Clones of *Mus musculus, Homo sapien, Bos taurus* and *Gallus gallus* ß-A2-crystallin exist, but this gene has not yet been cloned from rat. For this reason searching the database for homologies to the clone 246 insert sequence did not reveal any matches to the rat ß -A2-crystallin gene. The same explanation holds true for clone 841, since no sequence is presently available for the rat γ-S-crystallin gene or transcript. In the case of clone 2A the insert sequence does not have any significant sequence identity to the rat opsin mRNA sequence. However, it has sequence identity to the 3' untranslated region of the mouse opsin gene and the *C. griseus* rhodopsin gene and matches an EST (UI-R-Y0-lx-a-05-0-UI.S1) isolated from an adult rat eye library (figure 4-3). Since the sequence for the full rat rhodopsin gene is not available in the GenBank database it is not possible to determine if clone 2A is homologous to its 3' untranslated region.

The sequences of clones 1362A, and 1114 show similarity to human genes. The genes can be categorized under the enzyme (tyrosine kinase 7) and signaling pathway associated (proteasome inhibitor pI31) categories. The products of these genes could all be involved in the transmission of extracellular or intracellular signals. These signals could either be death or survival signals. Analysis of clones 1005, 1530, and 577 revealed sequence identity to the *M. musculus* sequences for guanine nucleotide binding protein, rab 3A gene, and hemochromatosis gene respectively. The expression pattern of a select number of these clones was examined over the course of LIRD (figure 4-4). **Clone 1005** has an expression pattern similar to that of clone 1114. mRNA levels of the smallest transcript are high only following 4 h light exposure while levels of the other transcripts decreased following light treatment until they reached undetectable levels following the 16 h light treatment.

Figure 4-3: Sequence Comparison of Clone 2A, Mouse Opsin Gene, and Rat Opsin Gene

The mouse opsin gene sequence (GenBank accession number M55171) is compared to the rat opsin gene coding region (GenBank accession number U22180) and to the sequences of clone 2A, EST UI-R-Y0-lx-a-05-0-UI.S1 , and clone 3A. Sequence identity between the rat exons and mouse exons is high (ranging from 91% to 96% identity). Clone 2A, matched to mouse opsin by sequence analysis, has 89% identity to the 3 untranslated region of the mouse opsin gene, between nucleotides 7007 and 7424. The corresponding rat sequence for this untranslated region of the opsin gene is unknown. The sequence of rat EST UI-R-Y0-lx-a-05-0-UI.S1, isolated from an adult rat eye cDNA library matches the sequence of Clone 2A. Clone 3A was also identified as differentially expressed in the differential cross-screen of the Commitment Phase cDNA library. It has sequence identity to rat opsin but not mouse opsin. This is due to the fact that it represents the partial sequence of two opsin exons.
The solid colour squares indicate regions that show sequence identity. The dashed lines correspond to regions of no sequence similarity, presumably indicating the location of introns.

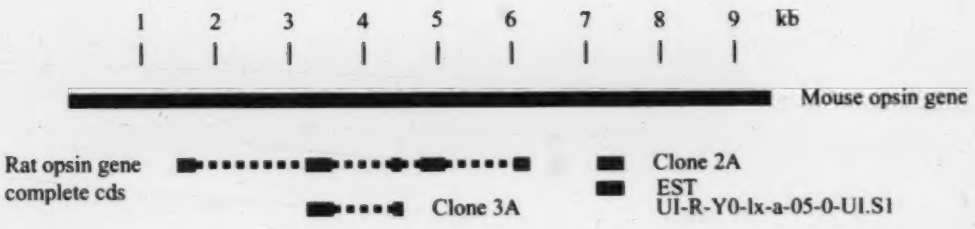
1
2
3
4
5
6
7
8
9
kb
Mouse opsin gene
Rat opsin gene
complete cds
Clone 3A
Clone 2A
EST
UI-R-Y0-lx-a-05-0-UI.S1

Figure 4-4: Hybridization Pattern on LIRD profile Northern Blots of Clones of Transcripts with Sequence Similarity

Clones containing transcripts that show no sequence similarities to known rat genes but did show similarity to known genes from other species were categorized under Sequence Similarity. The inserts of clones 1005, 114, and 830A were amplified, radiolabeled and used to probe LIRD profile Northern blots. A representative autoradiograph for each probe is shown. The Northern blots contain total RNA extracted from control and light treated rat retinae as indicated. The 18S ribosomal RNA detected on RNA gels was used as a loading standard. Densitometry and normalization to the 18S ribosomal RNA was performed for each band detected on the Northern blots. The results of this analysis are presented in graph form with each different sized transcript being represented by a different graph

Clone	Putative ID	Identity	Transcript size (bp)	Clone insert size (kb)	Sequence searched size (bp)	Score	e-value	Transcript Size (kb) on LIRD Northern Blots
1005	Mouse guanine nucleotide binding protein	360/381	1053	1.0	490	583	e-164	4.0, 2.0, 1.0
1114	Human protein tyrosine kinase 7	138/154	4187	0.3	384	151	1e-34	5.2, 3.8, 2.1, 0.4
830A	Mouse beta-B1 crystallin	430/472	873	1.5	497	595	e-168	0.9

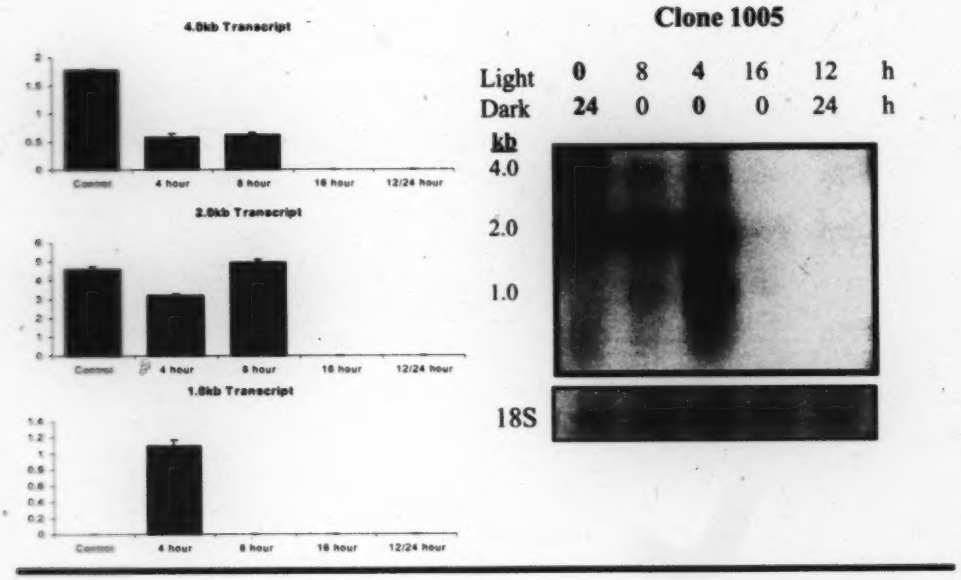
Clone 1005
4.0kb Transcript
2.0kb Transcript
1.0kb Transcript
Control
4 hour
8 hour
16 hour
12/24 hour
Light 0 8 4 16 12 h
Dark 24 0 0 0 24 h
kb
4.0
2.0
1.0
18S

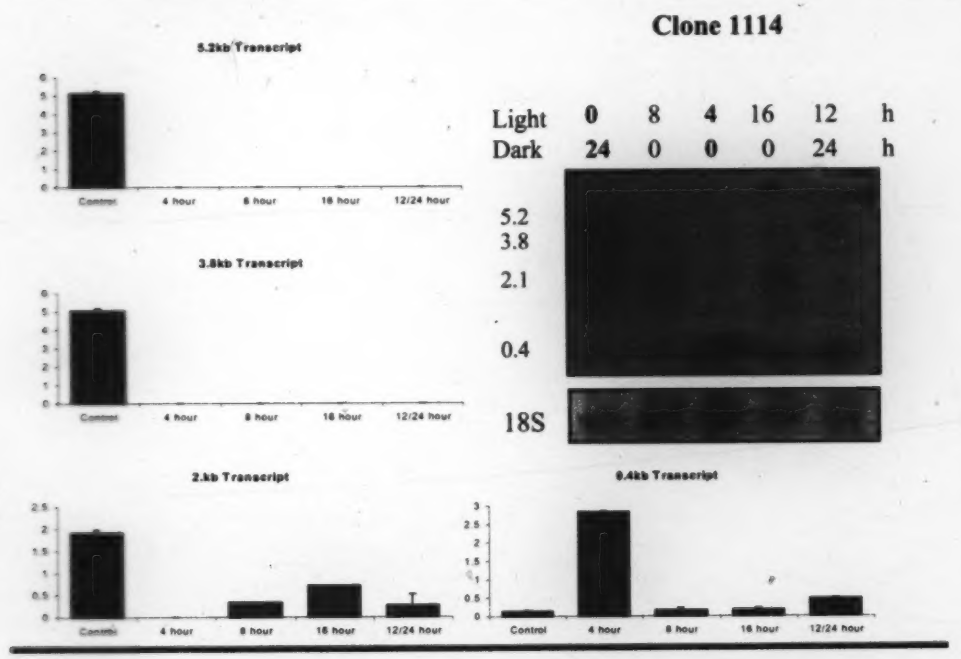
Clone 1114
5.2kb Transcript
3.8kb Transcript
2.kb Transcript
0.4kb Transcript
Control
4 hour
8 hour
16 hour
12/24 hour
Light 0 8 4 16 12 h
Dark 24 0 0 0 24 h
5.2
3.8
2.1
0.4
18S

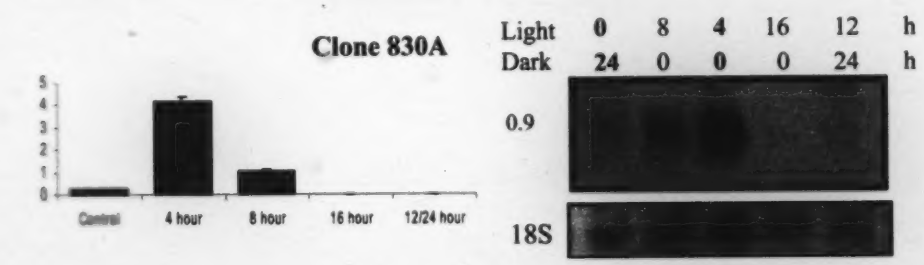
Clone 830A
Control
4 hour
8 hour
16 hour
12/24 hour
Light 0 8 4 16 12 h
Dark 24 0 0 0 24 h
0.9
18S

Clone 1114 hybridizes to several different transcripts. The larger transcript was down-regulated in response to 4 h light exposure while the smallest transcript was up-regulated. There are low or undetectable levels of the large transcript mRNA over the course of LIRD while levels of the smallest transcript are high only during the Commitment Phase (4 h light exposure) of LIRD.

Clone 830A hybridizes to a transcript whose expression increases substantially following 4 h light treatment. Following 8 h light treatment transcript levels decrease, but remain above control levels. Expression of this transcript is undetectable following the 16 h light treatment.

B-4 Matches to Known Rat Genes

B-4.1 Clones of Genes whose Products are Required in the Mitochondria Apoptosis is an active process, often requiring *de novo* protein synthesis (Wyllie *et al.*, 1995). The availability of ATP in a cell determines if the cell is able to undergo apoptosis or, must default to an undesirable necrotic fate (Leist *et al.*, 1999). Thus, the mitochondria, as the "power house of the cell", is central to apoptosis. Likewise, survival in an adverse environment would require energy. This energy could be used to increase transcription and translation of genes encoding proteins needed to repair damage inflicted on the cells as a result of light exposure. Therefore, the identification of differentially expressed genes encoding mitochondrial proteins following light treatment is expected.

Clones 1157, 716, and 130B all match sequences of known mitochondrial protein encoding genes. Northern analysis of **clone 1157** revealed a subtle change in the expression of this transcript over the course of LIRD (figure 4-5).

B-4.2 Eye & Central Nervous System Clones Sequence analysis of clone 3A revealed sequence identity to the rat opsin gene sequence. Clone 12 was identified as retina S-antigen (also known as arrestin). The three remaining clone inserts were all identified as crystallin transcripts. Two of them match rat alpha A-crystallin mRNA sequences (clones 1212A and 219) and the other matches the mRNA sequence for rat beta B3-crystallin (clone 1014).

Opsin mRNA levels have been observed to decrease during LIRD in previous experiments (Wong *et al.*, 1995). Clone 12 was identified as differentially expressed

Figure 4-5: Mitochondrial Clone 1157 on LIRD Northern Blots

The expression pattern of Clone 1157's insert was examined over the course of LIRD. The Northern blot contains total RNA extracted from control and light treated rat retinae as indicated. The 18S ribosomal RNA detected on RNA gels was used as a loading standard. Densitometry and normalization to the 18S ribosomal RNA was performed for each band detected on the Northern blot. The results of this analysis are presented in graph form with each transcript being represented by a different graph.

Clone	Putative Clone ID	Identity	Expected Size of Putative Transcript (bp)	Size of Clone Insert	Transcript Size(kb) on LIRD Northern Blots
1157	Mitochondrial cytochrome	265/265	7632	380bp	5.0 kb, 2.9 kb, 1.6 kb, 1.2

Light 0 8 4 16 12 h
Dark 24 0 0 0 24 h
kb
5.0
2.9
1.6
1.2
18S

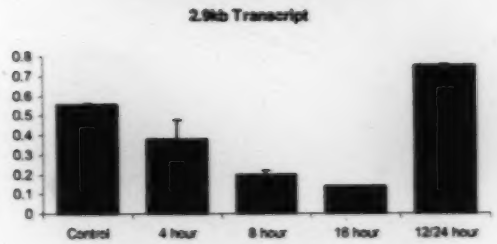
2.9kb Transcript
0.8
0.7
0.6
0.5
0.4
0.3
0.2
0.1
0
Control
4 hour
8 hour
16 hour
12/24 hour

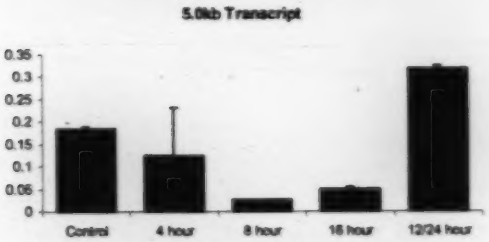
5.0kb Transcript
0.35
0.3
0.25
0.2
0.15
0.1
0.05
0
Control
4 hour
8 hour
16 hour
12/24 hour

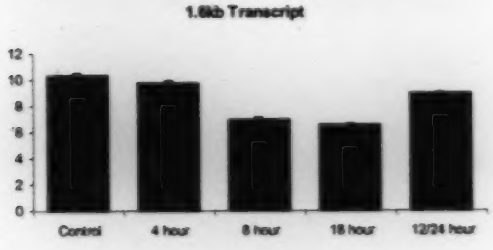
1.6kb Transcript
12
10
8
6
4
2
0
Control
4 hour
8 hour
16 hour
12/24 hour

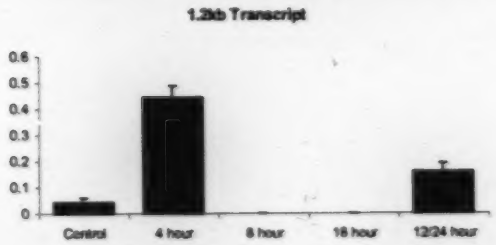
1.2kb Transcript
0.6
0.5
0.4
0.3
0.2
0.1
0
Control
4 hour
8 hour
16 hour
12/24 hour

using the differential cross-screen method and found to be a portion of the rat opsin gene. Identification of opsin as differentially expressed using the differential cross-screening technique provides additional proof that the screening of the Commitment Phase cDNA library was successful.

Clone 12 S-antigen transcript levels, increase following 4 h light treatment. mRNA levels decrease following 8 h light treatment, and further decreased following a 16 h light treatment to undetectable levels. During the 12 h light, 24 h dark treatment transcript levels increased but did not reach the levels observed in the control retinae (figure 4-6). The sharp increase in S-antigen transcript levels following the 4 h light treatment is interesting because of S-antigen's role in phototransduction. The large up-regulation of arrestin following 4 h light treatment suggests that the arrestin protein is required at a higher level than normal following this treatment. Arrestin's role in deactivating opsin (e.g. enabling the recycling of rhodopsin and inhibiting the re-activation of this molecule) combined with its induction following light exposure, suggests the presence of high levels of "activated" rhodopsin. This is consistent with the hypothesis that one of the key events that leads to light-induced retinal degeneration is a sharp increase in activated rhodopsin. An over-abundance of activated rhodopsin could lead to an over-stimulation of the phototransduction cascade and mimic the effects of mutations in rhodopsin that prevent its deactivation. Such mutations cause retinitis pigmentosa (reviewed in Rattner *et al.*, 1999).

The other eye-expressed genes were all identified as members of the crystallin gene family. For the most part these genes are regarded as genes expressed in the lens. However, recent experiments reveal that crystallin gene family expression has been observed in the retina (Magabo *et al.*, 2000; Jones *et al.*, 1999). The crystallins are an interesting class of proteins. They are associated with different functions depending on the cell type in which they are expressed. In the eye they are thought to function as heat shock proteins, enzymes, and structural proteins and are thought to play a role in stress response (Wistow *et al.*, 1993). The up-regulation of these genes could be occurring in response to the environmental stresses resulting from light exposure.

B-4.3 Enzymes Clone 748 was identified as γ-b3 glutathione-S-transferase cDNA and clone 1137 as a triosephosphate isomerase cDNA. The identification of clone 748 as

Figure 4-6: Hybridization Pattern of Clone 12 on LIRD Northern Blots

Clone 12 represents a clone of rat arrestin. The expression pattern of arrestin was examined over the course of LIRD by probing a LIRD profile Northern blot with Clone 12. The Northern blot contains total RNA extracted from control and light treated rat retinae as indicated. The 18S ribosomal RNA detected on RNA gels was used as a loading standard. Densitometry and normalization to the 18S ribosomal RNA was performed for each band detected on the Northern blots. The results of this analysis are presented in graph form with each different sized transcript being represented by a different graph.

Clone	Putative ID	Identity	Transcript size	Clone insert size	Sequence searched size	Score	E-value	Transcript Size (kb) on LIRD Northern Blot
12	S-antigen (arrestin)	290/322	1482	1.5	385	424	e-116	1.4

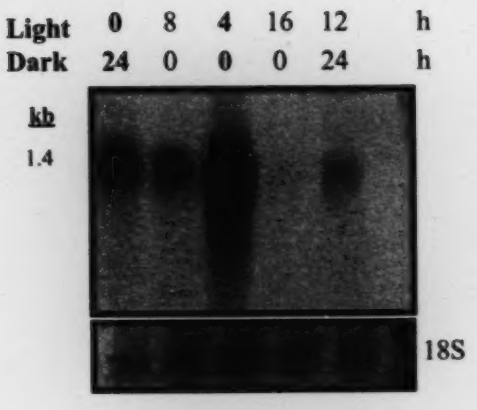
Light 0 8 4 16 12 h
Dark 24 0 0 0 24 h
kb
1.4
18S

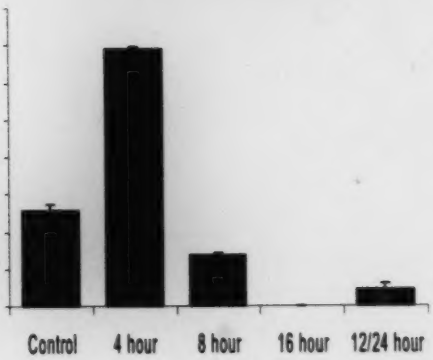
Control
4 hour
8 hour
16 hour
12/24 hour

γ-b3 glutathione-S-transferase is exciting because this enzyme plays an important role in protecting the mammalian eye from ultraviolet irradiation and oxidative stress. This enzyme is expressed in retinal nonpigmented and pigmented epithelial cells (RPE) (Escribano *et al.*, 1999). The majority of both these cell types survive light induced retinal degeneration (Noell *et al.*, 1966). The altered levels of γ-b3 glutathione-S-transferase mRNA in response 4 h light treatment suggest that this enzyme could be part of the survival response. Furthermore, since the RPE is not part of the neural retina no RPE cell derived RNA was used in the differential cross-screening experiments. Thus, γ-b3 glutatione-S-transferase must be expressed by surviving neural retina cells during LIRD.

B-4.4 Translational Machinery The majority of clones whose putative identities were determined upon sequencing belong to the translation associated group of proteins. Of the 42 clones with readable sequence, nine were ribosomal proteins and one was an elongation factor. A further discussion of this category of genes can be found in Chapter 6.

B-4.5 Signaling Pathway Associated Clones and Transcription Factors Four of the clones identified in the differential cross-screen contain sequences of signal pathway associated genes, including one clone containing a portion of an Otx-2 transcript (clone 1084). The other clones (clones M7, 1095, and 767) contain GTP-binding protein, neonatal glycine receptor and guanine nucleotide binding protein transcript sequences respectively.

Clone 1095 (neonatal glycine receptor) hybridized to one transcript whose expression is repressed by light exposure (figure 4-7).

Clone 1084 (Otx2) Northern analysis showed that the clone hybridized to five different transcripts in total retinal RNA (figure 4-7). Levels of the 0.8 kb and 0.4 kb transcripts were observed to increase following 4 h light treatment and then decrease as LIRD progressed. In the existing gene database only a partial, 211 nucleotide, mRNA sequence of Otx-2 has been cloned in R*attus norvegicus*. This makes it impossible to determine which, or if any, of the bands on the Otx-2-probed LIRD profile Northern blot correspond to the Otx-2 transcript. All of the bands to which the Otx-2 clone hybridizes on the LIRD

Figure 4-7: Hybridization Pattern of Signal Pathway Associated Clones on LIRD Northern Blots

Clones 1095 and 1084 were used as probes on LIRD profile Northern blots in order to determine their expression patterns during LIRD. The Northern blots contain total RNA extracted from control and light treated rat retinae as indicated. The 18S ribosomal RNA detected on the RNA gels was used as a loading standard. Densitometry and normalization to the 18S ribosomal RNA was performed for each band detected on the Northern blots. The results of this analysis are presented in graph form with each different sized transcript being represented by a different graph.

Clone	Putative ID	Identity	Transcript size (bp)	Clone insert size (kb)	Size of sequence searched (bp)	Score	e-value	Transcript size on LIRD Northern blot
1095	Neonatal glycine receptor	228/230	3865	0.8	452	434	e-120	3.6
1084	Otx2	196/197	211 (partial)	1.0	750	383	e-104	5.8, 3.4, 1.8, 0.8, 0.4

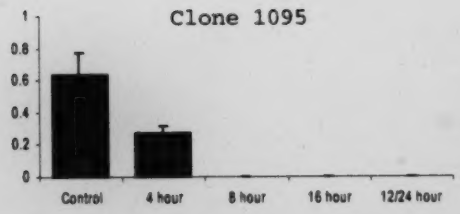
Clone 1095
1
0.8
0.6
0.4
0.2
0
Control
4 hour
8 hour
16 hour
12/24 hour

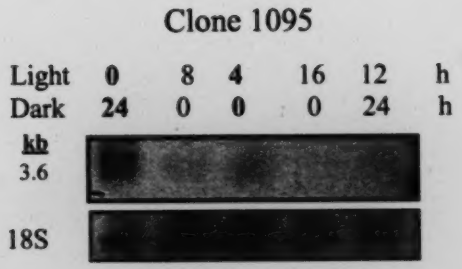
Clone 1095
Light 0 8 4 16 12 h
Dark 24 0 0 0 24 h
kb
3.6
18S

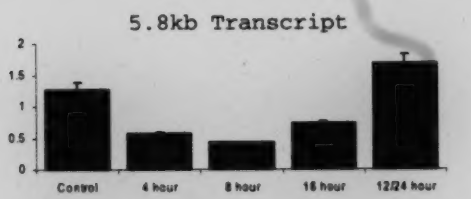
5.8kb Transcript
2
1.5
1
0.5
0
Control
4 hour
8 hour
16 hour
12/24 hour

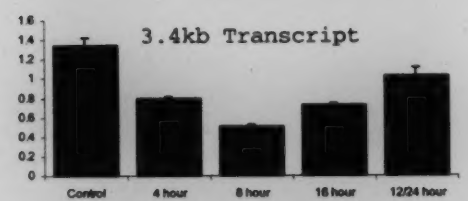
3.4kb Transcript
1.6
1.4
1.2
1
0.8
0.6
0.4
0.2
0
Control
4 hour
8 hour
16 hour
12/24 hour

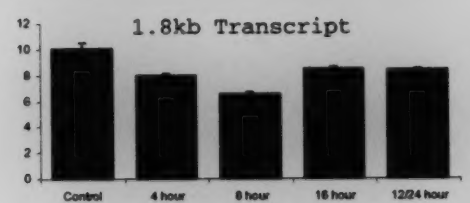
1.8kb Transcript
12
10
8
6
4
2
0
Control
4 hour
8 hour
16 hour
12/24 hour

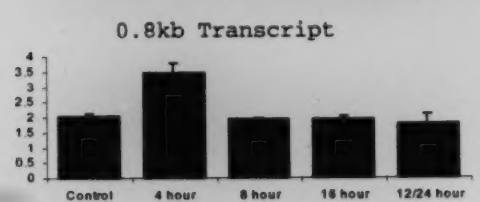
0.8kb Transcript
4
3.5
3
2.5
2
1.5
1
0.5
0
Control
4 hour
8 hour
16 hour
12/24 hour

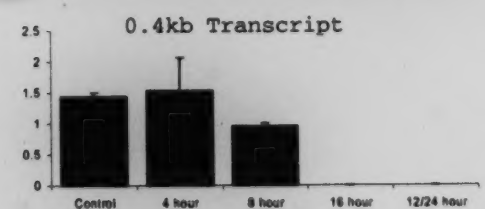
0.4kb Transcript
2.5
2
1.5
1
0.5
0
Control
4 hour
8 hour
16 hour
12/24 hour

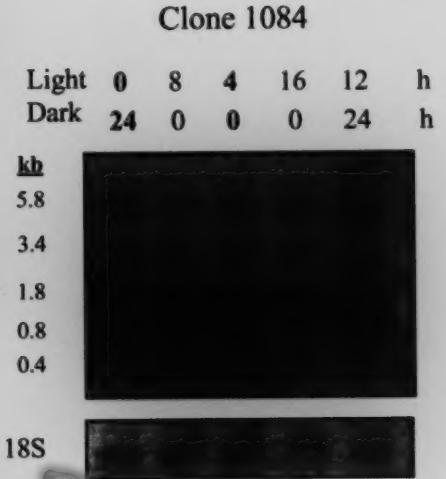
Clone 1084
Light 0 8 4 16 12 h
Dark 24 0 0 0 24 h
kb
5.8
3.4
1.8
0.8
0.4
18S

profile Northern blot are larger than 211 nucleotides, thus none can be eliminated based on size.

The nature of the molecular environment of the Commitment Phase retina makes it possible to uncover what changes in transcription need to occur in order for cells to commit to either apoptosis or survival. One way to identify these changes is by determining which genes are being targeted for altered transcription by identifying transcription factors whose levels of expression have been altered in response to light exposure. Therefore, to further pursue the characterization of transcription factor expression during LIRD the more sensitive, nuclease protection assay was employed. The results of these experiments are detailed in Chapter 5.

C. DISCUSSION

The majority of the transcripts identified as differentially expressed are up-regulated in response to the 4 h light treatment. This suggests a large amount of activity in retinal cells following light exposure, thus cells in the retina are responding to the alterations in the molecular environment caused by the light assault and not merely shutting down.

The technique of differential cross-screening is extremely laborious and time intensive. From 10,000 clones initially screened less than 1% were found to be differentially expressed. However, from the 54 clones that were isolated all 26 clones that were used to probe LIRD profile Northern blots were confirmed to be differentially expressed, demonstrating differential cross-screening is a reliable method for the isolation of differentially expressed transcripts.

Confirmation of clone differential status by Northern analysis and identification of a transcript previously described as differentially expressed during LIRD in this cross-screen, is evidence for the effectiveness and validity of the use of differential cross-screening to identify and isolate transcripts whose levels change over the course of LIRD. The effective use of this method is not isolated to the rat LIRD model. This protocol could be used to identify differences in transcript levels and isolate differentially expressed transcripts in any two molecular environments.

CHAPTER 5

EXPRESSION PATTERN OF TRANSCRIPTION FACTORS: EVALUATED USING NORTHERN ANALYSIS, NUCLEASE PROTECTION ASSAY AND RT-PCR

A. INTRODUCTION

The Commitment Phase of LIRD is predicted to represent a state in which intracellular and extracellular events come to dictate whether individual cells will undergo apoptosis or not. Thus, changes in the expression of specific genes are necessary. Alteration of gene expression is expected to occur through the action of transcription factors (TF) (Alberts *et al.*, 1994, Freund *et al.*, 1996). TF proteins can act in an independent, synergistic or antagonistic manner, to regulate the response to environmental signals or to initiate signals, and thus effect desired intracellular and extracellular changes. Since a substantial amount of experimental data on the signal pathways and target genes associated with many TFs is available, determining which TFs may be involved during the initial stage of LIRD will aid in predicting which gene products and signal transduction pathways could be involved in retinal degeneration.

In accordance with the prediction that the process of priming cells to activate an apoptotic or survival strategy in response to the light treatment involves a change in gene expression, a TF mRNA was isolated from the Commitment Phase cDNA library as a differentially expressed clone (clone 1084, putatively identified as TF Otx2). In the tertiary cross-screen of the cDNA library the 4 h light treatment cDNA probe hybridization signal with clone 1084 was more intense than that of the control cDNA probe. This suggested that the amount of TF clone 1084 transcript in the retina was increased in response to 4 hours of light treatment. Clone 1084 contains a 1 kb insert. A 750 kb section of this insert was sequenced. This sequence matched the 211bp partial sequence for the Otx2 mRNA in the GenBank database (score 383, identity 196/197). Clone 1084 detected five transcripts on LIRD profile Northern blots (refer to figure 4-7). Three of these transcripts were down-regulated in response to 4 h light treatment and the other two transcripts were up-regulated. Because the size of the full length rat Otx2 mRNA is not known it was not possible to determine if any of the transcripts detected by Northern analysis corresponded to Otx2. For this reason it was decided to use the Nuclease Protection Assay (NPA) to determine the expression pattern of Otx2 during LIRD and to resolve the question of which band on the Northern blot corresponds to the Otx2 transcripts. The NPA is regarded as a more sensitive method for the detection of low amounts of transcript (TF mRNAs are not expected to be abundant), requires less

template RNA than Northern analysis, and does not require the full length of the Otx2 sequence to be known. RT-PCR was then employed to verify the NPA results.

To gain a better perspective of what was occurring during LIRD the expression patterns of select retina-specific (Crx) and apoptosis related (c-fos, p53, NFκβ) transcription factors were also examined. The role of apoptosis related TFs p53 and c-fos has been studied by several groups in different models of human retinal degeneration (Wenzel *et al.*, 2000;Marti *et al.*, 1998; Hafezi *et al.*, 1998; Rich *et al.*, 1997). c-fos is a member of the Fos TF family which, together with members of the Jun TF family, comprise a group of TFs termed immediate early response (IER) TFs (Herdegen *et al.* 1998). TF p53's role in the initiation of apoptosis in response to DNA damage is well documented (reviewed in Li, 1999). The roles of these TFs appears to vary between the retinal degeneration models examined (Rich *et al.*, 1997;Marti *et al.*, 1998; Hafezi *et al.*, 1998; Wenzel *et al.*, 2000; Bussolino *et al.*, 1998). Therefore the expression of these TFs was chosen for examination during the course of LIRD. NFκβ is known to interact with p53 and to play a role in apoptosis, and therefore its expression pattern was also examined.

A role in retinal development and transcriptional regulation of photoreceptor cell specific genes has been proposed for TFs Otx2 and Crx (Furukawa *et al.*, 1997; Baas *et al.*, 2000; Fong *et al.*, 1999; Bobola *et al.*, 1999; Bovolenta *et al.*, 1997). Mutations in the Crx gene are associated with several forms of hereditary retinal degeneration (reviewed in Sohocki *et al.*, 1998). Expression patterns of Otx2 and Crx following 4 h light treatment and during the course of LIRD were examined.

B. RESULTS

B-1 Nuclease Protection Assay (NPA) Ribosomal 18S and 28S RNA oligonucleotide probes were used as loading controls for the five RNA samples (control, 4 h light treatment, 8 h light treatment, 16 h light treatment, and 12 h light treatment followed by 24 h dark recovery). Comparison of hybridization signal intensity of 18S and 28S between the 5 samples revealed inconsistency in the amount of total RNA present in each sample (figure 5-1).

Figure 5-1: Nuclease Protection Assay on Light-Induced Retinal Degeneration Profile RNA

Nuclease protection assays were employed to measure relative levels of Otx2, p53, c-fos, and CRX mRNA levels during the course of LIRD. The results of two different NPA assays are shown (panel A and panel B).
A) NPA experimental results visualized on autoradiographs after being size fractionated on 8M urea 12% polyacrylamide gels (15 minute exposure). The first lane serves as a positive control, containing full length radiolabeled oligonucleotide probes (undigested). The second lane serves as a negative control, containing nuclease treated radiolabelled oligonucleotide probes (digested). The remaining lanes are sample lanes. Each contains total RNA from the treatment group indicated, all five radiolabelled oligonucleotide probes and has been subjected to nuclease treatment. The bottom autoradiographs depicts a 2 hour exposure of the same NPA gel.
B) NPA experimental results visualized on autoradiographs after being size fractionated on 8M urea 12% polyacrylamide gels (15 minute exposure). The first lane serves as a positive control, containing full length radiolabelled oligonucleotide probes (undigested). The second lane serves as a negative control, containing nuclease treated radiolabelled oligonucleotide probes (digested). The third lane contains 28S radiolabelled oligonucleotide probe hybridized to rat liver RNA. Thus confirming the size of the 28S protected oligonucleotide probe. The remaining lanes are sample lanes. Each contains total RNA from the treatment group indicated, all five radiolabelled oligonucleotide probes and has been subjected to nuclease treatment. The bottom autoradiograph depicts a 3 hour exposure of the same NPA gel.

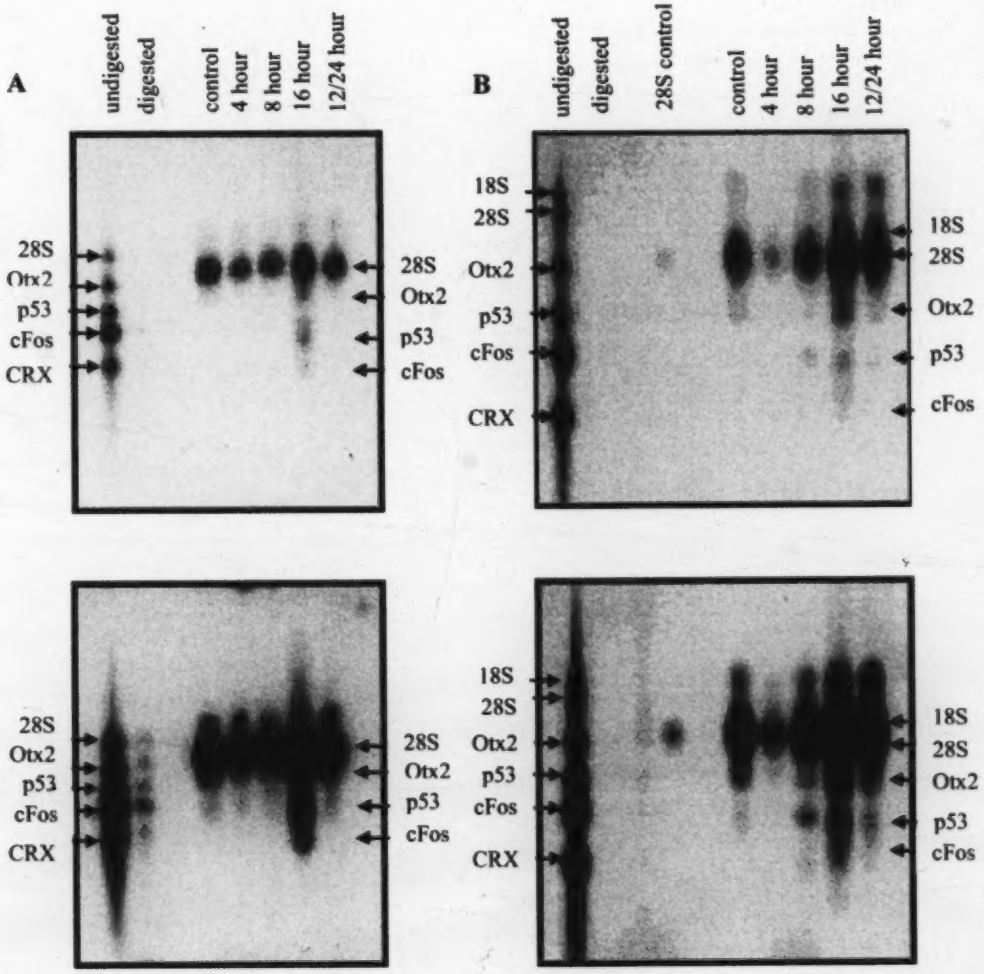
A
undigested
digested
control
4 hour
8 hour
16 hour
12/24 hour
28S
Otx2
p53
cFos
CRX
B
undigested
digested
28S control
control
4 hour
8 hour
16 hour
12/24 hour
18S
28S
Otx2
p53
cFos
CRX

The results of two separate NPA experiments were examined in order to determine the expression profile of Otx2, p53, c-fos, and Crx over the course of LIRD (figure 5-1 and 5-2). The results of the two sets of experiments are consistent. Briefly the profile shows: 1) In the control retinal RNA sample a weak signal was detected from the Otx2 oligonucleotide probe. 2) Following 4 h light treatment the Otx2 signal decreased. 3) TF expression levels of Otx2 following 8 h light treatment are similar to levels detected following 4 h light treatment. 4) Taking into account that there is approximately twice as much RNA in the 16 h treatment sample than in the 8 h treatment sample, following 16 h light treatment there appears to be an up-regulation of Otx2. 5) Following the 12 h light and 24 h dark treatment Otx2 transcript levels decreased and the hybridization signals from Otx2 approximate the intensity observed in the control. This profile shows that there is a decrease of Otx2 transcription during the Commitment phase of LIRD and that Otx2 transcription peaks during the Stress Response phase of LIRD.

In summary, based on amalgamated results of two separate NPA experiments, a down-regulation of Otx2 and p53 following 4 h light treatment is observed. Otx2 and p53 levels remain low following 8 h light treatment while c-fos levels increase. Transcript levels of Otx2, c-fos and, possibly Crx, all increase following 16 h light treatment and then decrease during the recovery phase (12 h light exposure, 24 dark recovery) of LIRD. p53 transcript levels peak following 8 h light treatment and then decrease.

B-2 Reverse-Transcriptase PCR (RT-PCR) analysis To confirm the expression pattern of Otx2, as determined by NPA, the expression pattern of Otx2 was further tested using the RT-PCR method. Ribosomal 18S RNA served as a loading control in this experiment. Control RT-PCR reactions were used to verify that the gene specific primers designed for the RT-PCR experiment amplified the targeted transcripts. Each set of primers was used in two control reactions, one with control total retinal RNA as a template and the other with 4 h light treated total retinal RNA as a template. In each case the amplified RT-PCR product was of the correct size indicating that the primers were gene specific (figure 5-3). In this analysis, NFκβ mRNA levels in the control and 4 h light treated rat retina were also tested.

Figure 5-2: Densitometric Analysis of NPA Autoradiographs

Densitometry readings of the hybridization signal intensities of the Otx2, p53 and c-fos oligonucleotide probes were taken. The signals were normalized to the 28S ribosomal RNA signal. These normalized expression patterns of Otx2, p53, and c-fos, over the course of LIRD, are presented in graph form.

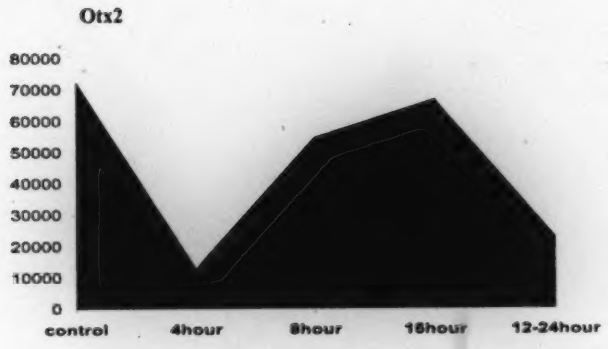
Otx2
80000
70000
60000
50000
40000
30000
20000
10000
0
control
4hour
8hour
16hour
12-24hour

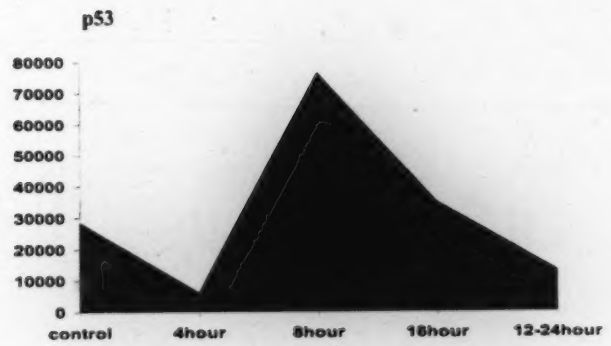
p53
80000
70000
60000
50000
40000
30000
20000
10000
0
control
4hour
8hour
16hour
12-24hour

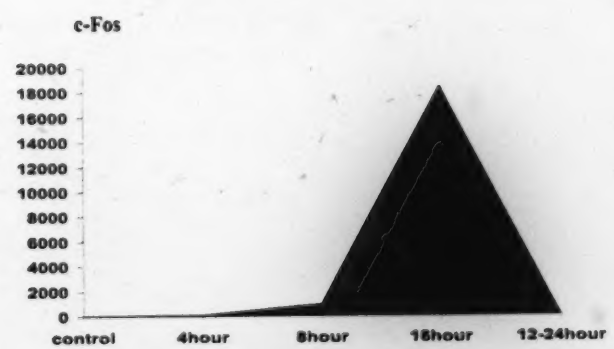
c-Fos
20000
18000
16000
14000
12000
10000
8000
6000
4000
2000
0
control
4hour
8hour
16hour
12-24hour

Figure 5-3: Detection of NFκβ and Otx2 Transcript in Control and 4 h Light Treated Retinal RNA Using RT-PCR

RT-PCR products were electophoresed on a 2% agarose gel.
lane 1: Gibco-BRL 1kb DNA ladder;
lane 2: Control retinae RNA with 18S RT-PCR primers (expected size 271bp),
lane 3: 4 h light treated retinae RNA with 18S RT-PCR primers (expected size 271bp),
lane 4: control retinae RNA with NFκβ RT-PCR primers (expected size 390bp),
lane 5: 4 h light treated retinae RNA with NFκβ RT-PCR primers (expected size 390bp),
lane 6: control retinae RNA with Otx2 RT-PCR primer (expected size 176bp),
lane 7: 4 h light treated retinae RNA with Otx2 RT-PCR primer (expected size 176bp).

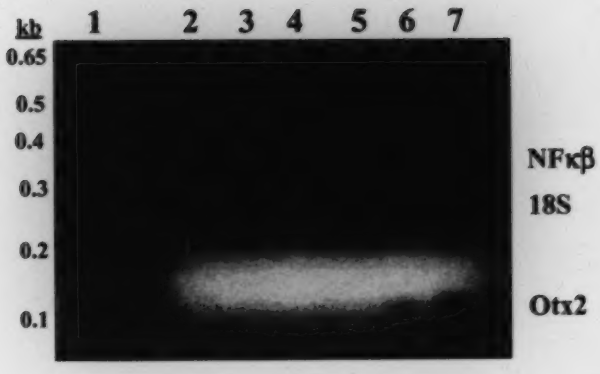
kb
1
2
3
4
5
6
7
0.65
0.5
0.4
0.3
0.2
0.1
NFκβ
18S
Otx2

Three primer sets (Otx2-specific, 18S-specific, NFκβ-specific) were used at the same time in the same reaction, first in a reaction containing total retinal RNA from control animals as template and second in a reaction containing total retinal RNA from 4 h light treated animals as template. RT-PCR products were size fractioned on a 2% agarose gel and visualized under UV light following ethidium bromide staining. In both the control RNA sample and 4 h light treated RNA sample the 18S product is visible. The Otx2 product is visible only in the 4 h light treated RNA sample lane. However, the expected NFκβ product was not visible in either the control RNA or 4 h light treated RNA sample lanes (figure 5-4).

To determine if the apparent absence of NFκβ and Otx2 products was a result of a paucity of amplified DNA, the two RT-PCR gels were blotted and the membranes probed with the RT-PCR amplified NFκβ and Otx2 fragments respectively. 18S ribosomal RNA was used as a loading control. Accurate normalization of the NFκβ autoradiography results to the 18S ribosomal loading control, using densitometry measurements , was difficult to accomplish. The measurements presented in figure 5-4G, reveal that levels of NFκβ transcript increase in response to 4 h light exposure. Examination of Otx2 autoradiography results following a 15 minute exposure shows hybridization of the Otx2 probe in experimental lane 1 (control rat retinal RNA) (figure 5-4). A longer exposure reveals Otx2 hybridization in experimental lane 2 (4 h light treated retina RNA). Thus, it appears that Otx2 transcript levels decrease following 4 h light exposure in the LIRD model. This is in agreement with the NPA experimental results.

B-3 Northern Analysis As a final confirmation of the results, LIRD profile Northern blots were probed with NFκβ and Otx2 RT-PCR products. This also made it possible to establish the expression pattern of these TFs over the course of LIRD. The NFκβ probe hybridized to three transcripts on the LIRD profile blot (figure 5-5). mRNA levels of the smallest of these transcripts (0.7 kb) decreases following 4 h light exposure and continues to decrease as LIRD progresses. No change is observed in the 2.3 kb transcript mRNA levels over the course of LIRD. Levels of the largest transcript (3.6 kb) increase following 4 h light exposure. This is consistent with the RT-PCR results. The hybridization signal of this transcript then decreases, until levels approximating control

Figure 5-4: Alterations in Otx2 and NFκβ Transcript Levels Following 4 h Light Treatment: RT-PCR Analysis

Southern transfers were preformed on the RT-PCR gel containing; lane 1: RT-PCR product from reaction containing control retinal RNA and all three gene specific primer sets (Otx2, NFκβ, and 18S), lane 2: RT-PCR product from reaction containing total retinal RNA from 4 h light treated animals and all three gene specific primer sets. The Southern blots were probed with Otx2 and NFκβ sequence obtained from the control RT-PCR reactions.

A) Photograph of RT-PCR gel. The 18S ribosomal RNA RT-PCR product visualized on the RT-PCR gel is present as a loading control.

B) An autoradiograph following a 15 minute exposure of the RT-PCR gel Southern blot probed with Otx2 sequence obtained from the control RT-PCR reaction.

C) An autoradiograph following a 3 h exposure of the same Southern blot.

D) Photograph of the RT-PCR gel showing the 18S ribosomal RNA RT-PCR product used as a loading control, and the approximately 400bp non-specific RT-PCR product (*).

E) An autoradiograph following a 15 minute exposure of the RT-PCR gel Southern blot probed with NFκβ sequence obtained from the control RT-PCR reaction. The NFκβ probe does not hybridize to the non-specific 400bp RT-PCR product but does hybridize to a fragment the same size as that observed in the control RT-PCR reaction for NFκβ.

F) An autoradiograph following a 3 h exposure to the same Southern blot.

G) Densitometry was performed to measure the intensity of the hybridization signals of the NFκβ probe in the control and 4 h sample lanes. The results were

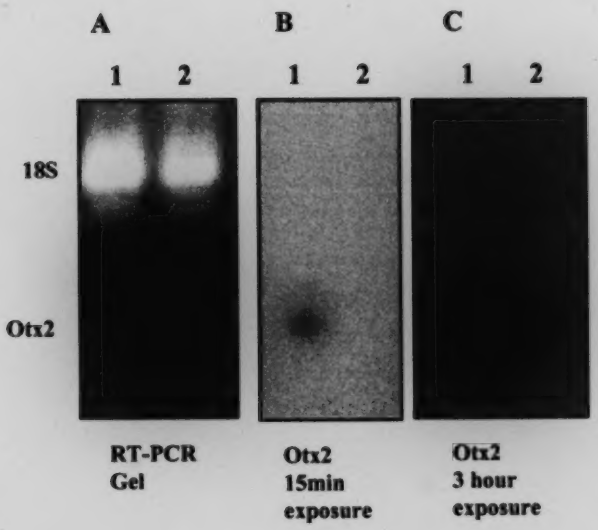
A
B
C
1
2
1
2
1
2
18S
Otx2
RT-PCR
Gel
Otx2
15min
exposure
Otx2
3 hour
exposure

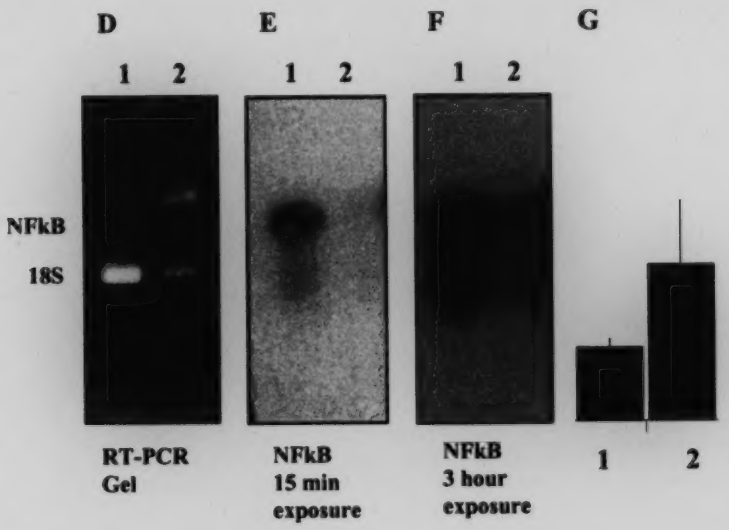
D
E
F
G
1
2
1
2
1
2
NFkB
18S
RT-PCR
Gel
NFkB
15 min
exposure
NFkB
3 hour
exposure
1
2

Figure 5-5: LIRD Profile Northern Blots Probed with RT-PCR Product NFκβ

LIRD profile Northern blot was probed with NFκβ derived from the RT-PCR reaction. The Northern blots contain total RNA extracted from control rat retinae, 4 h light treated (commitment phase) rat retinae, 8 h light treated (execution phase) rat retinae, 16 h light treated (stress response phase) rat retinae, and 12 h light-24 h dark treated (recovery phase) rat retinae. Densitometry was performed on each of the bands that appeared on the Northern blot. mRNA levels were then normalized with the 18S ribosomal RNA. The graphs depict a graphical representation of normalized transcript levels. Each transcript corresponds to a different graph.

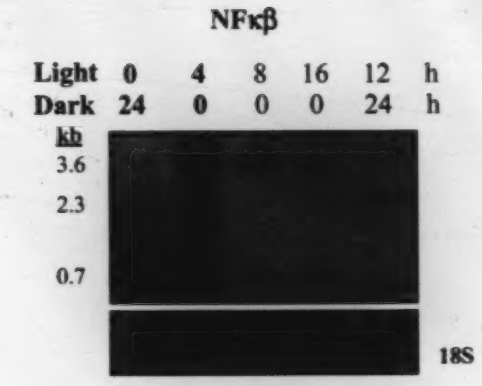
NFκβ
Light 0 4 8 16 12 h
Dark 24 0 0 0 24 h
kb
3.6
2.3
0.7
18S

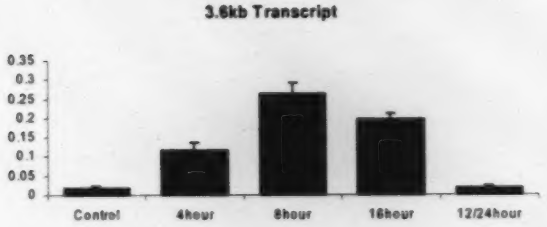
3.6kb Transcript
0.35
0.3
0.25
0.2
0.15
0.1
0.05
0
Control
4hour
8hour
16hour
12/24hour

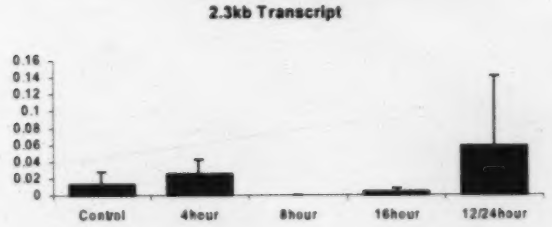
2.3kb Transcript
0.16
0.14
0.12
0.1
0.08
0.06
0.04
0.02
0
Control
4hour
8hour
16hour
12/24hour

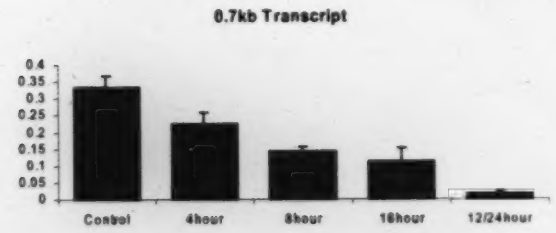
0.7kb Transcript
0.4
0.35
0.3
0.25
0.2
0.15
0.1
0.05
0
Control
4hour
8hour
16hour
12/24hour

levels are reached following the 12 h light; 24 h dark treatment, following a peak at the 8 h light treatment. The NFκβ transcript has been partially sequenced and measures 2245 nucleotides in length (Accession number AF079314), suggesting that either the 2.3 or 3.6 kb band on the NFκβ probed LIRD Northern blot corresponds to NFκβ transcript signal.

The Otx2, RT-PCR-derived probe, hybridized to four transcripts (7.2 kb, 4.1 kb, 3.0 kb, and 1.3 kb) on the LIRD profile Northern blot. mRNA levels of all four transcripts increase following 4 h light exposure and then decrease (figure 5-6). This hybridization pattern is opposite to that determined by NPA and RT-PCR experiments. Suggesting that clone 1084, putatively identified as Otx2, may not contain the Otx2 transcript.

The hybridization pattern of the Otx2 RT-PCR derived-probe was compared to that of the clone 1084 (figure 5-6) in an effort to determine if clone 1084 did contain Otx2 cDNA. Clone 1084 hybridized to five transcripts (5.8 kb, 3.4 kb, 1.8 kb, 0.8 kb, and 0.4 kb). Following a 4 h light exposure the levels of the 0.4 and 0.8 kb transcripts increase while levels of the 5.8 kb, 3.4 kb, and 1.8 kb transcripts decrease. Levels of the 1.8 kb transcript decrease following 8 h light treatment, increase following 16 h light treatment and remain high following the 12 h light; 24 h dark treatment. After the initial decrease of 5.8 kb and 3.4 kb transcripts the levels gradually increase to control levels. The hybridization patterns with the Otx2 RT-PCR product and clone 1084 are thus different. Indicating that it is unlikely that clone 1084 contains Otx2 cDNA.

C. DISCUSSION

The difference in hybridization patterns on LIRD profile blots between clone 1084 and the Otx2 RT-PCR product could be explained by suggesting that the putative identification of clone 1084 as Otx2 is incorrect and clone 1084 either represents a novel Otx2-like transcript or a new member of the Otx2 family or by suggesting that the Otx2 RT-PCR product and clone 1084 probes used were dissimilar enough to hybridize to different unrelated (non-Otx2) sequences. The insert size of clone 1084 is approximately 1.0 kb in length. 750 bp of this insert was sequenced and matches the 211 bp partial sequence available for Otx2 in its entirety (figure 5-7). The remaining clone insert sequence had no significant match to known

Figure 5-6: Comparison of Clone 1084 and Otx2 (RT-PCR Product) Hybridization Patterns on LIRD Profile Northern Blots

The RT-PCR product obtained using Otx2 specific primers was used as a probe on a LIRD profile Northern blot. The Northern blots contain total RNA extracted from control rat retinae, 4 h light treated (commitment phase) rat retinae, 8 h light treated (execution phase) rat retinae, 16 h light treated (stress response phase) rat retinae, and 12 h light-24 h dark treated (recovery phase) rat retinae. Densitometry and normalization to the 18S ribosomal RNA was performed. Results are presented in graph form bellow the autoradiograph. Clone 1084, which was putatively identified as Otx2 using the GenBank sequence database, was also used to probe a LIRD profile Northern blot (this Northern blot is the same as that shown in figure 4-7). Densitometry and normalization to the 18S rRNA was performed. Results are presented in graph form bellow the autoradiograph.

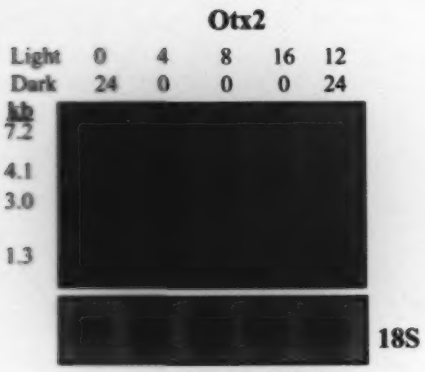
Otx2
Light 0 4 8 16 12
Dark 24 0 0 0 24
kb
7.2
4.1
3.0
1.3
18S

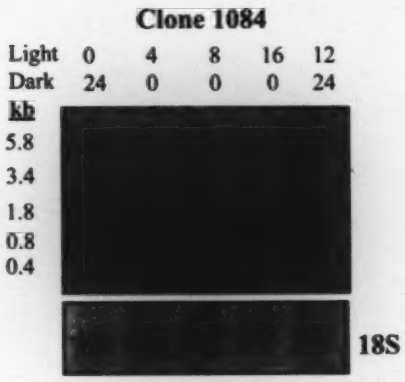
Clone 1084
Light 0 4 8 16 12
Dark 24 0 0 0 24
kb
5.8
3.4
1.8
0.8
0.4
18S

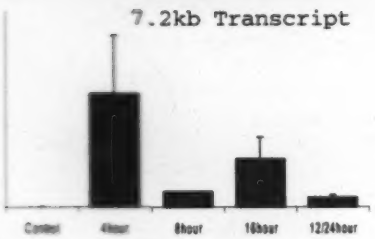
7.2kb Transcript
Control
4hour
8hour
16hour
12/24hour

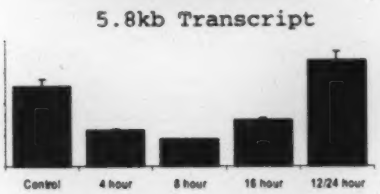
5.8kb Transcript
Control
4 hour
8 hour
16 hour
12/24 hour

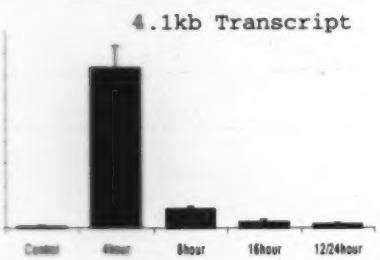
4.1kb Transcript
Control
4hour
8hour
16hour
12/24hour

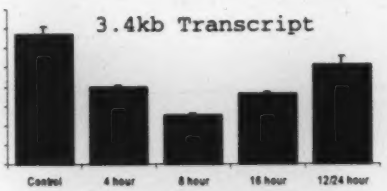
3.4kb Transcript
Control
4 hour
8 hour
16 hour
12/24 hour

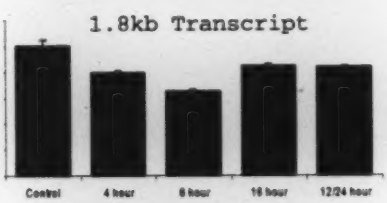
1.8kb Transcript
Control
4 hour
8 hour
16 hour
12/24 hour

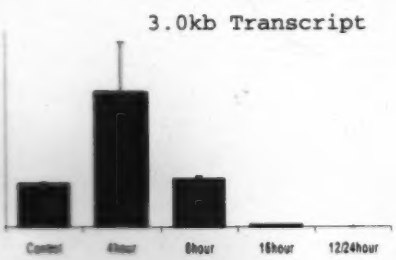
3.0kb Transcript
Control
4hour
8hour
16hour
12/24hour

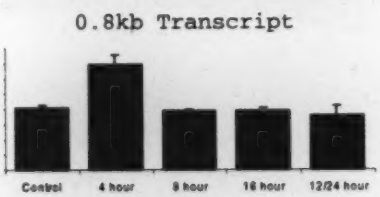
0.8kb Transcript
Control
4 hour
8 hour
16 hour
12/24 hour

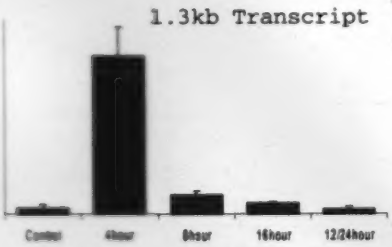
1.3kb Transcript
Control
4hour
8hour
16hour
12/24hour

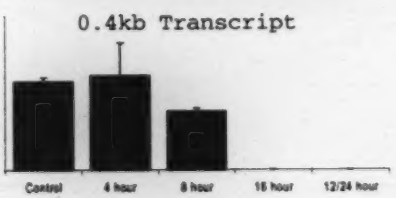
0.4kb Transcript
Control
4 hour
8 hour
16 hour
12/24 hour

Figure 5-7: Comparison of GenBank Otx2 Sequence to Sequence of Clone 1084 and Otx2 RT-PCR Product

Alignment of partial Otx2 sequence, available from GenBank database, clone 1084 insert sequence and RT-PCR product using Otx2 specific primers.

CCNGGGCTGCANGANTCGGCACGANCAGGCTTCAGGTTATAGTCAAGGCTATGCTGGC 58
CAGGCTTCAGGTTATAGTCAAGGCTATGCTGGC 47

TCGACTTCCTACTTTGGGGGCATGGACTGTGGATCTTACTTGACCCCTATGCATCACC 65
TCGACTTCCTACTTTGGGGGCATGGACTGTGGATCTTACTTGACCCCTATGCATCACC 116
TCGACTTCCTACTTTGGGGGCATGGACTGTGGATCTTACTTGACCCCTATGCATCACC 105

AGCTTCCTGGACCAGGGGCCACACTCAGTCCCATGGGTACCAATGCTGTTACCAGTCA 123
AGCTTCCTGGACCAGGGGCCACACTCAGTCCCATGGGTACCAATGCTGTTACCAGCCA 174
AGCTTCCTGGACCAGGGGCCACACTCAGTCCCATGGGTACCAATGCTGTTACCAGTCA 163

CCTCAATCAGTCCCCAGCTTCTCTTTCCACCCAGGGATATGGAGCTTC
CCTCAATCAGTCCCCAGCTTCTCTTTCCACCCAGGGATATGGAGCTTCAAGCTTGGGT 232
CCTCAATCAGTCCCCAGCTTCTCTTTCCACCCAGGGATATGGAGCTTC

TTTAACTCAACCACTGATTGCTTGGATTATAAGGACCAAACTGCCTCTTGGAAGCTTA 290

ACTTCAATGCTGACTGCTTGGATTATAAGGATCAGACATCCTCATGGAAATTCCAGGT 348

TTTGTGAANACCCGTAGGAGCTATTTTTTCTTTTTTTGTGGGTGATTTTTAAATATGCT 406

GGGCTGGACATTCCAGTTTTAGCCAGGCATTGGTTAAAAGANTTAGATGGGATGATGC 464

TCTCAGACTCCTGGTCAAAGTTACCGAGAGGCATANAAGGAAAAAGGAAGGGCCTTA 522

NAANGGTCCATCAACCANCAACCTGAGATGGATAAACTAATCTACTTAANATTCTGTT 580

ATAGTTCTANATCATTGGTTTTTCTGATTTGCAAATGATTGATCCAAATATATTCTAN 638

CAACACGCAACCAAACNCCACTCCAAGCGAAAATCAAACACAACTGAATTATGGGAAG 696

GAAGGTCNTGGNCTTCAAAACAGGCTTATCTGAATTTTTAACCAATCTTTGGTTGAAN 754

RT-PCR product using Otx2 specific primers
Clone 1084 sequence
GenBank partial Otx2 Sequence

gene sequences. The RT-PCR gene specific primers were designed based on available Otx2 sequence. Therefore a significant amount of sequence is present in the clone 1084 sequence and absent from the RT-PCR Otx2 product. It is possible that this non-overlapping region represents a fusion of a separate cDNA fragment that is hybridizing to another unrelated transcript and is therefore responsible for the differences in hybridization patterns observed. The results obtained for Otx2 (RT-PCR and NPA) and NFκβ (RT-PCR and Northern blot) are consistent. Since the full length of Otx2 is unknown the use of Northern analysis in this case is inconclusive. Thus, it seems that the NPA and RT-PCR methods are the best available indicators of Otx2 expression during LIRD. Based on these methods it appears that Otx2 transcript levels decrease following 4 h light treatment.

Based on the NPA results it appears that the expression levels of c-fos, p53, and Otx2 change over the course of LIRD. Whether Crx transcript levels also change cannot be determined from these experiments. Crx is normally expressed in photoreceptor cells (Furukawa *et al.*, 1997). Therefore, Crx transcripts are predicted to be present in the control retinal RNA sample. The absence of a Crx probe signal could be attributed to several factors. The oligonucleotide probe used for the detection of the Crx transcripts shared only a 10 bp region of identity with the Crx transcript. This very small amount of sequence identity may be insufficient for effective hybridization of the probe to the mRNA, resulting in the digestion of both the Crx transcript and oligonucleotide probe upon nuclease addition and thus absence of Crx probe signal. In future experiments a larger Crx oligonucleotide probe should be used. This would allow for a greater region of sequence similarity between the probe and transcript and promote effective hybridization.

The observed up-regulation of c-fos expression following 8 h light treatment is consistent with observations made by Rich *et al.* (1997) in rd (retinal degeneration) mice. In these experiments an up-regulation of c-fos photoreceptor cell expression was observed just prior to the peak of photoreceptor cell apoptosis. However, the absence of c-fos expression in the rd mouse model of retinal degeneration has no protective effect on the photoreceptor cells (Marti *et al.*, 1998). The degeneration in the rd; c-fos -/- mice is identical to that observed in rd; c-fos+/+ animals. Conversely, in a mouse model of

retinal degeneration, in which white light was used to induce degeneration, the absence of c-fos expression conferred full protection upon the photoreceptor cells of these mice (Wenzel *et al.*, 2000). Thus the precise mechanism that leads to the apoptotic loss of photoreceptor cells is diverse. Since p53 is capable of repressing c-fos expression (Tendler *et al.*, 1999) it is interesting that the up-regulation of c-fos occurs following the down-regulation of p53. However, the up-regulation of c-fos and the suggested interaction between c-fos and p53 do not necessarily indicate that either c-fos or p53 are participating directly in LIRD.

Using RT-PCR and NPA techniques respectively, an induction of NFκβ transcript and a reduction in p53 transcript levels following 4 h light treatment was observed. Northern analysis of NFκβ expression during LIRD confirms the up-regulation of transcript following a 4 h light treatment that was detected using RT-PCR methods. Interaction between NFκβ and p53 is known to be necessary for p53 dependent apoptosis (Ryan *et al.*, 2000). Interestingly, NFκβ can both induce and prevent apoptosis depending on how it is activated. Activation through the p53 pathway results in NFκβ participating in the induction of apoptosis while activation through the TNFα pathway results in NFκβ inhibiting apoptosis (Ryan *et al.*, 2000). An NFκβ site is present in the HO-1 promoter region suggesting that NFκβ may play a role in the induction of HO-1 expression (Lavrovsky *et al.*, 1993). Since HO-1 expression peaks following the 16 h light treatment, subsequent to the induction of NFκβ, this suggests that NFκβ could be involved in the induction of the oxidative stress response. It is unknown if induction of apoptosis during LIRD is p53 dependent. In a mouse model of retinal degeneration induced by white light treatment the absence of p53 does not prevent apoptosis suggesting that, at least in this system, photoreceptor cell apoptosis is occurring through a p53 independent pathway (Marti *et al*, 1998). However, considering the variable results obtained in experiments that have eliminated c-fos expression in the eye, no conclusion can be drawn as to the role of p53 in our LIRD model.

The expression profiles of TFs Otx2, p53, c-fos, Crx, and NFκβ were examined over the course of LIRD. The expression of these transcription factors changes in response to light treatment. The discrepancy in the expression profile of Otx2 when

using Northern analysis versus NPA and RT-PCR may indicate that clone 1084, putatively identified as Otx2, represents a new member of the Otx2 gene family.

CHAPTER 6

RIBOSOMAL PROTEIN EXPRESSION OVER THE COURSE OF LIRD

A. INTRODUCTION

Searching the GenBank database for sequence homologies to the sequences of the 54 differentially expressed clones revealed that a large proportion (9%) of these clones correspond to rat genes encoding ribosomal proteins (RP). Ribosomal proteins associate with either the large or small subunit of the ribosome. To date more than 80 such proteins have been identified (Davies and Fried, 1995; Wool, 1979). In prokaryotes the ribosomal protein genes are found in clusters, while in eukaryotes they are dispersed throughout the genome. Despite this dispersal of ribosomal protein genes, ribosomal proteins are maintained at approximately equimolar amounts and assembly of the ribosome occurs in a stoichiometrically precise manner. This suggests that the transcription and translation of ribosomal proteins is regulated by trans-acting factors (Davies and Fried, 1995; Kenmochi *et al.*, 1998; Wool, 1979). Most *Drosophila* ribosomal proteins have been mapped to polytene chromosome regions at or near Minute loci (Saeboe-Larssen *et al.*, 1996). Other RPs have extra-ribosomal roles as tumor suppressor, or regulators of oogenesis (Stewart & Denell, 1993; Crampton & Laski, 1994). In humans, ribosomal proteins have been implicated in a variety of cancers, as well as in DNA damage repair, cell cycle regulation, cell differentiation, apoptosis, and in human diseases (Pogue-Geile *et al.*, 1991; Watson *et al.*, 1992; Frigerio *et al.*, 1995; Chiao *et al.*, 1992; Seshadri *et al.*, 1993; Deutsch *et al.*, 1997; Neumann and Krawinkel, 1997; Horino *et al.*, 1998; Goldstone and Lavin, 1993; Naora *et al.*, 1998).

A total of 15 ribosomal protein cDNA clones were obtained to investigate the expression of ribosomal proteins during LIRD. Five of the clones were identified through the differential cross-screening of the Commitment Phase cDNA library, 3 were isolated in the differential cross-screening of the Execution Phase cDNA library (Michelle Chambers, unpublished results), one had been isolated previously, and the remaining six were purchased from Research Genetics (summarized in table 6-1). These additional RP cDNA clones were purchased because they have been reported in the literature as being associated with cellular changes during apoptosis or oncogenesis. Based on their expression pattern over the course of LIRD, the ribosomal proteins examined were divided into four categories. The initial RP probes that we had on hand (11 of the 15) were used to screen LIRD Slot blots. RP probes with a differential

Table 6-1: Summary of Ribosomal Protein Clones and Experiments

» indicates ribosomal proteins which were identified as differentially expressed clones in the Commitment phase cDNA differential cross-screen and were used to probe LIRD profile Northern blots to confirm differential status. This was done before their putative ID was known. Since their expression pattern was already known they were never subjected to Slot blot analysis.

† indicates that the experiment did not work.

* indicates that the ribosomal protein clone was not available at the time of the experiment.

- indicates that the experiment was not performed. In the case of RPS6, the experiment was not performed because Slot blot analysis showed no differential expression. In the case of RPS2/RPS4, the experiment was not performed because a separate RPS2 probe was purchased so that the hybridization signal from RPS2 could be observed without interference from the RPS4 hybridization signal.

✓ indicates that the experiment was performed.

Clone Number	Source	Slot Blot Analysis	LIRD profile Northern Analysis	Degenerative Prostate Northern Analysis
RPS16	Commitment Phase cDNALibrary	✓	✓	✓
RPL7	Commitment Phase cDNALibrary	»	✓	✓
RPL30	Commitment Phase cDNALibrary	»	✓	✓
RPL12	Commitment Phase cDNALibrary	✓	✓	✓
RPL19	Commitment Phase cDNALibrary	✓	✓	✓
RPS10	Execution Phase cDNALibrary	✓	✓	✓
RPS27a	Execution Phase cDNALibrary	✓	†	✓
RPL5	Execution Phase cDNALibrary	✓	✓	✓
RPS28	Independent Experiment	✓	✓	✓
RPS3	Research Genetics	✓	✓	†
RPS3a	Research Genetics	✓	✓	✓
RPS6	Research Genetics	✓	-	✓
RPS2	Research Genetics	*	✓	✓
RPS2/S4	Research Genetics	✓	-	-
RPS24	Research Genetics	*	✓	✓

hybridization pattern on these Slot blots, together with RP probes we obtained after the Slot blot study, were used to screen Northern blots of the LIRD profile. The expression pattern of RP in a non-retinal model of model of cell death (androgen deprivation-induced rat prostate degeneration) was also examined (Tenniswood *et al.*, 1992)

B. RESULTS

B-1 Slot Blot Analysis Through Slot blot analysis it was determined that the transcript levels of 10 of the 11 RP genes tested (the exception being RPS6), were affected by the 4 h light treatment (figure 6-1). To verify this observation Northern blot analysis was performed with RPs that showed altered expression in response to light exposure (figure 6-2). The Northern blot results confirmed Slot blot results by detecting a change in the level of RP gene expression and allowed for further evaluation of ribosomal protein expression over the entire course of LIRD.

B-2 Northern Blot Analysis Twelve RP genes (table 6-1) were examined by Northern analysis (RPL12, RPS16, RPS28, RPS2, RPS10, RPS3a, RPS3, RPL5, RPL19, RPL7, RPL30, and RPS24). Northern blot analysis revealed that during each phase of LIRD a different set of RP genes is upregulated (figure 6-2). During the commitment phase of LIRD all the RP genes examined are up-regulated. However, the degree to which the genes are induced varies. Genes encoding RPS24, RPL12 and RPS28 are up-regulated only slightly while RPL19, RPS16, RPS3, RPL30, RPL7, RPS3a, RPL5, RPS2, and RPS10 show pronounced increases in transcript levels compared to controls. Following the 8 h light treatment transcript levels of RPL7, RPS3a, RPL5, RPS10, RPS16, and RPS2 decrease. Transcript levels of RPL19, RPL30, RPL12, RPS24 and RPS28 remain high or constant following the 8 h light treatment. Thus, a change is observed in the RP genes expressed during the commitment and execution phase of LIRD. A different set of RP genes are expressed during the stress response phase (16 h light treatment). RPS16, RPS3 and RPL19 transcripts continue to be present at high levels although the level of expression is approaching levels seen in the control. Levels of RPS3a, and RPL5 continue to decrease but remain above levels detected in the control retinae. RPL7, RPL12, and RPL30 transcript levels are lower than control levels while RPS24 transcript

Figure 6-1: Hybridization Pattern of Ribosomal Protein Clones on Slot Blots Containing Control and 4 h Light Treated Retinal RNA

Clones encoding eleven different ribosomal proteins were used as probes on eleven different Slot blots containing total RNA from control and 4 h light treated rat retinae. Ribosomal 18S RNA was used as a loading control.

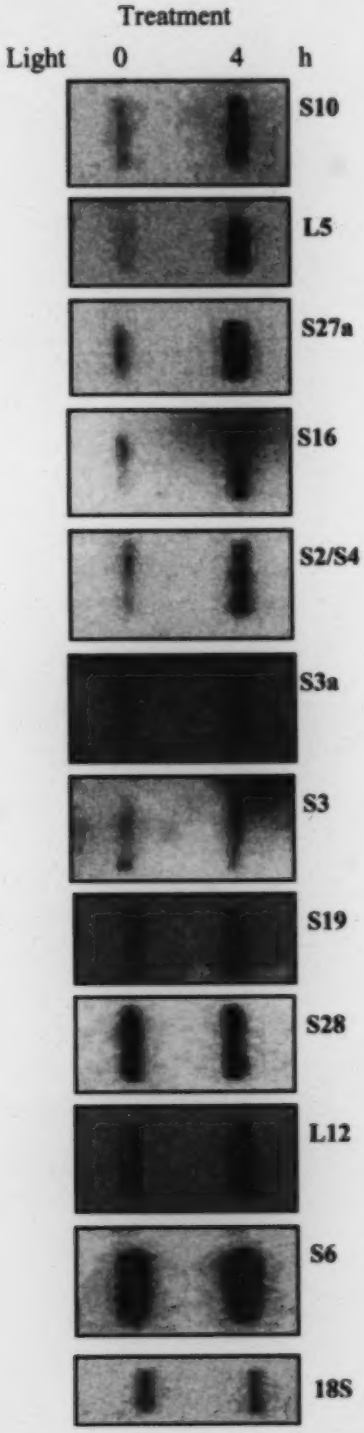
Treatment
Light 0 4 h
S10
L5
S27a
S16
S2/S4
S3a
S3
S19
S28
L12
S6
18S

Figure 6-2: Change in Ribosomal Protein Gene Expression Pattern Over LIRD

LIRD profile Northern blots were probed with 12 different ribosomal protein gene clones to examine the expression pattern of ribosomal protein genes over the course of LIRD. The Northern blots contain total RNA extracted from control and light treated rat retinae as indicated. During each of the 4 phases of LIRD (commitment, execution, stress response, and recovery) there is an high level of expression of a different set of ribosomal protein genes.

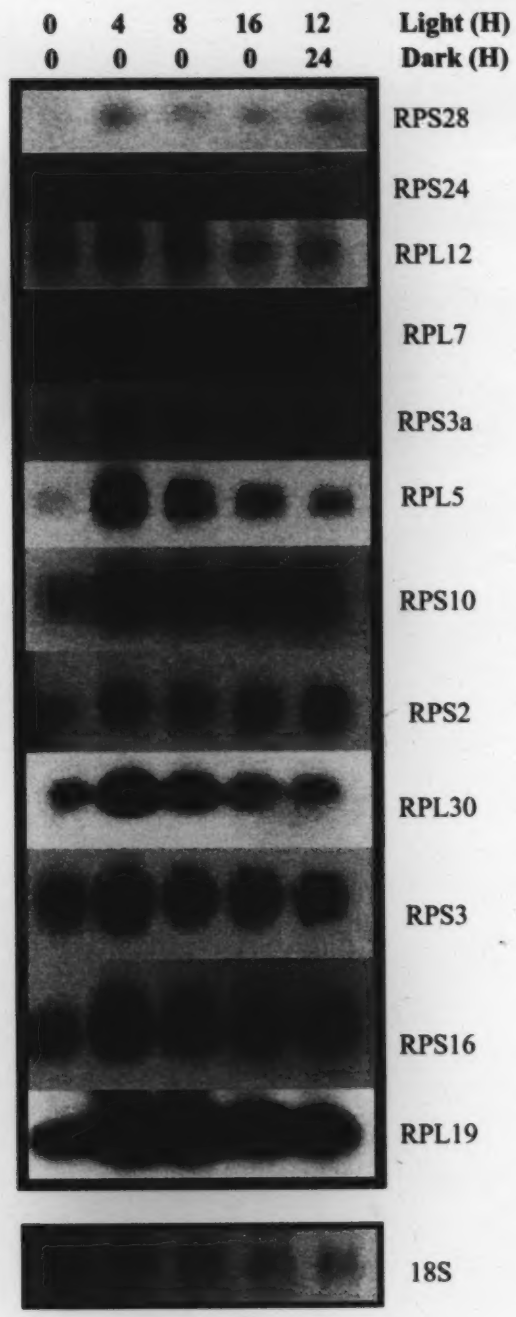
0 4 8 16 12 Light (H)
0 0 0 0 24 Dark (H)
RPS28
RPS24
RPL12
RPL7
RPS3a
RPL5
RPS10
RPS2
RPL30
RPS3
RPS16
RPL19
18S

levels have decreased to control levels. Expression of RPS2, RPS10, and RPS28 remain approximately the same as those detected following 8 h of light treatment. During the recovery phase high levels of RPS16, RPS3, RPL30, RPS2 and RPS10 expression are observed, while RPL5, RPS3a, RPL7, RPL12, and RPS28 transcript levels are low. The level of RPL7 and RPL12 mRNA is below control levels while the level of all other ribosomal proteins is higher than or approximates transcript levels observed in the control retinae. Based on observed RP gene expression patterns each phase of LIRD can be defined based on a unique RP gene expression signature and the RP genes examined can be grouped into four categories.

Category 1: Ribosomal Proteins L5, S3a, L30, S3, S16 Northern blot analysis revealed that ribosomal proteins in this category showed a marked induction of transcript levels following a 4 h light exposure. Transcript levels peaked after either 4 h or 8 h of light exposure, after which time levels gradually decrease to levels approximating those found in the control (figure 6-3).

Category 2: Ribosomal Proteins L7, L12 Members of the second category of ribosomal proteins are characterized by a hybridization pattern showing an increase of mRNA levels between the control group and the 4 h and 8 h light treatments. The high levels of mRNA after 4 h and 8 h of light exposure sharply decrease following the 16 h light exposure. In the recovery phase (12 h light/24 h dark) the mRNA levels are lower than those found in the control retinae (figure 6-4).

Category 3: Ribosomal Proteins S10, L19, S2 The expression pattern of this category of RPs shows a marked increase in mRNA levels, compared to control levels, following a 4 h light exposure. mRNA levels decrease gradually as degeneration progresses. Recovery phase mRNA levels are still higher than those detected in control retinae (figure 6-4).

Category 4: Ribosomal Protein S24, S28 The hybridization patterns of RPS24, and RPS28 show no significant fluctuation over the course of rat LIRD (figure 6-2). There is

Figure 6-3: Graphical Representation of Category 1 RP Expression Over the Course of LIRD

Northern blots containing total RNA extracted from the retinae of control rats and from the retinae of rats subjected to each of the four experimental treatments were probed with individual ribosomal protein cDNA clones. Densitometry was performed on hybridization signals from each ribosomal protein gene clone. The signals were then normalized to the 18S ribosomal RNA. The normalized expression profile over the course of LIRD is depicted in graph form.

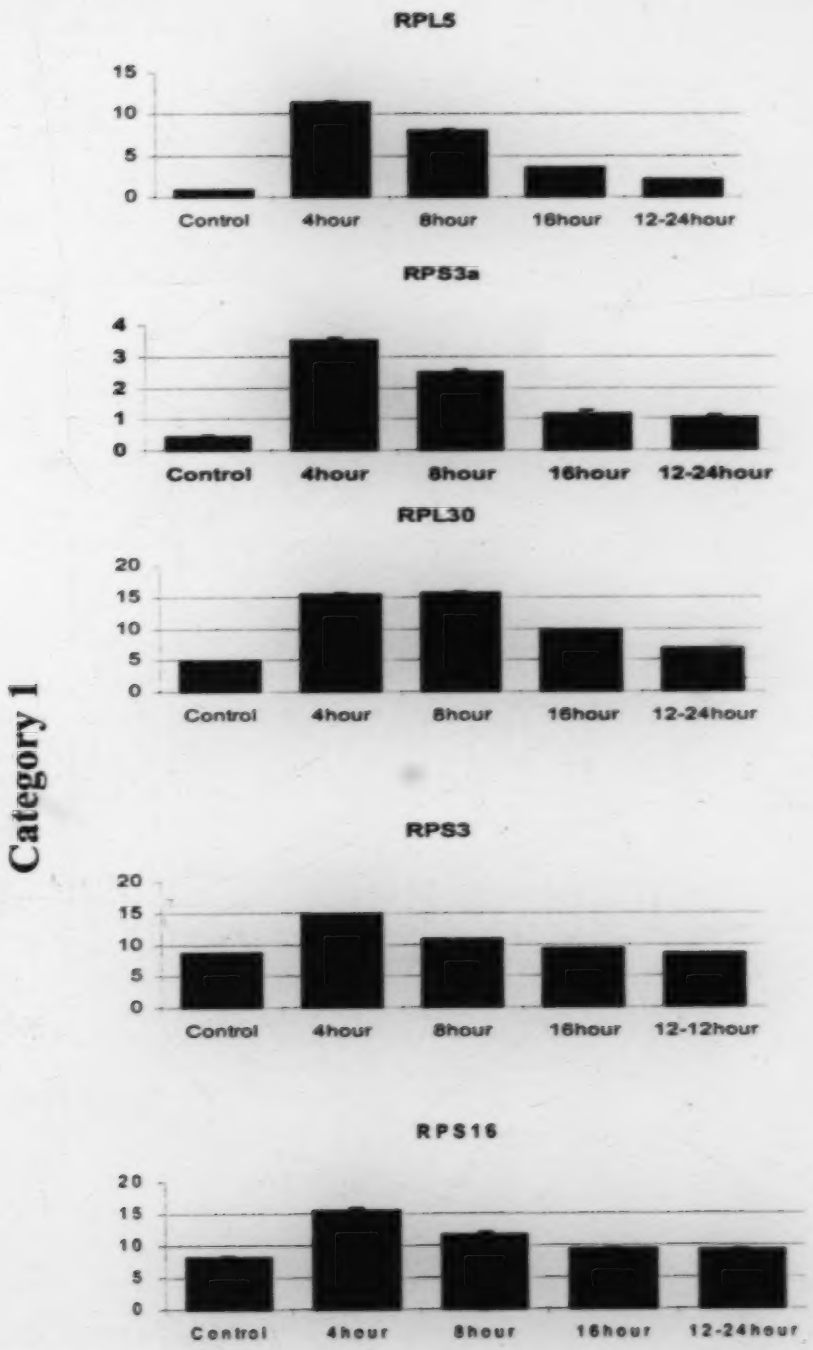
RPL5
15
10
5
0
Control
4hour
8hour
16hour
12-24hour
RPS3a
4
3
2
1
0
Control
4hour
8hour
16hour
12-24hour
RPL30
20
15
10
5
0
Control
4hour
8hour
16hour
12-24hour
Category 1
RPS3
20
15
10
5
0
Control
4hour
8hour
16hour
12-12hour
RPS16
20
15
10
5
0
Control
4hour
8hour
16hour
12-24hour

Figure 6-4: Graphical Representation of Category 2 and 3 RP Expression Over the Course of LIRD

Northern blots containing total RNA extracted from the retinae of control rats and from the retinae of rats subjected to each of the four experimental treatments were probed with individual ribosomal protein cDNA clones. Densitometry was performed on hybridization signals from each ribosomal protein gene clone. The signals were then normalized to the 18S ribosomal RNA. The normalized expression profile over the course of LIRD is depicted in graph form.

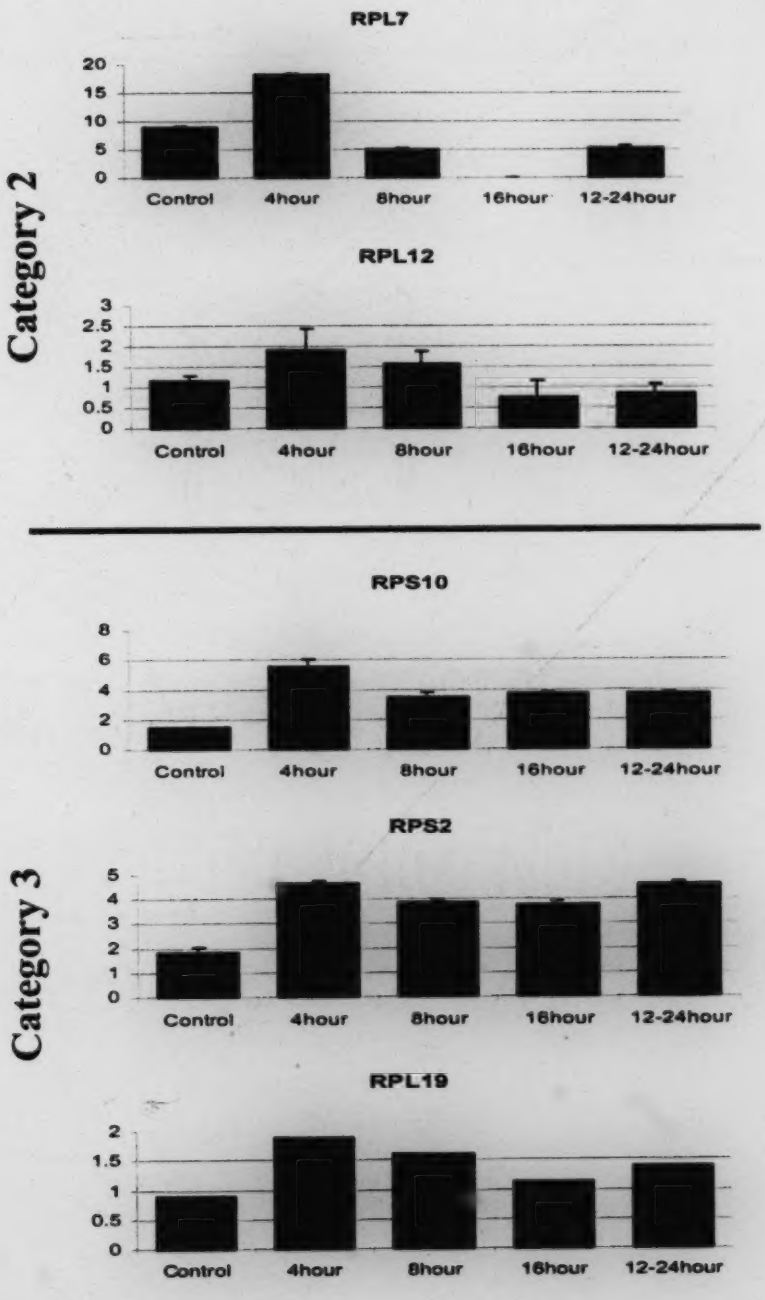
Category 2
RPL7
20
15
10
5
0
Control
4hour
8hour
16hour
12-24hour
RPL12
3
2.5
2
1.5
1
0.5
0
Control
4hour
8hour
16hour
12-24hour
Category 3
RPS10
8
6
4
2
0
Control
4hour
8hour
16hour
12-24hour
RPS2
5
4
3
2
1
0
Control
4hour
8hour
16hour
12-24hour
RPL19
2
1.5
1
0.5
0
Control
4hour
8hour
16hour
12-24hour

a very gradual increase in mRNA peaking at 4 and 8 h light treatment at levels not significantly higher than those detected in control retinae, and gradually decreasing to levels approximating those detected in the control retinae in the recovery phase (12 h light 24 h dark treatment).

B-3 Expression Patterns During Prostate Degeneration The expression pattern of RP genes prior to androgen deprivation, and 1, 2, 3, and 4 days following androgen deprivation was examined. The expression of all RP genes examined increased over this time frame (figure 6-5). Similar to what was observed during LIRD the degree of the up-regulation varied, although the range of variation in the prostate model was more limited than that observed in LIRD.

C. DISCUSSION

C-1 Slot blot vs. Northern blot Analysis In an effort to conserve RNA, Slot blot analysis was first used to examine the expression of 11 RP genes. The same amount of total RNA (5ug) that is required in a single lane for one Northern blot can be used to make 16 Slot blots. Because of the limited amount of tissue available, Slot blot analysis is more practical. Upon visual inspection of Slot blot results it appeared that all of the ribosomal protein genes tested, with the exception of RPS6, were up-regulated in response to 4 h light treatment. The up-regulation of these RP genes was confirmed by Northern blot analysis demonstrating that Slot blot analysis can be used to predict expression profiles. This method is especially valuable when conservation of RNA is necessary.

C-2 Ribosomal Proteins and Function During LIRD Ribosomal protein genes, as a whole, represent a highly conserved group of genes (Wool *et al.*, 1995). A general concept is that alterations of proteins that can interact with the ribosome may alter the mechanism by which the translation machinery functions. Some question has arisen as to whether these genes initially code for proteins explicitly involved in ribosome function, or whether they represent preexisting genes that were responsible for other cellular functions and were recruited into a role in protein synthesis over the course of evolution

Figure 6-5: Expression Pattern of Ribosomal Proteins on Degenerative Prostate Northern Blots

Ribosomal protein clones were used to probe degenerative prostate Northern blots. These Northern blots contain total RNA isolated from the prostate 0, 1, 2, 3, and 4 days after castration. The 18S ribosomal RNA is used as a loading control.. Similar changes in expression were observed for all ribosomal protein gene tested.

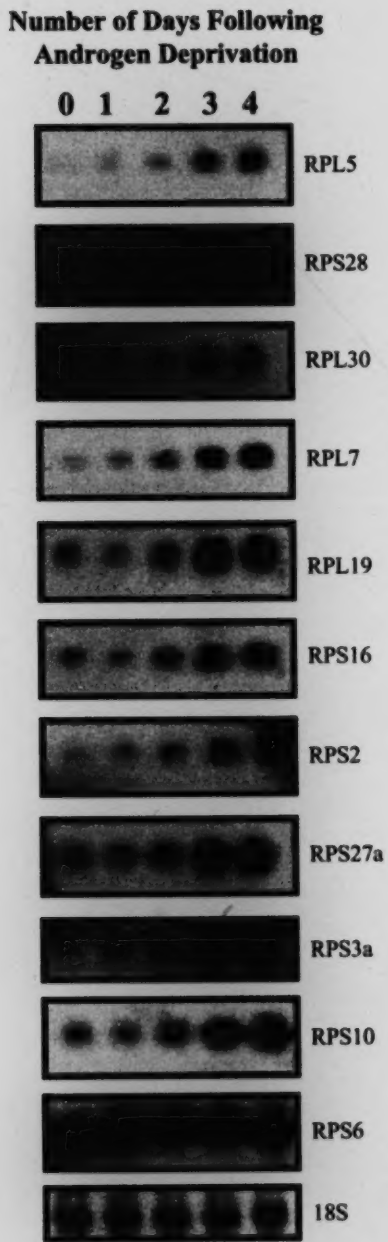
Number of Days Following
Androgen Deprivation
0 1 2 3 4
RPL5
RPS28
RPL30
RPL7
RPL19
RPS16
RPS2
RPS27a
RPS3a
RPS10
RPS6
18S

(Wool *et al.*, 1995; Wool *et al.*, 1996). A number of ribosomal proteins are associated with other biological processes or conditions such as cancer, DNA damage repair, cell cycle regulation, cell differentiation, and apoptosis (reviewed in Naora and Naora, 1999).

C-2.1 Ribosomal protein up-regulation in cancer cell lines. Of the ribosomal proteins examined in this series of experiments, RPS10, RPL5, RPS3, and RPS3a are associated with cancer. Interestingly, some of these RPs were identified through the use of differential cross-screening methods (Lecomte *et al.*, 1996, Pogue-Geile *et al.*, 1991). Variable expression patterns of RPS10 have been detected in colo-rectal cancers but no correlation has been made between mRNA levels and the severity of the disease (Frigerio *et al.*, 1995). RPL5 and RPS3 mRNA levels increase in both adenomatous polyps (the precursors of adenocarcinoma) and in adenocarcinoma itself (Pogue-Geile *et al.*, 1991). Increased RPS3a transcript levels have been documented in transformed rat liver cells, and cat T-lymphoid malignancies (Lecomte *et al.*, 1996). Evidence indicating that cell cycle deregulation can lead to cancer raises the possibility that these ribosomal proteins may have a role in cell cycle regulation. The suggestion that these ribosomal proteins could have a function as regulatory molecules fits with their expression pattern over the course of LIRD. It is hypothesized that a 4 h light treatment induces the Commitment Phase of LIRD. During this phase regulatory molecules likely direct the cellular response to the damage or changes caused by the light treatment. Genes involved in committing cells to an apoptotic fate, as well as those involved in repair are therefore expected to be up-regulated following this treatment. Transcript levels of RPS10, RPL5, RPS3 and RPS3a are all up-regulated in response to 4 h light treatment.

C-2.2 Cell cycle regulation. The role of RPS16 in determining cell fate was proposed based on its observed over-expression in the undifferentiated pancreatic tumor cell line, Panc 1 (Batra *et al.*, 1991). The observed 30-fold increase in RPS16 mRNA in Panc-1 is the consequence of there being 20-fold more copies of the RPS16 gene. A screen of 13 other differentiated pancreatic tumors showed no increase in RPS16 levels. Thus, it was proposed that the increased levels of RPS16 mRNA were more likely involved in maintaining the undifferentiated state of the Panc1 cells rather than contributing to their transformed state. Hence, RPS16 is proposed to play a role in cell differentiation.

Ribosomal proteins S3a, S2, and L7 are associated with cell cycle regulation. Increased transcript levels of the *Catharanthus roseus* RPS3a homologue cyc07, are associated with S phase of the cell cycle. This suggests that, like cyc07, RPS3a plays a role in cell cycle control (Lecomte *et al.*, 1996). In yeast, RPS3a homologues PLC1 and PLC2 are involved in cell proliferation (Lecomte *et al.*, 1996). RPS2 has been associated with cell cycle regulation since *Drosophila* RPS2 mutants arrest oogenesis at developmental stage 5 (Watanabe *et al.*, 1991). A role for RPL7 in cell cycle regulation has also been proposed based on the observation that constitutive expression of RPL7 causes G-phase arrest in Jurkart T-lymphoma cells (Neumann & Krawinkel, 1997). Interestingly, a reduction in RPL7 mRNA is associated with cell senescence (Seshadri *et al.*, 1993).

C-2.3 Ribosomal Proteins and Regulation Ribosomal proteins could be involved in retinal degeneration either in association with translation, as part of the ribosomal translation machinery, or by performing a specific extra-ribosomal function. As part of the ribosomal machinery, ribosomal proteins could be involved in regulating which transcripts are translated into proteins. In this way they may alter the balance of anti- and pro-apoptotic factors. Such a role has been attributed to RPL7. High, constitutive expression of RPL7 in Jurkart T-lymphoma cells inhibits the translation of two unidentified nuclear proteins, p25 and p18 and also induces the cells to undergo apoptosis (Neumann & Krawinkel, 1997). These two nuclear factors may be anti-apoptotic and apoptosis in these cells may be a result of RPL7 inhibiting the translation of these anti-apoptotic factors, thus allowing an increase in pro-apoptotic factors and subsequently apoptosis (Neumann & Krawinkel, 1997). Alternatively, RPL7 may be acting as a transcription factor and inducing the expression of pro-apoptotic genes. The basic region-leucine zipper (BZIP) motif found in RPL7's N-terminal is a motif common to eukaryotic transcription factors, including c-Fos and c-Jun (Hemmerich *et al.*, 1993). RPL7 is localized to both the nucleus and cytoplasm (Neu *et al.*, 1995), and thus RPL7 may act as a regulatory factor of both transcription and translation. When in the nucleus RPL7 may act as a transcription factor, while when in the cytoplasm RPL7 could inhibit translation of specific mRNA species. A role in association with regulation could also be ascribed to other RPs. RPL5 interacts with MDM2, a regulator of transcription factor p53 (Marechal *et al.*, 1997), presenting the possibility that RPL5 could be acting

upstream to regulate p53 expression and thus be effecting cellular changes independent of translation. A nuclear binding factor site and multiple transcription start sites are found in the RPL19 gene (Davies & Fried, 1995), suggesting the possibility that a nuclear factor or factors may be specifically inducing variable transcription of RPL19. Although no extra-ribosomal role has been identified for RPL19 to date, its role may be controlled through variable transcription. Different transcripts could encode proteins of different function. The RPS3a protein is found at the interface of the large and small ribosomal subunits, an area associated with the initiation of translation (Lecomte *et al.*, 1996). From this location RPS3a may also be playing a role in regulating the translation of specific mRNAs. All of these ribosomal proteins are expressed at high levels during the commitment phase, during which the induction of regulatory genes is expected.

C-2.4 Ribosomal proteins and apoptosis. Ribosomal proteins, RPL7 and RPS3a are directly associated with apoptosis. An increase in their mRNA levels results in the sensitization of cells to apoptotic stimuli (Naora *et al.*, 1999; Neumann & Krawinkel, 1997). The approximately 6-fold increase in RPL7 transcript levels during the Commitment Phase, prior to a decrease in transcript levels as apoptosis is executed, supports the hypothesis that RPL7 could be sensitizing cells or priming cells for apoptosis. The up-regulation of RPL7 during the Commitment Phase could allow for an increase in the cells' sensitivity to new insults. A transient increase followed by a decrease of RPS3a mRNA levels induces apoptosis in NIH 3T3 derived cells and mouse thymic cells (Naora *et al.*, 1998). In LIRD RPS3a mRNA levels increase during the commitment phase and then decrease during the execution phase, fulfilling the requirement of a transient induction followed by down-regulation shown to be sufficient for the induction of apoptosis.

C-2.5 Ribosomal Proteins and Repair. RPS3 has an extra-ribosomal role in DNA damage repair (Deutsch *et al.*, 1997). Deutsch *et al.*, (1997) have demonstrated that RPS3 has an apurinic/apyrimidinic (A/P) lyase activity, N-glycosylase activity, and a 3'and 5' deoxyribophosphodiesterase activity. RPS3 specifically excises 8-oxoGua and FapyGua from damaged DNA. This is of interest since 8-oxoGua is produced under the type of oxidative conditions present during LIRD (Organisciak *et al.*, 1995). Following its up-regulation in response to 4 h light treatment, RPS3 mRNA levels remain high over

the entire LIRD profile. Even during the recovery phase RPS3 transcript levels are higher than detected in the control retinae. RPS3 may be recruited to its DNA damage repair role during LIRD.

C-3 Ribosomal Proteins as a Common Phenomenon in Degeneration A comparison between the expression patterns of ribosomal proteins in the prostate and retinal degeneration models could shed light on the mechanism involved in both. If the expression patterns are similar then perhaps the mechanisms are similar also. If the expression patterns differ, then the role of ribosomal proteins may be unique in each tissue. The up-regulation of ribosomal proteins following androgen deprivation in the rat prostate mirrors the up-regulation of these ribosomal proteins in the rat retina following light exposure, suggesting that this phenomenon is not unique to retinal degeneration. Thus, the up-regulation of these ribosomal proteins can be added to the list of similarities between the retinal and non-retinal systems of tissue regression or degeneration.

D. CONCLUSION

It seems plausible that some ribosomal proteins may influence the LIRD independently of their function during translation. The ribosomal proteins could be involved in retinal degeneration either in association with translation, as part of the ribosomal translation machinery, or by performing a specific extra-ribosomal function. As part of the ribosomal machinery, ribosomal proteins could be involved in regulating which transcripts are translated into proteins. In this way they may alter the balance of anti-and pro-apoptotic factors. Such a role has been attributed to RPL7. Of the 15 ribosomal protein genes examined by Northern analysis and Slot blot analysis 11 are light-inducible, suggesting that a change in the translational machinery may represent a characteristic event in the progression to a degenerate phenotype. Several of the genes studied such as RPL7, RPS3a, and RPS3 are associated with active cell death or DNA damage repair. The variation in relative steady state levels of each ribosomal protein gene over the degeneration profile from gene to gene suggests that the changes in expression levels that are observed do not represent a uniform change due to changes in cell numbers and cell type populations. In all cases the initial induction in mRNA levels

was detectable after a 4 h light exposure, a light exposure that does not cause immediate detectable DNA fragmentation. Thus changes in the expression of genes underlying macromolecular synthesis precedes DNA fragmentation and represents a signature event that marks an early process in light-induced retinal degeneration.

CHAPTER 7
CONCLUSION

Despite the prevalence of retinal degenerative disease and the years of research in this area, the mechanism of retinal degeneration remains elusive. The objective of this thesis was to attempt to elucidate the mechanism of retinal degeneration by identify differences in gene expression between a healthy retina and a retina in the early stages of degeneration. A four hour exposure to green (498-580 nm), 1500 lux light was used to induce this early stage of retinal degeneration in albino Sprague-Dawley rats. This stage of retinal degeneration, termed the Commitment Phase, is predicted to define the time during which extracellular and intracellular events in the neural retina dictate whether individual cells will be committed to undergo apoptosis.

A differential cross-screen of a Commitment Phase cDNA library, using 4 h light treated retinae cDNA and control retinae cDNA probes, identified 54 differentially expressed transcripts. mRNA levels of the majority of these transcripts increase following 4 h light treatment, suggesting that an active cellular response is occurring in response to this light assault. Sequencing of the cloned cDNA transcripts revealed that the clones that could be identified as known rat genes fit into five gene classes: mitochondria associated, eye and central nervous system specific, enzyme, translational machinery, and signal pathway associated and transcription factor. Moreover, 9% of these 54 transcripts were identified as unique sequences. This analysis defines the specific categories of genes acting in concert during the initial stages of retinal degeneration. Further characterization of two categories of differentially expressed genes, the ribosomal proteins and transcription factors, was undertaken.

Assessment of TF expression over the course of LIRD was accomplished using NPA, RT-PCR, and Northern blot analysis. Based on these experiments it was concluded

that Clone 1084, putatively identified as containing Otx2 cDNA, does not contain Otx2 transcript but may contain a new member of the homeo-box domain containing-class of TFs. Of the retina-specific TF examined the expression pattern of the photoreceptor cell specific TF Crx, could not be determined due to the short length of the NPA oligonucleotide probe used, while the expression of Otx2 appeared to decrease following 4 h of light exposure (NPA results). The expression patterns of the three apoptosis associated TFs, p53, c-fos, and NFκβ, examined were shown to change over the course of LIRD. An inverse expression pattern for c-fos and p53 and a peak of NFκβ expression prior to the crest in p53 expression were observed. Although, these experiments cannot substantiate the existence of interactions between these TF during LIRD or that these TF are actively participating in LIRD, they do suggest that both events may be occurring. Hence, further pursuit in this area of research could provide answers as to the regulation of the LIRD and also offer insight into the regulation of apoptosis in general.

Analysis of the expression pattern of a variety of ribosomal protein (RP) transcripts showed that each phase of LIRD has its own unique complement of up-regulated and down-regulated RP genes, thus demonstrating that RP gene expression can contribute to the further definition of each phases' molecular phenotype. This study is the first to examine the expression of ribosomal proteins during retinal degeneratio. The expression of all RP genes examined was shown to increase following 4 h light exposure, however, the degree of induction differed between the RP genes examined. This result indicates that the induction of genes precedes DNA fragmentation and puts forth the possibility that specific RPs could be involved in extra-ribosomal or regulatory functions. Ribosomal proteins L7, S3a, and S3 are especially well suited for participation in such

roles since they have already been implicated in the regulation or induction of apoptosis and in the repair of damaged DNA (Kenmochi *et al.*, 1998, Nora *et al.*, 1999, Deutsch *et al.*, 1997). Experiments that explore the possible dual function of these three RPs as well as that of other RPs with interesting expression patterns over the course of LIRD, could reveal novel regulatory mechanisms and further the understanding of RP function. Results presented in this thesis are the first to suggest the involvement of RPs in the process or retinal degeneration.

My thesis project represents a beginning stage in a long-term research directive. The results, therefore, create a framework from which future research can be developed in order to dissect and characterize the diverse mechanisms that underlie light induced retinal degeneration, with the hope that this will lead to better diagnosis, treatment or a cure for retinal degenerative disease.

References

Adler R, Curcio C, Hicks D, Price D, Wong F. Cell death in age-related macular degeneration. Molecular Vision. **5**:31. 1999.

Alberts, B., Bray D., Lewis J., Raff., Roberts., Watson J.D. Molecular Biology of the Cell, 3rd ed., New York: Garland Publishing, Inc. 1994.

Allikmets R., Singh N., Sun H., Shroyer N.F., Hutchinson A., Chidamberam A., Gerrard B., Baird L., Stauffer D., Peiffer A., Rattner A., Smallwood P., Li Y. A photoreceptor cell-specific ATP-binding transporter gene (ABCR) is mutated in recessive Stargardt macular dystrophy. Nature Genetics. **15(3)**:236-46. 1997.

Baas D, Burnsted K.M, Martinez J.A, Vaccarino F.M, Wikler K.C, Barnstable C.J. The subcellular localization of Otx2 is cell-type specific and developmentally regulated in the mouse retina. Brain Research Molecular Brain Reasearch. **78(1-2)**:26-37. 2000.

Batra S.K., R.S. Metzgar, M.A. Hollingsworth. Molecular cloning and sequence analysis of the human ribosomal protein S16. Journal of Biological Chemistry **266(11)**: 6830-6833. 1991.

Biel M, Seeliger M, Pfeifer A, Kohler D, Gerstner A, Ludwig A, Jaissle G, Fauser S, Zrenner E, Hofmann F. Selectove loss of cone function in mice lacking the cyclic nucleotide-gated channel CNG3. Proceeding of the National Academy of Science USA. **96(19)**: 7553-7. 1999.

Bobola N, Briata P, Ilengo C, Rosatto N, Craft C, Corte G, Ravazzolo R. OTX2 homeodomain protein binds a DNA element necessary for interphotoreceptor

retinoid binding protein gene expression. Mechanisms of Development. **82 (1-2)**: 165-9. 1999.

Bovolenta P, Mallamaci A, Briata P, corte G, Boncinelli E. Implication of OTX2 in pigment epithelium determination and neural retina defferentiation. Journal of Neuroscience. **17(11)**: 4242-52. 1997

Bursch W, Kleine L, Tenniswood M. The biochemistry of cell death by apoptosis. Biochemical Cell Biology. **68(9)**: 1071-4. 1990.

Bussolino D.F., de Arriba Zerpa G.A., Grabois V.R., Conde C.B., Guido M.E., Caputto B.L. Light affects c-fos expression and phospholipid synthesis in both retinal ganglion cells and photoreceptor cells in an opposite way for each cell type. Molecular Brain Research. **58**:10-15. 1998.

Cai J, Nelson K.C, Wu M, Sternberg P Jr, Jones D.P. Oxidative damage and protection of the RPE. Progress in Retinal Eye Research. **19(2)**:205-21. 2000.

Chang G.Q, Hao Y, Wong F. Apoptosis: final common pathway of photoreceptor death in rd, rds, and rhodopsin mutant mice. Neuron. **11(4)**:1254-62. 1993.

Chen K., Gunter K., Maines M.D. Neurons overexpressing heme oxygenase-1 resist oxidative stress-mediated cell death. Journal of Neurochemistry. **75**: 303-313. 2000.

Chiao P.J., Shin D.M., Sacks P.G., Hong W.K., Tainsky MA. Elevated expression of the ribosomal protein S2 gene in human tumors. Molecular Carcinogenesis. **5**: 219-231. 1992.

Chomczynski P., Sacchi N. Single-step method of RNA isolation by acid guanidinium thiocyanate-phenol-chloroform extraction. Analytical Biochemistry. **162**:153-159. 1987.

Cicerone C.M. Cones survive rods in the light-damaged eye of albino rat. Science. **194(4270)**: 1183-5. 1976.

Cideciyan A.V., Hood D.C., Huang Y., Banin E., Li Z., stone EM., Milam AH., Jacobson SG. Disease sequence from mutant rhodopsin allele to rod and cone photoreceptor degeneration in man. Proceedings of the National Academy of Science USA. **95**:7103-7108. 1998.

Cohen A.I. The retina. Adler's Physiology of the Eye 9th edition. Edited by W.M.Hart Jr. Mosby Year Book. St. Louis. Missouri. 1992.

Colombo L.L, Mazzoni E.O, Meiss R.P. The time of tumor cell division and death depends on the site of growth. Oncological Report. **7(6)**:1363-6. 2000.

Cramton S.E, Laski F.A. String of pearls encodes Drosophila ribosomal protein S2, has Minute-like characteristics, and is required during oogenesis. Genetics. **137(4)**: 1039-48. 1994

Darrow, R.A., Darrow, R.M., Organisciak D.T. Biochemical characterization of cell specific enzymes in light-exposed rat retinae: oxidative loss of all-trans retinal dehydrogenase activity. Current Eye Research. **16**:144-151. 1997.

Davies B., M. Fried. The L19 ribosomal protein gene (RPL19): gene organization, chromosomal mapping, and novel promoter region. Genomics **25**: 372-380. 1995.

Deutsch W.A., A. Yacoub, P. Jaruga, T.H. Zastawny, M. Dizdaroglu. Characterization and mechanism of action of Drosophila ribosomal protein S3 DNA glycosylase activity for the removal of oxidatively damaged DNA bases. Journal of Biological Chemistry. **272(52)**: 32857-32860. 1997.

Diaz B, Pimentel B, de Pablo F, de La Rosa E.J. Apoptotic cell death of proliferating neuroepithelial cells in the embryonic retina is prevented by insulin. European Journal of Neuroscience. **11(5)**:1624-32. 1999

Dingle J.T. Action f vitamin A on the stability of lysosomes in vivo and in vitro. Ciba Foundation Symposium on Lysosomes. 1963.

Dryja T.P., Hahn L.B., Kajiwara K., Berson E.L. Dominant and digenic mutations in the Peripherin/RDS and ROM1 genes in retinitis pigmentosa. Investigative Ophthalmology and Visual Science. **38(10)**: 1972-1981. 1997.

Ellis R.E., Yuan J., Horvitz H.R. Mechanisms and functions of cell death. Annual Review Cell Biology. **7**: 663-698. 1991.

Escribano J., Ortego J., Coca-Prados M. Isolation and characterization of cell-specific cDNA clones from a subtractive library of the ocular ciliary body of a single normal human donor: transcription and synthesis of plasma proteins. Journal of Biochemistry. **118**:921-931. 1995.

Freund C., Horsford F.J., McInnes R.R. Transcription factor genes and the developing eye: a genetic perspective. Human Molecular Genetics. **5**: 1471-1488. 1996.

Freund C.L., Wang Q.L., Chen S., Muskat B.L., Wiles C.D., Sheffield B.C., Jacobson S.G., McInnes R.R., Zack D.J., Stone E.M. De novo mutations in the CRX homeobox gene associated with Leber congenital amaurosis. Nature Genetics **18**: 311-313. 1998.

Frigerio J.-M., P. berthezene, P. Garrido, E. Ortiz, S. Barthellemy, S. Vasseur, B. Sastre, I. Selezneff, J.-C. Dagorn, J. L. Iovanna. Analysis of 2166 clones from a human colorectal cancer cDNA library by partial sequencing. Human Molecular Genetics. **4(1)**: 37-43. 1995.

Furukawa T., Morrow E.M., Cepko C.L. Crx, a novel otx-like homeobox gene, shows photoreceptor-specific expression and regulates photoreceptor differentiation. Cell. **91**: 531-541. 1997.

Gal A, Li Y, Thompson D.A, Weir J, Orth U, Jacobson S.G, Apfelstedt-Sylla E, Vollrath D. Mutations in MERTK, the human orthologue of the RCS rat retinal dystrophy gene, cause retinitis pigmentosa. Nature Genetics. **26(3)**: 270-1. 2000.

Goldstone S.D., Lavin M.F. Isolation of a cDNA clone, encoding the ribosomal protein S20, downregulated during the onset of apoptosis in a human leukaemic cell line. Biochemical and Biophysical Research Communications. **196(2)**: 619-623. 1993.

Grimm C, Wenzel A, Hafezi F, Yu S, Redmond T.M, Reme C.E. Protection of Rpe65-deficient mice identifies rhodopsin as a mediatior of light-induced retinal degeneration. Nature Genetics. **25(1)**: 63-6. 2000.

Guenette R.S, Mooibroek M, Wong K, Wong P, Tenniswood M. Cathepsin B, a cysteine protease implicated in metastatic progression, is also expressed during regression of the rat prostate and mammary glands.
European Journal of Biochemistry. **226(2)**:311-21. 1994.

Hafezi F., Abegg M., Grimm C., Wenzel A., Munz K., Sturmer J., Farber D.B., Reme C.E. Retinal degenerationin the rd mouse in the absence of c-fos. Investigative Ophthalmology and Visual Science. **39(12)**: 2239-2244. 1998.

Hafezi, F., Grimm, C., Simmen, G.C., Wenzel, A., Reme, C.E. Molecular ophthalmology: an update on animal models for retinal degenerations and dystrophies. British Journal of Ophthalmology. **84**: 922-927. 2000.

Hemmerich P., A. vonMikecz, F. Neumann, O. Sozeri, G. Wolff-Vorbeck, R. Zoebelein, U. Krawinkel. Structural and functional properties of ribosomal protein L7 from humans and rodents. Nucleic Acids Research **21(2)**: 223-231. 1993.

Herdegen T, Leah J.D. Inducible and constitutive transcripton factors in the mammalian nervous system control of gene expression by Jun, Fos, and Krox and CREB/ATF proteins. Brain Research. Brain Research Reviews. **28(3)**:370-490. 1998.

Honig L.S., Rosenberg R.N. Apoptosis and neurologic disease. American Journal of Medicine. **108(4)**: 317-30. 2000.

Horino K., Hiroshi N., Ohsako T., Shibuya Y., Hiraoka T., Kitamura N., Yamamoto T. A monocyte chemotactic factor S19 ribosomal protein dimmer, in phagocytic clearance of apoptotic cells. Laboratory Investigation. **78(5)**: 603-617. 1998.

Ishida Y, Agata Y, Shibahara K, Honjo T. Induced expression of PD-1, a novel member of the immunoglobulin gene superfamily, upon programmed cell death. EMBO Journal. **11(11)**:3887-95. 1992.

Jacobson S.G., Cideciyan A.V., Huang Y., Hanna D.B., Freund C.L., Affatigato L.M., Carr R.E., Zack D.J., Stone E.M., McInnes R.R. Retinal degenerations with truncation mutations in the cone-rod homeobox (CRX) gene. Investigative Ophthalmology and Visual Science. **39(12)**: 2417-2426. 1998.

Jones S.E, Jomary C, Grist J, Makwana J, Neal M.J. Retinal expression of gamma-crystallins in the mouse. Investigative Ophthalmology and Visual Science. **40(12)**:3017-20. 1999.

Kenmochi N., T. Kawaguchi, S. Rozen, E. Davis, N. Goodman, T.J. Hudson, T. Tanaka, D.C. Page. A map of 75 human ribosomal protein genes. Genome Research. **8**: 509-523. 1998.

Kutty R.K., Kutty, G., Wiggert, B., Chader, G.J., Darrow, R.M., Organisciak, D.T. Induction of heme oxygenase 1 in the retina by intense visible light: suppression by the antioxidant dimethylthiourea. Proceedings of the National Academy of Science U.S.A. **92**:1177-1181. 1985.

Kuwabara T, Funahashi M. Light damage in the developing rat retina. Archives of Ophthalmology. **94(8)**: 1369-74. 1976.

LaVail, M.M. Rod outer segment disk shedding in rat retina: relationship to cyclic lighting. Science. **194(4269)**:1071-4. 1976

LaVail, M.M., Gorrin, G.M., Repaci, M.A., Thomas, L.A., Ginsberg, H.M. Genetic regulation of light damage to photoreceptors. Investigative Ophthalmology and Visual Science. **28**:1043-1048. 1987.

Lavrovsky Y, Schwarzman M.L, Abraham N.G. Novel regulatory sites of the human heme oxygenase-1 promoter region. Biochemical Biophysical Research Communications. **196(1)**: 336-41. 1993.

Lecomte F., Szpirer J., Szpirer C. The S3a ribosomal protein gene is identical to the Fte-1 (v-fos transformation effector) gene and the TNF-a-induced TU-11 gene, and its

transcript level is altered in transformed and tumor cells. Gene. **186**: 271-277. 1997.

Le W.D., Xie W.J., Appel S.H. Protective role of heme oxygenase-1 in oxidative stress-induced neuronal injury. Journal of Neuroscience Research. **56(6)**: 652-8. 1999.

Leist M. Single B., Naumann H., Fava E., Simon B., Kuhule S., Nicotera P. Inhibibition of mitochondrial ATP generation by nitric oxide switches apoptosis to necrosis. Experimental Cell Research. **249(2)**: 396-403. 1999.

Li G.M. The role of mismatch repair in DNA damage-induced apoptosis. Oncology Research. **11(9)**:393-400. 1999.

Li, S., Chang, C-J., Abler A.S., Tso, M.O.M. Inhibitory effects of cycloheximide and flunarizine on light-induced apoptosis of photoreceptor cells. Degenerative Diseases of the Retina. Edited by Anderson, R.E., LaVail, M.M., Hollyfield, J.G. Plenum Press, New York. Pp. 27-38. 1995A.

Li Z-Y, Milam A.H. Apoptosis in retinitis pigmentosa. Degenerative Diseases of the Retina. Edited by RE Anderson, MM LaVail and JG. Hollyfield. Plenum Press. New York. p. 1. 1995B.

Lucy J.A., Luscombe H., Dingle J.T. Studies on the mode of action of excess of vitamin A.8. mitochondrial swelling. Journal of Biochemistry. **84**:611 1962.

Maines M.D. Heme Oxygenase Clinical Applications and Functions. CRC Press, Inc. Florida. 1992.

Magabo K.S, Horwitz J, Piatigorsky J, Kantorow M. Expression of betaB(2)-crystallin mRNA and protein in retina, brain and testis. Investigative Ophthalmology and Visual Science. **41(10)**:3056-60. 2000

Marechal V., Elenbaas B., Taneyhill L., Piette J., Mechali M., Nicolas J-C., Levine A.J., Moreau J. Conservation of structural domains and biochemical activities of the MDM2 protein from Xenopus laevis. Oncogene. **14**:1427-1433. 1997.

Marti A., Hafezi F., Lansel N., Hegi M.E., Wenzel A., Grimm C., Niemeyer G., Reme C. Light-induced cell death of retinal photoreceptors in the absence of p53. Investigative Ophthalmology and Visual Science. **39**:846-849. 1998.

Maslim J., Valter K., Egensperger R., Hollander H., Stone J. Tissue oxygen during a critical developmental period controls the death and survival of photoreceptors. Investigative Ophthalmology and Visual Science. **38(9)**:1667-77. 1997.

Morimura H., Fishman G.A., Grover S.A, Fulton A.B, Berson E.L, Dryja T.P. Mutations in the RPE65 gene in patients with autosomal recessive retinitis pigmentosa or leber congenital amaurosis. Proceedings of the National Academy of Science USA. **95(6)**: 3088-93. 1998.

Morrow E.M, Furukawa T, Cepko C.I. Vertebrate photoreceptor cell development and disease. Development. **126(1)**: 23-36. 1999.

Naora H., Naora H. Involvment of ribosomal proteins in regulating cell growth and apoptosis: translational modulation or recruitment for extraribosomal activity? Immunology and Cell Biology. **77**: 197-205. 1999.

Naora H., Takai I., Adachi M., Naora H. Altered cellular responses by varying expression of a ribosomal protein gene: sequential coordination of enhancement

and suppression of ribosomal protein S3a gene expression induces apoptosis. Journal of Cell Biology. **141(3)**: 741-753. 1998.

Neu E., A.H. VonMikecz, P.H. Hemmerichc, H.H. Peter, M. Fricke, H. Deicher, E. Genth, U. Krawinkel, and Members of the SLE Study Groups. Autoantibodies against eukaryotic protein L7 in patients suffering from systemic lupus erythematosus and progressive systemic sclerosis: frequency and correlation with clinical, serological and genetic parameters. Clinical and Experimental Immunology. **100**: 198-204. 1995.

Neumann F., Krawinkel U. Constitutive expression of human ribosomal protein L7 arrests the cell cycle in G1 and induces apoptosis in Jurkat T-lymphoma cells. Experimental Cell Research. **230**: 252-261. 1997.

Nickerson J.M, Li GR, Lin Z.Y, Takizawa N, Si J.S, Gross E.A. Structure-function relationships in the four repeats of human interphotoreceptor retinoid-binding protein (IRBP). Molecular Vision. **4**:33. 1998.

Nicolas M.G, Fujiki K, Murayama K, Suzuki M.T, Mineki R, Hayakawa M, Yoshikawa Y, Cho F, Kanai A. Studies on the mechanism of early onset macular degeneration in cynomolgus (Macaca fascicularis) monkeys. I. Abnormal concentrations of two proteins in the retina. Experimental Eye Research. **62(3)**:211-9. 1996.

Noell W.K., Walker VS., Kang B.S., Berman S. Retinal damage by light in rats. Investigative Ophthalmology. **5(5)**: 450-472. 1966.

Noell, W.K., Albrecht, R. Irreversible effects of visible light on the retina: role of vitamin A. Science. **172**:76-80. 1971.

Nolte J. The Human Brain An Introduction to Its Functional Anatomy Fourth Edition. Mosby Inc. Chicago. 1999.

Nolte D., Taimor G., Kalff-Suske M., Seifart K.H. The human S3a ribosomal protein: sequence, location and cell-free transcription of the functional gene. Gene. **169**: 179-185. 1996.

Oppenheim, R.W., Prevette, D., Tytell, M., Homma, S. Naturally occurring and induced neuronal death in the chick embryo in vivo requires protein and RNA synthesis: evidence for the role of cell death genes. Developmental Biology. **138**: 104-113. 1990.

Organisciak D.T, Darrow R.M, Barsalou L, Kutty R.K, Wiggert B. Circadian-dependent retinal light damage in rats. Investigative Ophthalmology and Visual Science. **41(12)**:3694-701. 2000.

Organisciak D.T., Darrow R.A., Barsalou L., Darrow R.M., Lininger L.A. Light-induced damage in the retina: differential effects of dimethylthiourea on photoreceptor survival, apoptosis and DNA oxidation. Photochemistry and Photobiology. **70(2)**: 261-268. 1999.

Organisciak, D.T., Darrow, R.M., Jiang Y.-L., Blanks, J.C. Retinal light damage in rats with altered levels of rod outer segment docosahexaenoate. Investigative Ophthalmology and Visual Science. **37**:2243-2257. 1996

Organisciak, D.T., Darrow, R.M., Jiang, Y.-L., Marak, G.E., Blanks, J.C. Protection of dimethylthiourea against retinal light damage. Investigative Ophthalmology and Visual Science. **33**:1599-1609.1992.

Organisciak, D.T., R.M., Darrow, R.A., Darrow, L.A. Lininger. Environmental light and age-related changes in retinal proteins. Photostasis and Related Phenomena. Editor Williams and Thistle. Plenum Press, New York. 1998.

Organisciak, D.T., Wang, H.-M., Li, Z.-Y., Tso, M.O.M. The protective effect of ascorbate in retinal light damage of rats. Investigative Ophthalmology and Visual Science. **26**: 1580-1588. 1985.

Organisciak D.T., Kutty R.K., Leffale M., Wong P., Messing S., Wiggert B., Darrow R.M., Chader G.J. Oxidative damage and responses in retinal nuclei arising from intense light exposure. Degenerative Diseases of the Retina. Edited by R.E. Anderson, M.M. LaVail, J.G. Hollyfield. Plenum Press, NY. 1995.

Organisciak, D.T., Winkler, B.S. Retinal light damage: practical and theoretical considerations. In: Osborn, N.N., and Chader, G.J., eds. Progress in Retinal and Eye Research. Vol 13. Pergamon Press. New York . pp. 1-29. 1994.

Penn, J.S., Anderson, R.E. Effect of light history on rod outer segment membrane composition in the rat. Experimental Eye Research. **44**:779-788. 1987.

Phelan J.K., Bok D. A brief review of retinitis pigmentosa and the identified retinitis pigmentosa genes. Molecular Vision. **6**:116-24. 2000.

Pogue-Geile K., Geiser J.R., Shu M., Miller C., Wool I.G., Meisler AI., Pipas J.M., Ribosomal protein genes are overexpressed in colorectal cancer: isolation of a cDNA clone encoding the human S3 ribosomal protein. Molecular and Cellular Biology. **11(8)**: 3842-3849. 1991.

Portera-Cailliau C., Sung C.H., Nathans J., Adler R. Apoptotic photoreceptor cell death in mouse models of retinitis pigmentosa. Proceeding of the National Academy of Science USA. **91(3)**: 974-8. 1994.

Rattner A., Sun H., Nathans J. Molecular genetics of human retinal disease. Annual Review of Genetics. **33**: 89-131. 1999.

Redmond T.M, Yu S., Lee E., Bok D., Hamasaki D., Chen N., Goletz P., Ma J.X., Crouch R.K., Pfeifer K. Rpe65 is necessary for production of 11-cis-vitamin A in the retinal visual cycle. Nature Genetics. **20(4)**: 344-51. 1998.

Rhoades R., Pflanzer R. Human Physiology Third Edition. Saunders College Publishing, Harcourt Brace College Publishers. Toronto. 1996.

Rich K.A., Zhan Y., Blanks J.C., Aberrant expression of c-fos accompanies photoreceptor cell death in the rd mouse. Journal of Neurobiology. **32**:593-612. 1997.

Rozet J.M., Gerber S., Ghazi I., Perrault I., Ducroq D., Souied E., Cabot A., Dufier J.L., Munnich A., Kaplan J. Mutations of the retinal specific ATP binding transporter gene(ABCR) in a single family segregating both autosomal recessive retinitis pigmentosa RP19 and Stargardt disease: evidence of clinical heterogeneity at this locus. Journal of Medical Genetics. **36(6)**: 447-451. 1999.

Ruifrok A.C, Weil M.M, Thames H.D, Mason K.A. Diurnal variations in the expression radiation-induced apoptosis. Radiation Research. **149(4)**:360-5. 1998.

Ryan K.M., Ernst M.K, Rice N.R., Vousden K.H. role of NF-kB in p53-mediated programmed cell death. Nature. **404**:892-896. 2000.

Saari J.C. The biochemistry of sensory transduction in vertebrate photoreceptors. Adler's Physiology of the Eye 9th edition. Edited by W.M. Hart Jr. Mosby Year Book. St. Louis. Missouri. p. 460. 1992.

Sachs L.M, Damjanovski S, Jones P.L, Li Q, Amano T, Ueda S, Shi Y.B, Ishizuya-Oka A. Dual functions of thyroid hormone receptors during Xenopus development. Comparative Biochemical Physiology and Biochemistry and Molecular Biology. **126(2)**:199-211. 2000.

Saeboe-Larssen S., Lambertsson A. A Novel Drosophila Minute Locus Encodes Ribosomal Protein S13. Genetics. **143**: 877-885. 1996.

Sambrook J., Fritsch E.F., Maniatis T. Molecular Cloning A Laboratory Manual Second Edition. Cold Spring Harbor Laboratory Press. Plainview, New York. 1989.

Sapi E., Flick M.B., Kacinski B.M. The first intron of human c-fms proto-oncogene contains a processed pseudogene (RPL7P) for ribosomal protein L7. Genomics. **22**: 641-645. 1994.

Seshadri T., Uzman J.A., Oshima J., Campisi J. Identification of a transcript that is down-regulated in senescent human fibroblasts. Journal of Biological Chemistry. **268(25)**: 18474-18480. 1993.

Shroyer N.F., Lewis R.A., Allikmets R., Singh N., Dean M., Leppert M., Lupski J.R. The rod photoreceptor ATP-binding cassette transporter gene ABCR, and retinal disease: from mongenic to multifunctional. Vision Research. **39(15)**: 2537-44. 1999.

Smith S.B, Bora N, BcCool D, Kutty G, Wong P, Kutty R.K, Wiggert B. Photoreceptor cells in the vitiligo mouse die by apoptosis. TRPM-2/clusterin is increased in the neural retina and in the retinal pigment epithelium. Investigative Ophthalmology and Visual Science. **36(11)**: 2193-201. 1995.

Sohocki M.M., Sullivan L.S., Mintz-Hittner H.A., Birch D., Heckenlively Jr., Freund C.L., McInnes R.R., Daiger S.P. A range of clinical phenotypes associated with

mutations in CRX, a photoreceptor transcription-factor gene. American Journal of Human Genetics. **63**: 1307-1315. 1998.

Southern E.M. Detection of specific sequences among DNA fragments separated by gel electrophoresis. Journal of Molecular Biology. **98(3)**:503-17. 1975.

Spect S., Leffak M., Darrow R.M., Organisciak D.T., Damage to rat retinal DNA induced in vivo by visible light. Photochemistry and Photobiology. **69(1)**: 91-98. 1999.

Stewart M.J, Denell R. Mutations in the Drosophila gene encoding ribosmal protein S6 cause tissue overgrowth. Molecular Cell Biology. **13(4)**:2524-35. 1993.

Stocker R. Induction of haem oxygnease as a defence against oxidative stress. Free Radical Research Communications. **9(2)**: 101-12. 1990.

Tendler Y., Weisinger G., Coleman R., Diamond E., Lischinsky S., Kerner H., Rotter V., Zinder O. Tissue-specific p53 expression in the nervous system. Molecular Brain Research. **72**:40-46. 1999

Tenniswood M.P, Guenette R.S, Lakins J, Mooibroek M, Wong P, Welsh J.E. Active cell death in hormone-dependent tissues. Cancer Metastasis Review. **11(2)**:197-220. 1992

Watson K.L., Konrad K.D., Woods D.F., Bryant P.J. Drosophila homolog of the human S6 ribosomal protein is required for tumor suppression in the hematopoietic system. Proceedings of the National Academy of Science U.S.A. **89**: 11302-11306. 1992.

Weiss E.R, Hao Y, Dickerson C.D, Osawa S, Shi W, Zhang L, Wong F. Altered cAMP levels in retinal from transgenic mice expressing a rhodopsin mutant. Biochemical Biophysical Research Communications. **216(3)**: 755-61. 1995.

Wenzel A., Grimm C., Marti A., Kueng-Hitz N., Hafezi F., Niemeyer G., Reme C.E. C-fos controls the " private pathway' of light-induced apoptosis of retinal photoreceptors. Journal of Neuroscience. **20(1)**: 81-88. 2000.

Wiegand R.D., N.M. Giusto, I.M., Rapp, R.E., Anderson. Evidence for rod outer segment lipid peroxidation following constant illumination of the rat retina. Investigative Ophthalmology and Visual Science. **24**: 1433-1435. 1983.

Wistow G. Lens crystallins: gene recruitment and evolutionary dynamism. Trends in Biochemichal Science. **18(8)**:301-6. 1993.

Wong P. Apoptosis, retinitis pigmentosa, and degeneration. Biochemical Cell Biolgoy. **72**:489-498. 1994

Wong, P., Kutty, R.K., Darrow, R.M., Shivaram S, Kutty G, Fletcher RT, Wiggert B, Chader G, Organisciak DT. Changes in clusterin expression associated with light-induced retinal damage in rats. Biochemical Cell Biology. **72(11-12)**: 499-503. 1994.

Wong P, Ulyanova U, Darrow R, Shivaram S, vanVeen T, Chader G, and Organisciak D. Correlation of light-induced retinal damage in rats with changes in TRPM-2/Clusterin (TRPM-2) expression. (ARVO, Ft. Lauderdale, U.S.A., May 1995). Investigative Ophthalmology and Visual Science **36**:S860. 1995

Wool I.G. The structure and function of eukaryotic ribosomes. Annual Review of Biochemistry. **48**: 719-54. 1979.

Wool I.G, Chan Y.L, Gluck A. Structure and evolution of mammalian ribosomal proteins. Biochemical Cell Biol. **73(11-12)**: 933-47. 1995

Wool I.G. Extraribosomal functions of ribosomal proteins. Trends Biochemical Science. **21(5)**:164-5. 1996.

Wyllie A.H. The genetic regulation of apoptosis. Current Opinion in Genetic Development. **5(1)**:97-104. 1995.

Zhang K. Nguyen T.H., Crandall A., Donoso L,A. Genetic and molecular studies of macular dystrophies: recent developments. Survey of Ophthalmology. **40(1)**:51-61. 1995

APPENDEX I

SOLUTIONS

ELECTROPHORESIS BUFFERS

10X TBE

To 800 mL of deionized H_2O add:

109g	Tris base
55g	boric acid
40 mL	0.5 M EDTA pH8

Dissolve the solutes

Adjust volume to 1L with deionized H_2O

* Use 1X concentration for Gel Running Buffer

50X TAE

To 600 mL of deionized H_2O add:

242g	Tris base
57.1 mL	glacial acetic acid
100 mL	0.5M EDTA (pH 8.0)

Adjust volume to 1L with deionized H_2O

Formaldehyde Gel Electrophoresis Buffer

Electrophoresis buffer is prepared to a final volume of 1 L

83 mL	formaldehyde
15 mL	10X MOPs buffer
817 mL	deionized H2O

GELS

1% Agarose Gel

To desired volume of 1X TAE buffer add 1% (w/v) of agarose

Dissolve agarose in buffer by heating

Allow agarose to cool prior to pourning into gel casting tray

1% Formaldehyde Gel

For a 150 mL gel:

1.5g	agarose
108 mL	deionized H2O

Dissolve the agarose in the deionized H2O

Once the agar has cooled but not solidified add:

15 mL	10X MOPs buffer
27 mL	formaldehyde

Swirl to mix ingredients and pour into gel casting tray.

12% Polyacrylamide 8M Urea Gel

To clean flask add:

14.4g	urea
3 mL	10X TBE
8.6 mL	40% polyacrylamide

Adjust volume to 30 mL with deionized H_2O

Dissolve solutes

Add:

240ul	100% ammonium persulfate in H_2O
36ul	TEMED

The addition of the above will result in the gel setting very quickly

MEDIA

lB Medium (Luria-Bertani Medium)

To 950 mL of deionized H_2O add:

- 10g bacto-tryptone
- 5g bacto-yeast extract
- 10g NaCl

Dissolve the solutes

Adjust pH to 7.0 with 5N NaOH

Adjust volume to 1L with deionized H2O

Autoclave on liquid cycle

LB Agar

To 900 mL of deionized H_2O add:

- 10g NaCl
- 10g tryptone
- 5g yeast extract
- 20g agar

Dissolve the solutes

Adjust pH to 7.0 with 5N NaOH

Adjust volume to 1L with deionized H_2O

Autoclave on liquid cycle

NZY Agar

To 900 mL of deionized H_2O add:

- 5g NaCl
- 2g MgSO4-7H2O
- 5g yeast extract
- 10g NZ amine (casein hydrolysate)
- 15g agar

Dissolve the solutes

Adjust pH to 7.5 with NaOH

Adjust volume to 1L with deionized H_2O

Autoclave on liquid cycle

NZY Top Agar

To 900 mL of deionized H_2O add:

5g NaCl

2g MgSO4-7 H_2O

5g yeast extract

10g NZ amine (casein hydrolysate)

1% (w/v) agar

Dissolve the solutes

Adjust pH to 7.5 with NaOH

Adjust volume to 1L with deionized H_2O

Autoclave on liquid cycle

PCR COMPONENTS

10X PCR Buffer

200mM Tris-HCl (pH 8.4)

500mM KCl

15mM $MgCl_2$

HYBRIDIZATION SOLUTIONS

Hybrisol II

10% Dextra Sulfate

1% SDS

6X SSC

20X SSC

In 800 mL of deionized H_2O dissolve:

175.3g NaCl

88.2g sodium citrate

Adjust pH to 7.0 with 10N NaOH

Adjust volume to 1L with deionized H_2O

Autoclave on liquid cycle

10% SDS (Sodium dodecyl sulfate)

In 900 mL of deionized H_2O dissolve:

100g of electrophoresis-grade SDS

Heat to 68°C to aid in dissolving the SDS

Adjust pH to 7.2 with HCl

Adjust volume to 1L

DO NOT Autoclave

SM Buffer

To 880 mL of deionized H_2O add:

5.8g NaCl

2.0g MgSO4-7 H_2O

50 mL 1M Tris-HCl pH 7.5

5 mL 2% gelatin

Adjust volume to 1L with deionized H_2O

Autoclave on liquid cycle

EDTA

To 800 mL of deionized H_2O add:

186.1g EDTA

Adjust pH to 8.0 with NaOH

*the EDTA will not dissolve until the pH is 8.0

Adjust volume to 1L with deionized H_2O

RNA Sample Master Mix for Formaldehyde Gel Electrophoresis

To approximately 1.5ug RNA sample add:

4ul 10X MOPS

7ul Formaldehyde

20ul Deionized Formaldehyde

1ul Ethidium bromide (1μg/μL)

adjust volume to 35ul with DEPC treated water

1M Tris-HCl

In 800 mL of deionized H_2O dissolve:

121.1g Tris base

Adjust pH to desired value with concentrated HCl

Make sure solution is at room temperature when adjusting pH

Adjust volume to 1L with deionized H_2O

Autoclave on liquid cycle

* if solution has yellow colour discard it.

5M NH_4OAc (m=77.08)

To 50 mL deionized H_2O add:

38.5g ammonium acetate

Adjust volume to 100 mL with deionized H_2O

DEPC (Diethylpyrocarbonate) Water

Add DEPC to double-distilled, deionized H_2O to a concentration of 0.1% (i.e. add 1 mL per leter of H_2O)

Stir into solution

Incubate several hours or overnight

Autoclave for at least 45 minutes, or until DEPC scent is gone

APPENDIX II

ABBREVIATIONS

ABCR	ATP binding transporter gene
cDNA	copy DNA
Crx	cone-rod homeobox gene
DEPC	Diethylpyrocarbonate
DMTU	Dimethylthiourea
EST	Expressed Sequence Tag
h	hour(s)
HO-1	Heme oxygenase 1
IER	Immediate Early Response genes
IRBP	Interphotoreceptor Retinol Binding Protein
LIRD	Light Induced Retinal Degeneration
LRAT	Lecithin:Retinol Acyltransferase
MMLV-RT	Murine leukemia virus reverse transcriptase
NPA	Nuclease Protection Assay
OD	Optical Density
PCR	Polymerase Chain Reaction
PDE	Phosophodiesterase
PR-PCR	Reverse Transcriptase- Polymerase Chain Reaction
ROS	Rod Outer Segment
RP	Ribosomal Protein
RPE	Retinal Pigment Epithelium
SSC	Sodium Chloride tri-sodium Citrate
TF	Transcription Factor
UV	Ultra-violet